Effect of Reflow Process on Glass Transition Temperature of Printed Circuit Board Laminates and Model for Prediction of Package-on-Package (PoP) Warpage and The Effect of Process and Material Parameters

by

Vikalp Narayan

A thesis submitted to the Graduate Faculty of
Auburn University
in partial fulfillment of the
requirements for the Degree of
Master of Science

Auburn, Alabama
December 14, 2013

Keywords: Glass transition temperature, Peak temperature, Time above liquidus, Warpage, Package-on-Package (PoP), ANOVA, PCR, Electronic Packaging

Copyright 2013 by Vikalp Narayan

Approved by

Pradeep Lall, Chair, Thomas Walter Professor of Mechanical Engineering
George T. Flowers, Professor of Mechanical Engineering and Dean of the Graduate School
Michael J. Bozack, Professor of Physics Department

Abstract

The effect of temperature exposure encountered both during assembly and in fielded products, has a known influence on glass transition temperature of printed-circuit board (PCB) laminate materials. Printed circuit board laminates such as FR4 are composites of epoxy resin with woven fiberglass reinforcement. Interaction between manufacturing process variables that impact the changes in glass transition temperature (T_g) has been studied. The laminates studied have been broadly classified into high-T_g, and mid-T_g laminates. Different sets of reflow profiles were created by varying the process variables including, time above liquidus, peak temperature, ramp rate and cooling rate. The effect of multiple reflows encountered in normal assembly or board rework has been studied by exposing the assemblies to multiple reflows between 2x-6x. Changes to the glass transition temperature have been classified by measurement of the glass transition temperature were measured via Thermo Mechanical Analysis (TMA). Statistical analysis of the variables has been used to determine the statistical significance of the measured changes for large populations.

Package-on-Package (PoP) assemblies may experience warpage during package fabrication and later during surface mount assembly. Excessive warpage may result in loss-of-coplanarity, open connections, mis-shaped joints, and reduction in package board-level reliability (BLR) under environmental stresses of thermal cycling, shock and vibration. Previous researchers have shown that warpage may be influenced by a number of design and process factors including underfill properties, mold properties, package geometry, package architecture,

board configuration, underfill and mold dispense and cure parameters, package location in the molding panel. A comprehensive inverse model incorporating a full set of design and process parameters and their effect on PoP package and PoP assembly warpage is presently beyond the state of art. In this paper, data has been gathered on multiple package-on-package assemblies under a variety of assembly parameters. The packages have been speckle coated. The warpage of the PoP assemblies have been measured using a glass-top reflow oven using multiple cameras. Warpage measurements have been taken at various temperature of the reflow profile between room temperature and the peak reflow temperature. Finite element models have been created and the package-on-package warpage predictions have been correlated with the experimental data. The experimental data set has been augmented with the simulation data to evaluate configurations and parameter-variations, which were not available in the experimental dataset. Statistical models have been developed to capture the effect of single and multiple parameter variations using principal components regression, and ridge regression. Best subset variables obtained from stepwise methods, have been used for model development. The developed models have been validated with experimental data using a single factor design of experiment study and are found to accurately capture material and geometry effects on part warpage. The results show that the proposed approach has the potential of predicting both single and coupled factor effects on warpage.

Acknowledgments

First of all I would like to thank my parents Mr. Sheoganga Narayan Singh and Mrs. Kiran Singh for having faith in me and providing endearing love, encouragement and moral support.

I would like to express my deep gratitude to my research advisor and teacher Dr. Pradeep Lall for giving me the opportunity to work under his guidance and mentorship at NSF Center for Advanced Vehicle and Extreme Environment Electronics (CAVE^3) as a Graduate Research Assistant at Auburn University. Thanks to his invaluable guidance, support and patience during the course of this degree. I would also like to thank my other committee members Dr. George T. Flowers and Dr. Michael Bozack for their constant support and guidance while completing this thesis.

I would also like to thank all my friends especially Ajit, Aditya, Sadhwi and Smita for their priceless friendship and camaraderie all throughout my graduate studies.

It was also a privilege to work with all my colleagues: Kewal, Mahendra, Geeta, Dinesh and others who are not mentioned here. It was a pleasure working with them all of you and I would like to thank you for all the help.

Table of Contents

Abstract…………………………………………………………………………………….ii

Acknowledgments……………………………………………………………..………....iv

Table of Contents……………………………………………………………………….v

List of Figures……………………………………………………………………....viii

List of Tables…………………………………………………………………………...xi

CHAPTER 1 Introduction

1.1 Overview of Electronic Packaging……...1

1.2 Reliability Concerns..7

1.3 Effect of Lead Free on PCB Reliability...9

1.4 Statistical Analysis……….…………………………..……………………….…...10

1.5 Finite Element Analysis…………………………………………………………….13

1.6 Digital Image Correlation…………………………………………………….....15

1.7 Thesis Layout………………………………………………………………………..17

CHAPTER 2 Literature Review

2.1Glass Transition Temperature of Printed circuit Board………..……....……..…………20

2.2 Package Warpage………..……..………………………………...….……………...22

2.3 Statistical Prediction Method………..…………….……………………..………………26

2.4 Digital Image Correlation………………………………..………………..…….........28

2.5 Finite Element Modeling………………………………………………………….....30

CHAPTER 3 Effect of Reflow Process on Glass Transition Temperature of Printed Circuit Board Laminates

3.1 Introduction……………………………………………………....……..……………32

3.2 Test Vehicle ………………………………………………………………...……....34

3.3 Measurement of Tg…..36

3.4 Result and Analysis…………………………..……………………...........................40

3.4.1 Mid Tg Laminates...40

3.4.2 Statistical Analysis of TAL Effect on Tg...42

3.4.3 Statistical Analysis of Peak Temperature Effect on Tg...46

3.4.4 Statistical Analysis of Number of Reflows Effect on Tg.......................................50

3.5 High Tg Laminates...54

3.5.1 Statistical Analysis of TAL Effect on Tg...56

3.5.2 Statistical Analysis of Peak Temperature Effect on Tg...60

3.5.3 Statistical Analysis of Number of Reflows Effect on Tg.......................................64

CHAPTER 4 Model for Prediction of Package-on-Package Warpage and Effect of Material and Process Parameters

4.1 Introduction…………………..…………………………………………………...........68

4.2 Test Vehicle…………………………...……………………………………………..72

4.3 Experimental Set Up...75

4.4 Finite Element Analysis…………………………………………………………………80

4.5 Source of Data for Statistical Analysis……………………………………………………82

4.6 Statistical Model Development……………………………………………………......83

4.7 Failure Modes……………………………………………………………………........90

4.8 Convergence of Predicted vs Measured Values……………………………………………92

4.8.1 Effect of Process Variable……………………………………………………..92

4.8.2 Effect Material Properties………………………………………………….......95

4.8.3 Effect of Assembly Dimension………………………………………………....101

4.9 Inverse Determination of Desired Material Properties, Process Condition and Package Element Dimension…………………………………………………………………....106

CHAPTER 5 Summary and Future Work…………………………………………………110

Bibliography………………………………………………………………………………113

List of Figures

Figure 1.1: Electronic packaging hierarchy [Lau 1995 Page #2]…………………………….……….....2

Figure 1.2: Moore's Law ……...…………..…………………………………………………..3

Figure 1.3: Electronic packaging industry: Trends [JISSO Japan Technology Roadmap, 2001 Edition]…………………………………………………………………………….4

Figure 1.4: Package trend [Courtesy Amkor]…………………………………………......5

Figure 1.5: Roadmap for 3D interconnects [Source Yole Development]……………………....6

Figure 1.6 Schematic drawing of excessive warpage at reflow temperature resulting in shorts (left) or opens (right) after soldering [Courtesy Imec]………………………………8

Figure 1.7: Tracking movement of a point..15

Figure 1.8: Strain evaluation [Courtesy lavision]..16

Figure 1.9: Set-up for 3D digital image correlation [J. M. Dulieu-Barton]…………………....17

Figure 2.1: Open circuit induced by warpage in SMT process I…………………………….24

Figure 2.2: Open circuit induced by warpage in SMT process II………………….................24

Figure 3.1: Reflow profile..35

Figure 3.2.a: TMA (Thermo mechanical Analyzer)…………………………………….....36

Figure 3.2.b: Sample holder...37

Figure 3.2.c: Sample holder with heater...38

Figure 3.3: Representative CTE measurements from Thermo mechanical Analyzer……………..39

Figure 3.4: Analysis of statistical significance of TAL effect on Tg of Mid-Tg Laminate............43

Figure 3.5: Analysis of statistical significance of peak temperature effect on Tg of Mid-Tg laminate...46

Figure 3.6: Analysis of statistical significance of number of reflows effect on T_g of Mid-T_g laminate…………………………………………………………………………..50

Figure 3.7: Analysis of statistical significance of TAL effect on T_g of High-T_g laminate……..56

Figure 3.8: Analysis of statistical significance of peak temperature effect on T_g of High-T_g laminate…………………………………………………………………………..60

Figure 3.9: Analysis of statistical significance of number of reflows effect on T_g of High-T_g laminate…………………………………………………………………………..64

Figure 4.1: A common PoP configuration...69

Figure 4.2 : Warpage sign convention..70

Figure 4.3: Test vehicle 1 package architecture...72

Figure 4.4: Test vehicle 2 package architecture…………………………………………...74

Figure 4.5: Temperature profile for reflow..75

Figure 4.6: Experimental set up..76

Figure 4.7: Digital image correlation for a 3D case [Lall 2010]..77

Figure 4.8: DIC out-of-plane displacement contour…………………………………......79

Figure 4.9: Experimental warpage Vs. FEA warpage [Patel 2013]...................................81

Figure 4.10: PCR predicted vs measured for change in initial warpage……………….......93

Figure 4.11: PCR predicted vs measured for change in temperature…………………………94

Figure 4.12: PCR predicted vs measured for change in peak temperature……………………94

Figure 4.13: PCR predicted vs measured for change in die E……………………………...95

Figure 4.14: PCR predicted vs measured for change in mold CTE2………………….......96

Figure 4.15 PCR predicted vs measured for change in mold E1………………………………..96

Figure 4.16: PCR predicted vs measured for change in mold E2…………………………….....97

Figure 4.17: PCR predicted vs measured for change in core CTE………………………………98

Figure 4.18: PCR predicted vs measured for change in core E……………………………..…...100

Figure 4.19: PCR predicted vs measured for change in die CTE……………………………....100

Figure 4.20: PCR predicted vs measured for change in die width...101

Figure 4.21: PCR predicted vs measured for change in die thickness…………………….......102

Figure 4.22: PCR predicted vs measured for change in mold thickness…………………….....102

Figure 4.23: PCR predicted vs measured for change in core thickness…………………..........104

Figure 4.24: PCR predicted vs measured for change in package width……………………….104

List of Tables

Table 3.1: Effect of time above liquidus on T_g for Mid-T_g laminates.…………………………......41

Table 3.2: Effect of peak temperature on Tg for Mid-T_g laminates……………………………...41

Table 3.3: Effect of number of reflows on Tg for Mid-T_g laminates…………….……………42

Table 3.4: ANOVA for effect of TAL on Tg of Mid-Tg laminate…………………….……43

Table 3.5: Means and confidence intervals for effect of TAL on Tg of Mid-Tg laminate………44

Table 3.6: Comparison of Tg from each TAL treatment using student's t-test………………….45

Table 3.7: Pairwise p-values for various TAL treatments on T_g for Mid-T_g laminates………....45

Table 3.8: ANOVA for effect of peak temperature on T_g of Mid- T_g laminate………………..47

Table 3.9: Means and confidence intervals for effect of peak temperature on T_g for mid-T_g laminate………………………………………………………………………..47

Table 3.10: Comparison of T_g from each peak temperature treatment using student's t-test……48

Table 3.11: Pairwise p-values for various peak temperature treatments on T_g for mid-T_g laminates…………………………………………………………………………49

Table 3.12: ANOVA for effect of number of reflows on T_g of mid-T_g laminate……………....51

Table 3.13: Means and confidence intervals for effect of number of reflows on T_g for mid-T_g laminate………………………………………………………………………...51

Table 3.14: Comparison of T_g from each number of reflows treatment using student's t-test……………………………………………………………………………..52

Table 3.15: Pairwise p-values for various number of reflow treatments on Tg for mid-Tg laminates……………………………………………………………………...53

Table 3.16: Effect of time above liquidus on T_g for high-T_g laminates………………………....54

Table 3.17: Effect of peak temperature on Tg for high Tg laminates……………………………55

Table 3.18: Effect of number of reflows on Tg for high Tg laminates………………….........55

Table 3.19: ANOVA for effect of TAL on T_g of mid-T_g laminate……………………………..57

Table 3.20: Means and confidence intervals for effect of TAL on T_g for high-T_g laminate…....58

Table 3.21: Comparison of Tg from each TAL treatment using student's t-test………………….58

Table 3.22: Pairwise p-values for various time above liquidus treatments on Tg for high-Tg laminates……………………………………………………………………...59

Table 3.23: ANOVA for effect of peak temperature on T_g of high-T_g laminate……………….61

Table 3.24: Means and confidence intervals for effect of peak temperature on T_g for high-T_g laminate……………………………………………………………………….62

Table 3.25: Comparison of Tg from each peak temperature treatment using student's t-test……62

Table 3.26: Pairwise p-values for various peak temperature treatments on T_g for high-T_g laminates……………………………………………………………………….63

Table 3.27: ANOVA for effect of number of reflows on T_g of high-T_g laminate……………...65

Table 3.28: Means and confidence intervals for effect of number of reflow on T_g for high-T_g laminate……………………………………………………………………….66

Table 3.29: Comparison of T_g from each number of reflow treatment using student's t-test…...66

Table 3.30: Pairwise p-values for various number of reflow treatments on T_g for high-T_g laminates……………………………………………………………………….67

Table 4.1: Range of values examined………………………………………………………71

Table 4.2: Test vehicle 1 package specifications…………………………………………....73

Table 4.3: Test vehicle 2 package specifications…………………………………………....74

Table 4.4: PCR beta coefficients…………………………………………………………......91

Table 4.5: Example base configuration for Package-on-Package warpage………………...….107

Table 4.6: Effect of mold CTE1 on the Package-on-Package warpage………………………..108

Table 4.7: Usability of PCR model…………………………………………………………..109

CHAPTER 1

Introduction

1.1 Overview Electronic Packaging

Over the past few decades, technology has developed rapidly and is being used in day to day life for many applications. People rely more on devices like computers, cell phones, and so many other electronic devices for both personal and industry purposes and this has led to the boom in the industry. With such a reliance on electronic devices, the cost, manufacturing, and reliability of such devices are of great concern. The functionality of such devices has led to the creation of the integrated chips that are predominantly used in all these applications.

Electronic packaging is an art based on placing and interconnecting different levels of electronic systems. Packaging brings together the basics of mechanical engineering, physics and electronics towards the development of better functioning devices. It alters bare integrated circuits into useful products. This acts as a bridge between micron IC as well as provides electrical signal connections, power supply, environmental protection and a path heat dissipation. The process of electronic packaging involves the placement, creation and connection of integrated circuits on semiconductors. The most commonly used semiconductor is Silicon, as it abundantly present. The electronic packaging may be viewed at three levels: *chip, board* and *system*. The process of cutting the silicon wafer into smaller pieces called, as "chips" is the first step. This chip is housed in a carrier or chip container. The interconnections between this chip and carrier are made using gold wire bonds. Solder bumps are also created and used as means of interconnection

between such chips and carriers. This assembly of the chip and carrier is called as first level package. The second level package consists of one or more chip carriers connected to a Printed Circuit Board (PCB). These PCBs have conductive wire traces that are connecting different electrical components. The third level package consists of several PCBs that are connected to a motherboard or bus. The PCBs are allowed to communicate by using edge connectors between multiple PCBs. The hierarchy of electronic packaging can be seen in the Figure 1.1.

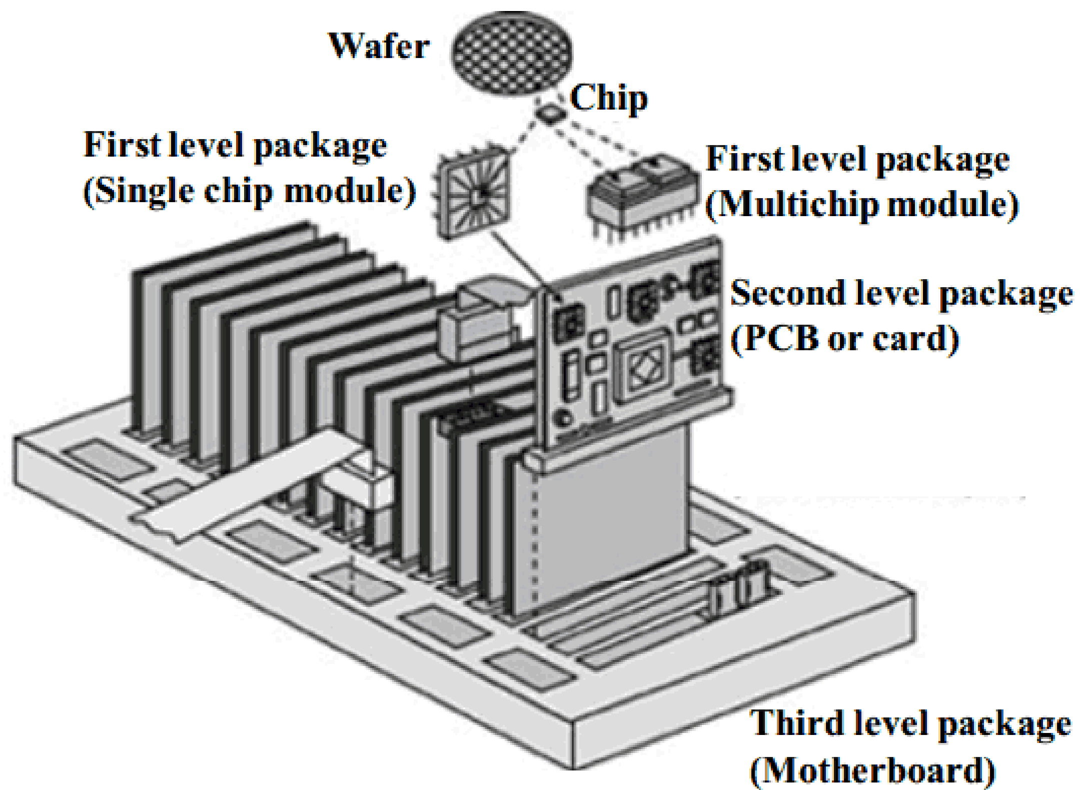

Figure 1.1: Electronic Packaging Hierarchy [Lau 1995 Page #2]

Gordon Moore, co-founder of Intel, famously stated in 1965 " The amount of transistors which can be inexpensively placed on an Integrated Circuit device doubles every 18 months". This statement has been widely accepted and become the trend driving the semiconductor industry [Moore et al,1998].

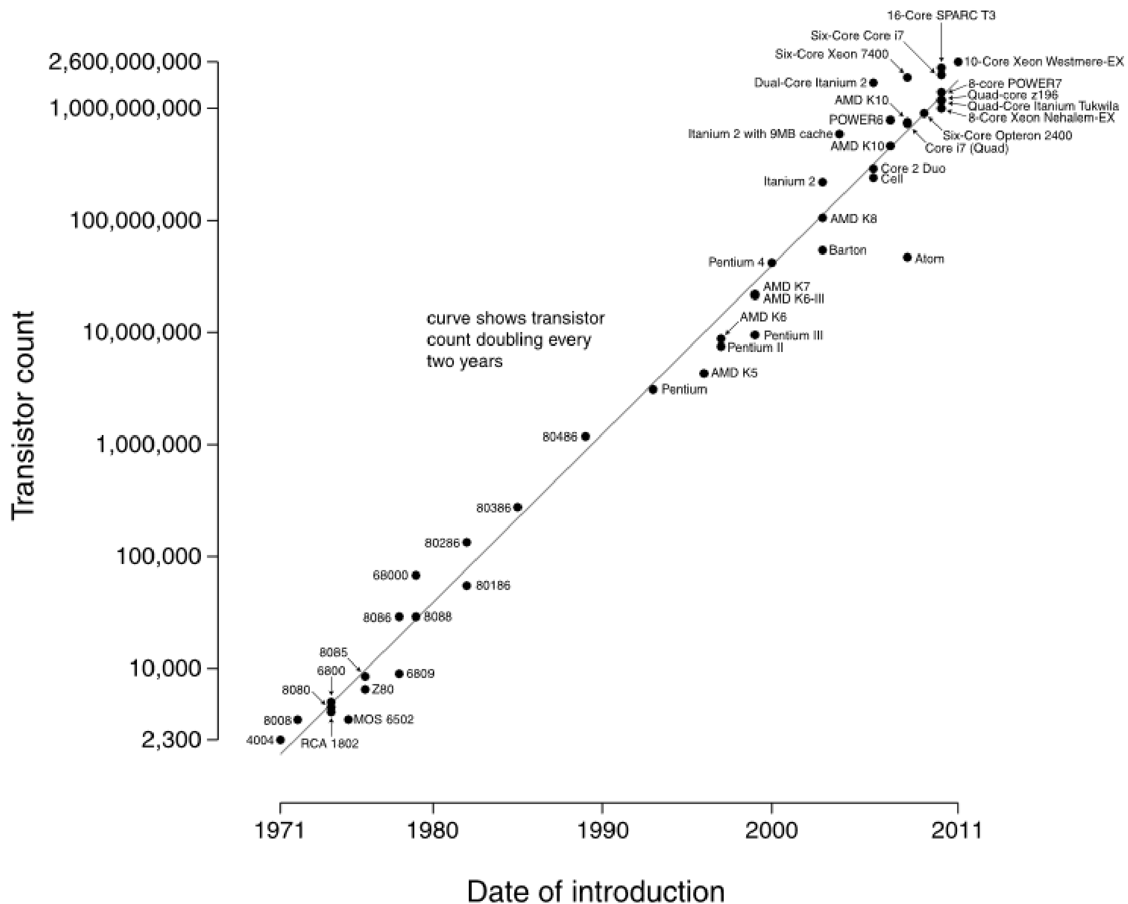

Figure 1.2: Moore's Law

Thus in smaller size more and more functions can be fabricated on a specific chip for each succeeding generation of semiconductor. This led to several challenges faced by the packaging industry. The small devices should be able to handle several numbers of external inputs and output connections, the reduction in areas can cause an increase in line resistance which may degrade the signal and there may an increase in the amount of heat dissipated. In order to deal with these issues, electronic industry has come up with surface mount technology. The following

Figure 1.3 shows the schematic depicting the trend of electronic packaging carriers over the years.

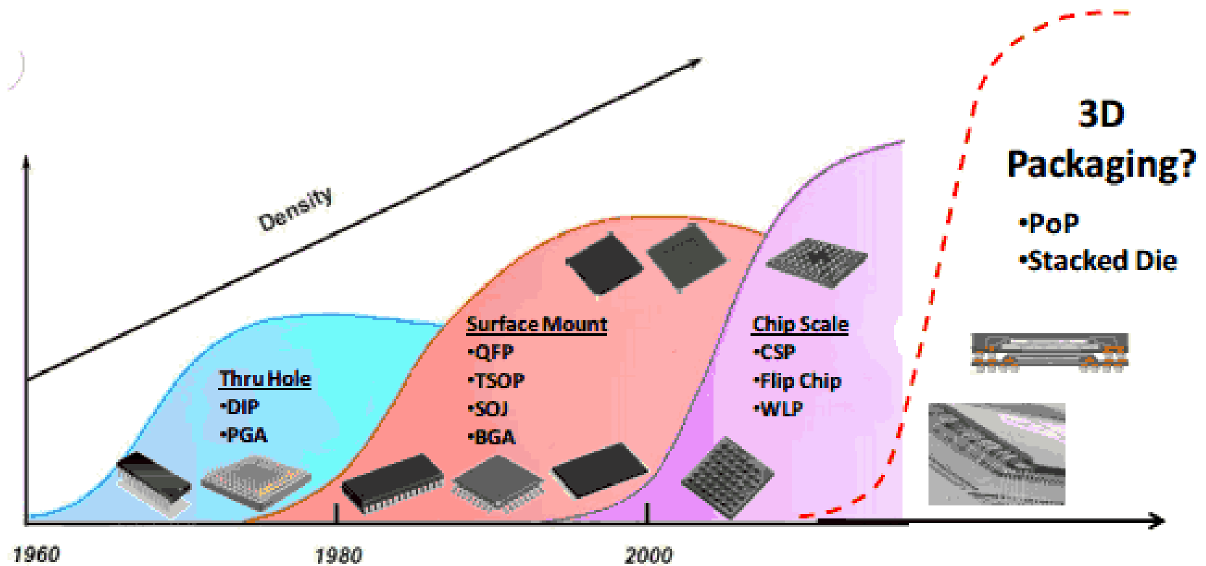

Figure 1.3: Electronic Packaging Industry: Trends [JISSO Japan Technology Roadmap, 2001 Edition]

Electronic packaging can be classified based on their mounting types such as (i) Surface Mount Components and (ii) Through Hole Components; or based on their packaging type as (i) Hermetically Packaged or (ii) Plastic Encapsulated Packages, the most accepted one being the former one. For the first three decades the semiconductor packaging technology was majorly based on only three major packaging technologies plat forms, through hole packages followed by Surface mount package and Wire bond packages.

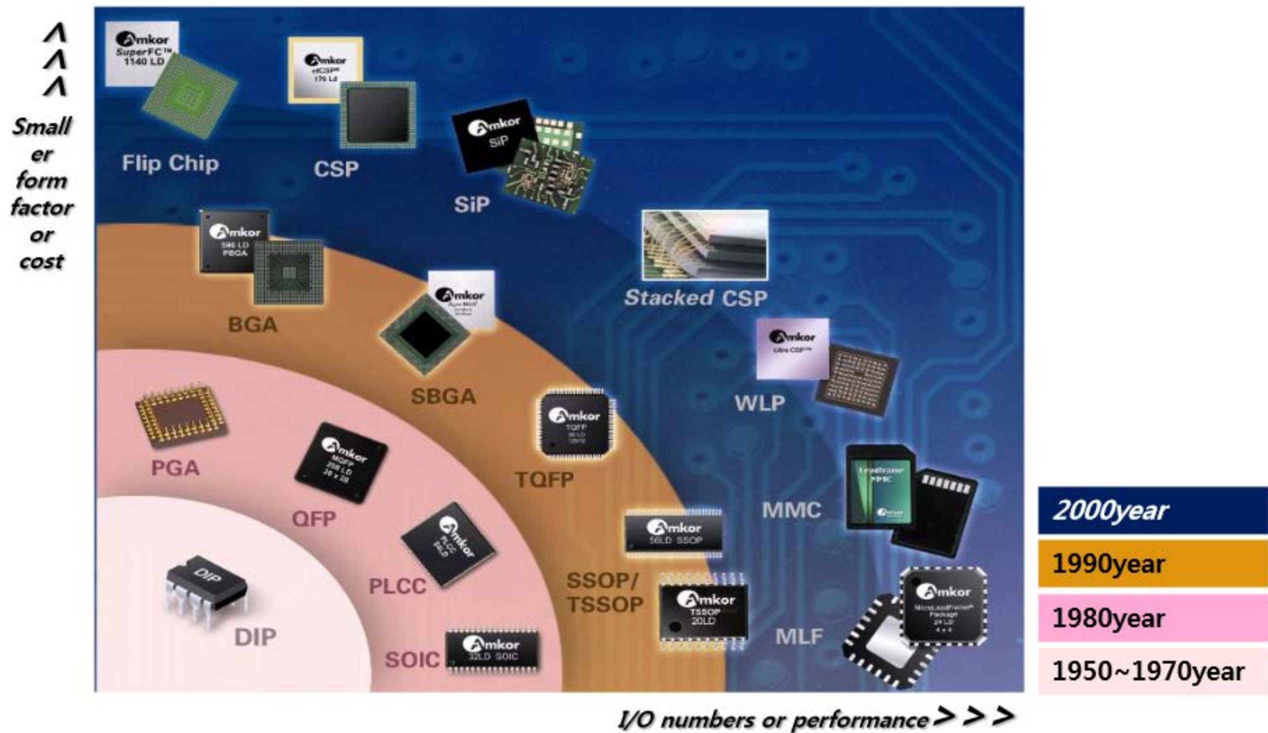

Figure 1.4: Package Trend [Courtesy Amkor]

It was in the 1990's only that SMT became the predominant packaging technology mostly due to smaller form factor and ease of board mounting advantages. Surface Mount Technology involves placing the components on the board using landing pads and solder attachments instead of hole interconnect. The advantage of using the technique over others is that the number of inputs and outputs can be increased as both sides of the board can be used. Thus the density of interconnects on the board will be higher. Some examples of Surface Mount Components are small outline package (SOP) and the quad flat package (QFP). These devices use gull wing interconnects as a means of interconnection. The final lead pitch could be achieved using gull wings interconnects. Recent demands for higher functionality and performance have resulted in newer packaging types like stacked-chip packages, 3D packages, and chip on board packages

(COB). This led to an increase in functionality and performance but has also resulted in concerns about the reliability.

Advances in packaging technology have added more functionality to the packages. 3D packaging technology is one such advancement with some future visionary functionality such as an autonomous electronic system housing multiple functionalities like signal processing, power management and nano storage devices. Over the years 3D packaging has evolved in three phases. The first phase was during the time when technology was developed to house multiple chips within the same package. 3D packaging succeeded owing to its ability to stack several memory devices in the same package, to support the demand of memory rich requirements and cellular phones and portable devices.

The shift from single die package to multiple die packages using the out of plane direction and its impact on miniaturization and integration are shown in Figure 1.5 shows the 3D packaging trend.

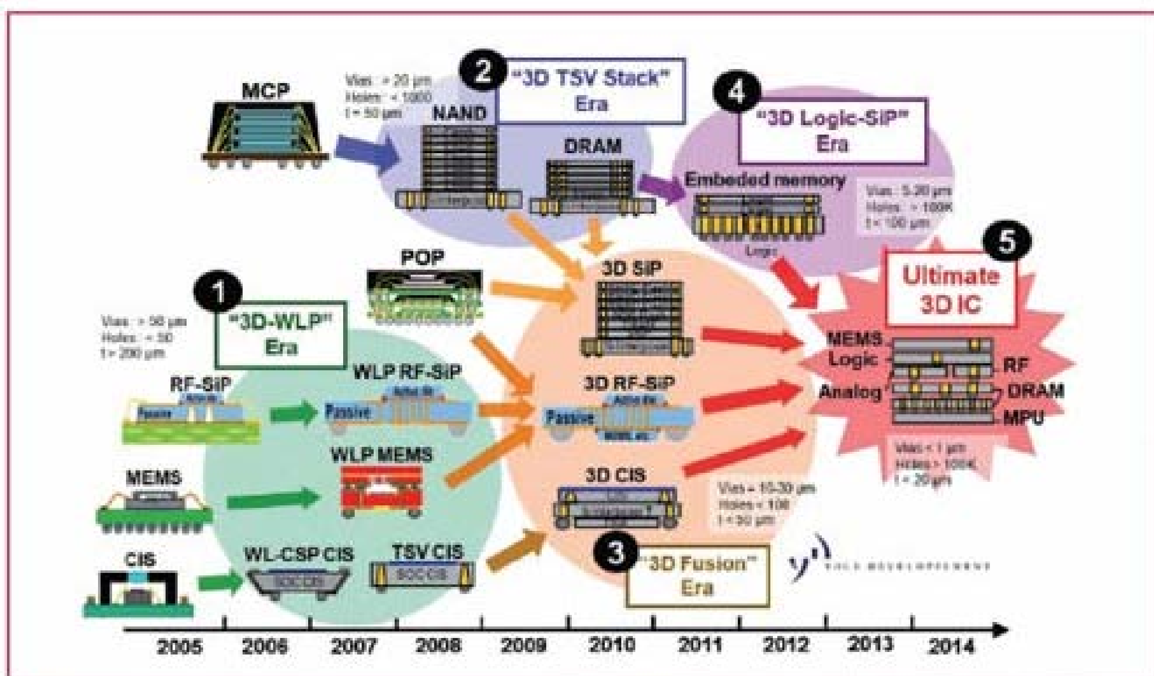

Figure 1.5: Roadmap for 3D Interconnects [Source Yole Development]

The second phase started with the introduction of package on package (PoP) technology. This technology catered the need of more efficient 3D packaging alternative by combining the logic and memory chips on the same package. Right now the packaging industry is in early stage of third phase through the development of chip stacking using through silicon vias (TSV).

1.2 Reliability Concerns

Reliability is defined as the probability that the component, assembly or system, under consideration, will survive the next period of interest. The current trend in electronic packaging is driven by market's requirement to minimal cost, increase circuit density and small real state. This demand led to miniaturization and increased functionality, the components are manufactured smaller and more complex. With the advent of these novel packaging technologies such as System-on-Chip (SoC), System-in-Package(SiP), Multi- Chip-Modules (MCM) and 3D packaging technologies such as PoP and Stacked-Die components, the complexity of packaging designs have increased exponentially. As the number of interconnect counts For increases, the pitch between them decreases and their susceptibility to failure increases. In the competitive market these days it is very important to manufacture devices of high quality and reliability. A careless design may cause the package to fail which may be dangerous for the entire device. It is very essential for the packages to possess high thermal and mechanical reliability under extreme conditions.

Electronic packages are often exposed to high loadings and different environments. The failures in electronic packages are mainly due to mechanical, thermal, electrical or manufacturing issues. The thermal failure is mostly due to mismatch in coefficients of thermal expansion (CTE). The

electronic packages are made up of different layers of materials like the molding compound, a laminate substrate, a silicon die, silicon adhesive and solder interconnects. The following FIG shows the cross section schematic showing the many layers of an electronic package. One of the common types of packages is Ball Grid Arrays (BGA). Thermal failures occur in these packages due to mismatch of CTE between the silicon die and Printed Circuit Board (PCB). The CTE of the die is much lower when compared to the PCB and this leads to the difference in the expansion rate. This difference will lead to thermally induced stresses occurring in the solder ball interconnect. This especially poses as a problem in electronic packages exposed to thermal cycling environments where there are changes in temperature. These stresses can cause fatigue and often failure in the electronic packages.

For surface mounted device one of the important issues is loss of co-planarity which leads to failure during manufacturing process. Printed circuit boards and electronic packages may appear to be flat, a small warpage often exist. Warpage may get induced in the components during thermal processing. If the warpage is large, it results in faulty solder joints during manufacturing process. Figure below shows a typical faulty joint after solder reflow due to warpage.

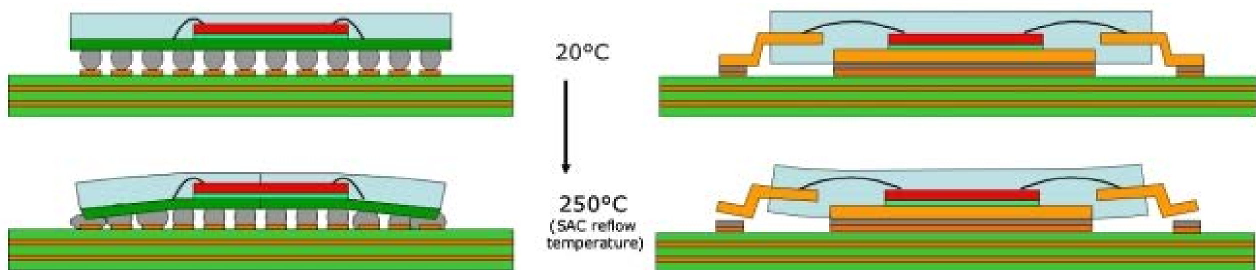

Figure 1.6: Schematic drawing of excessive warpage at reflow temperature resulting in shorts (left) or opens (right) after soldering [Courtesy Imec]

1.3 Effect of Lead Free on PCB Reliability

As the electronics industry is pushing towards lead-free solder assembly, it has led to many investigations into PCB materials and finishes. The major focus of the investigation is to discern the ability of the materials to withstand the high temperatures associated with lead-free soldering process. Printed circuit boards face major reliability threat due to exposure to high temperature during the soldering process for the assembly of components onto PCB. The temperature attained by PCB is higher than most of the other components in the assembly. When soldering with SnPb solders, the temperature can be between 230^0C to 245^0C and for lead free solder between 265^0C to 280^0C. The PCB assembly is also often exposed to multiple reflow cycles during assembly and multiple cycles can have additive effect on the material. The PCB material should be able to withstand these multiple exposures to high temperature reflow cycles.

FR-4 is the most commonly used material for fabrication of PCBs. It is a composite material composed of woven fiberglass cloth with an epoxy resin binder that is flame retardant. The disadvantage of this material lies in their inadequate capability to withstand high temperature during lead free soldering process. When exposed to such high temperature, the material properties of PCB changes especially if the temperature is very close to glass transition temperature (Tg) of PCB. The glass transition temperature (Tg) is an important normative dimension for the base material that determines the temperature at which the resin matrix converts from a glassy, brittle state condition into soft, elastic one. The glass transition temperature of the base material sets an upper boundary, at which the resin matrix decomposes and a subsequent delamination occurs. It is thus not the value of the maximum operational temperature, but rather that which the material can endure for only very short time. In past couple of years FR-4's has improved significantly and the improvement has occurred primarily

with one property-glass transition temperature (Tg). Therefore it is important to understand the behavior of printed circuit board in terms of variation in its glass transition temperature.

Apart from glass transition temperature, coefficient of thermal expansion (CTE) and decomposition temperature (Td) too play important part in improvement of printed circuit board capabilities. Improvement in glass transition temperature (Tg) and coefficient of thermal expansion (CTE) helps maintaining the integrity of the PCB interconnect structures while improvement in glass transition temperature (Tg) and decomposition temperature (Td) is necessary for the stability of the PCB resin. The material properties of PCB laminate are altered when exposed to high temperature associated with lead-free soldering thereby compromising the performance and reliability of the PCB and entire electronic assembly. It is therefore important to have knowledge of PCB material properties, their dependence on the material constituents along variations due to exposure to lead-free soldering.

1.4 Statistical Analysis

It is essential to know while planning an experiment that the results can be analyzed. Type of statistical analysis to be used is an integral part of planning the experiment. Researchers have used different statistical methods for the collection, organization, analysis, interpretation and presentation of experimental test data. It is particularly useful when dealing with noisy data. It provides a conclusion on the effect of changes in the values of predictors on response. Some well-known statistical tests and procedure are Analysis of variance (ANOVA), Student's *t*-test and Regression analysis. An experimental data usually consists of means or proportion affected of different groups. Means will differ because every individual sample is different where as proportion affected could differ by chance but means and proportion can also vary as a result of

treatment. The common goal of statistical analysis is to determine the probability that differences as great as or greater than those observed could be due to chance. Variation can be due to chance if this probability is high but if it is low then treatment effect can be the explanation. If the goal is to compare the mean of measured that then analysis of variance (ANOVA) or *t*-test are best suited.

The purpose of analysis of variance (ANOVA) is to test for significant differences between means. The total variability found within a data set is divided into two components namely systematic and random. Systematic factors have statistical influence on the given data set while random factors do not. For a set of means resulting from number of treatment groups the ANOVA will calculate the probability that the observed or greater differences among them could have occurred by chance sampling variation. For more than two means in comparison ANOVA does not tell which mean differs from which and is determined by extension of the ANOVA or by using post-hoc comparisons.

With certain assumptions ANOVA and Student's *t*-test are often the best way of analyzing measured data. When comparing only two treatment groups the ANOVA and *t*-test are mathematically identical. Student's *t*-test is used to determine how significantly two data sets are different from each other while ANOVA can incorporate more than two groups and more complex designs. Effect of variation in peak temperature, time above liquidus and number of reflow on glass transition temperature of PCB was studied. The changes in glass transition temperature were measured and the means were analyzed using ANOVA, *t*-test and other statistical procedure to determine their statistical significance along with corresponding standard error and confidence interval.

There are experiments, which are designed to estimate the response in one dependent variable to changes in predictor (independent) variable. Regression analysis is more appropriate in such cases for investigation of relationships between variables. The goal in such investigation is to ascertain the casual effect of one variable on another— the effect of material and process parameter on Warpage. To explore such issues, data is collected on the underlying variables of interest and regression technique is applied to estimate the quantitative effect of the predictor variables on the response variable. Regression model is an effective tool not only to understand and explain relationship between variables but also to predict the actual outcome based on historical behavior.

One of the simplest forms of regression is multiple linear regression, which defines the relationship between predictor and response variable by fitting a linear equation to observed data. A single response measurement is related to a single predictor for each observation. For a population of p explanatory variables $x_1, x_2, \ldots, x_p$ the regression line is defined to be $\mu_y = \beta_0 + \beta_1 x_1 + \beta_2 x_2 + \ldots\ldots + \beta_p x_p$. This equation describes the changes in mean response μ_y with respect to predictor variables. The observed values for y vary about their means μ_y and are assumed to have same standard deviation σ. The fitted values $b_0, b_1, \ldots\ldots, b_p$ estimate the parameters $\beta_0, \beta_1, \ldots\ldots, \beta_p$ of the population regression line.

Multiple regression model also includes a term to estimate the effect of variation of observed values of y about their means μ_y. The model is expressed as DATA = FIT + RESIDUAL, where FIT corresponds to expression $\beta_0 + \beta_1 x_1 + \beta_2 x_2 + \ldots\ldots + \beta_p x_p$ and Residual represents the variation of observed values of y about their means μ_y with mean 0 and variance σ. In mathematical model this deviation is denoted by ε.

The most widely used method of solving a regression problem is using correlation matrix (X'X) and is given by formula $\beta = (X'X)^{-1} X'Y$ where 'Y' is the response matrix and 'X' is called predictor matrix. The limitation of this method is that it holds good if and only if the determinant of the X'X matrix is approximately one. Thus if the predictor variables (column of X matrix) are related to each other, the determinant of X'X matrix tends to move towards zero. In many engineering applications the factors that significantly contribute to the response can be derived functions of each other. This results in numerical snag and regular solution to multiple linear regression $\beta = (X'X)^{-1} X'Y$ would fail to explain the actual significance of the variable.

There have been a lot of techniques developed over the years to circumvent this problem. Principal component based regression analysis is one of the predominant methods for combating multicollinearity and results in estimation and prediction better than ordinary least squares when used successfully. In this method the original predictor variables are transformed into new set of uncorrelated variables called principal components of correlation matrix. This transformation nulls the effect of correlation.

This method was used to develop the statistical model for prediction of PoP Warpage based on material properties of package and process parameters. The developed model was validated against the experimental as well as finite element results.

1.5 Finite Element Analysis

Finite Element Method is a numerical method for solving a differential or integral equation. It has been applied to a number of physical problems related to engineering and mathematical physics. It is very useful for problems with complicated geometries, loadings and material properties where analytical solutions cannot be obtained. It can be used to understand the

dynamic phenomenon of electronic systems and is an effective tool to verify the data obtained from experiment. In todays competitive market where time to launch, rectify or improve a product is highly critical, exhaustive testing of all the design iterations of a product has become unfeasible. Owing to the complex nature of package design and problems associated with their failure, analytical methods have established their superiority over experimental methods.

With the development of new packaging materials, designs and assembly process finite element method can be used to approximate the actual solution to a problem. Finite element analysis involves approximating functions determined in terms of nodal values of a physical field which is sought. A continuous physical problem is transformed into a discretized finite element problem with unknown nodal values. For linear problem a system of linear algebraic equations should be solved. Values inside finite elements can be recovered using nodal values. The FE method based simulations make it easier to account for scale differences between the dimensions of the individual layers of an electronic assembly, such as solder interconnects, copper pad and chip interconnects [Dally, 2008]. Finite element solution is an approximation of the actual solution which can be improved by using appropriate element types and increased mesh density. Piece-wise approximation of physical fields on finite elements provides good precession even with simple approximating functions. Locality of approximation leads to sparse equations for discretized problem. This helps to solve problems with very large number of nodal unknowns. In this study, finite element method is used to determine warpage response of package for variation in material and process parameter.

1.6 Digital Image Correlation (DIC)

Digital Image correlation is a non-contacting optical method of measuring surface displacements of an object subjected to driving force. It uses speckle pattern to track the movement of a geometric point. This method obtains the incremental displacement and strain field on surface of a planar specimen by comparing a pair of digital images taken before and after deformation. Figure 1.7 below shows the schematic of undeformed and deformed image of speckle coated sample.

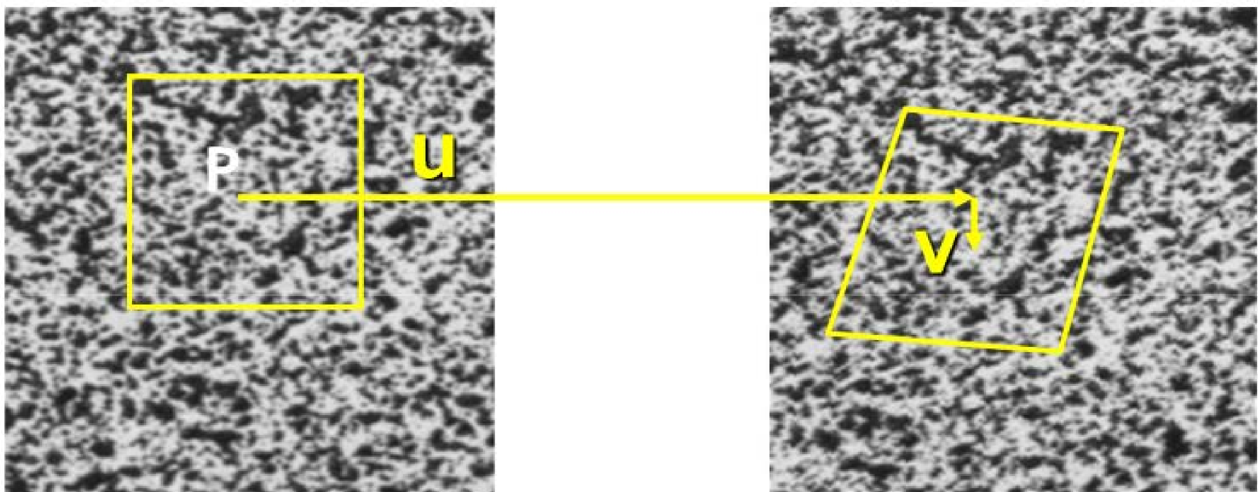

Figure 1.7: Tracking Movement of a Point

Gray value patterns in small subsets of the deformed and undeformed images are determined. As the interested surface of specimen is coated with white paint and with black speckle coats, the tracking of pixels are much easier and makes distinct pixel recognition possible. One major advantage of this technique is that sample preparation is simple and quick. Transient deformation data is recorded by high speed cameras, which is then processed to evaluate full field strain. Figure 1.8 describes the strain evaluation process.

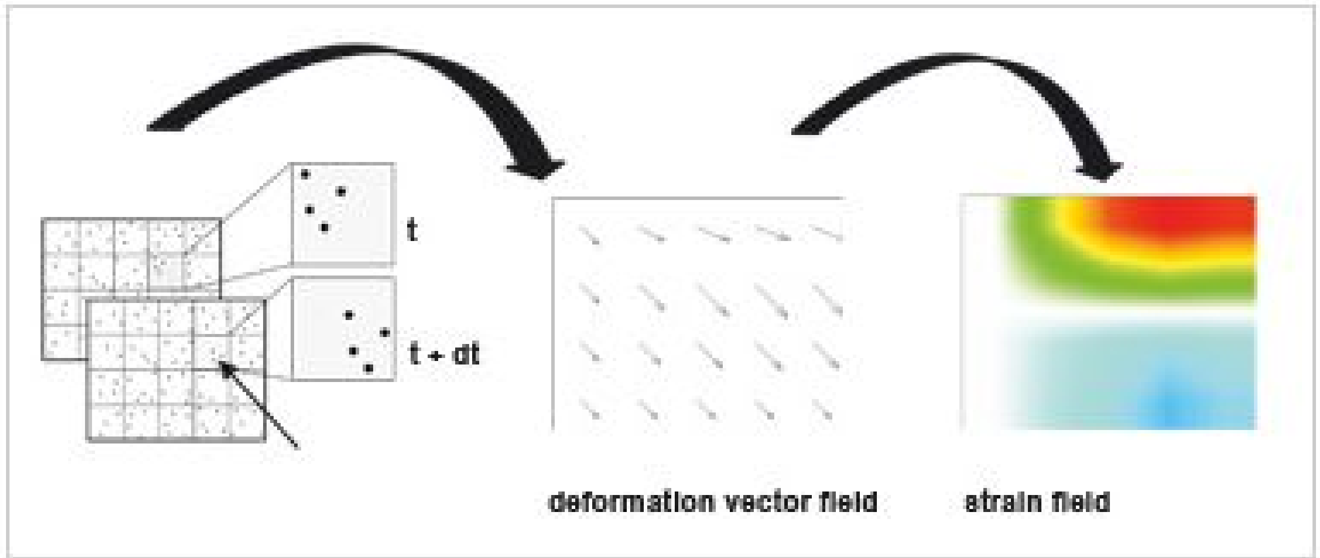

Figure 1.8: Strain Evaluation [Courtesy lavision]

Two dimensional deformations requires only one camera to capture the event where as for three dimensional deformations requires the use of two cameras. The full field data captured from DIC analysis is then used to determine localized strain and deformation contours. Figure 1.8 shows the schematic layout of process to capture 3D deformation.

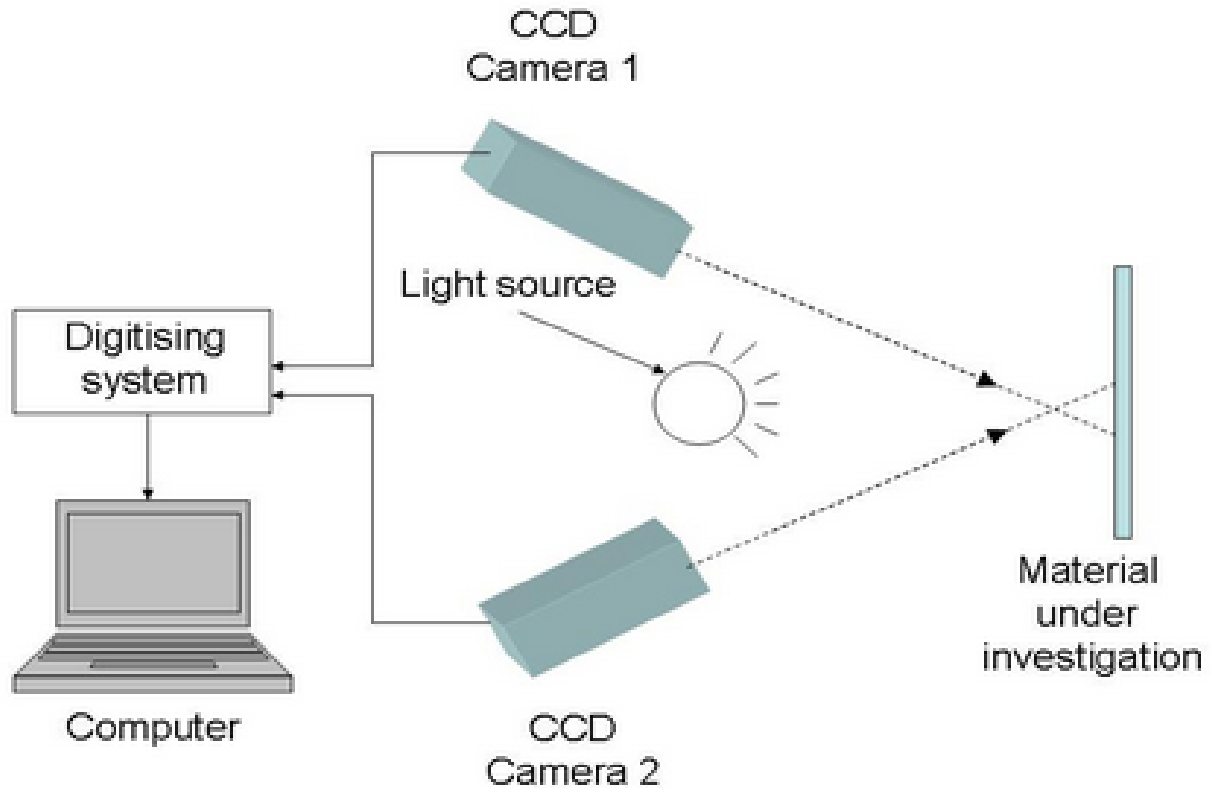

Figure 1.9: Set-up for 3D digital image correlation [J. M. Dulieu-Barton]

Previously researchers have used digital image correlation with great effect in the field of electronic packaging science. Digital image correlation was used by [Lall, 2009, 2010] to study crack propagation in solder interconnects in drop/shock, material characterization at high strain rates [Tiwari 2005, Lall 2010], stresses in BGA package solder interconnects under thermal loading [Zhou 2001; Zhang 2004; Lall 2009, 2010].

1.7 Thesis Layout

This thesis showcases the research done to study the behavior of printed circuit board and packages when exposed to thermal loading. The glass transition temperature of printed circuit board is an important design variable for defining assembly, testing and operating temperature range. This work aims to study the interaction between manufacturing process variables that

impact the changes in glass transition temperature (Tg). The focus of this work was to perform statistical analysis of the test data accumulated from the tests that were conducted at the CAVE[3] to check for their statistical significance and to infer meaningful conclusion from the test result. This study also investigates the effect of material and process parameters along with geometric and temperature definition of package on its warpage response. Finite element models was developed to simulate warpage response and to augment the experimental data matrix. The data accumulated was based on various package types, material and dimensional configurations. The accumulated data was used to run regression analysis and develop a statistical model to predict the Warpage of PoP package. The model was validated with FE simulations and experimental result.

Chapter 2 presents the literature survey on the current state of art for the various techniques used in this study. The section summarizes the available literature related to this research topic. The first portion of the reviewed literature in this section relates to various issues concerning to glass transition temperature of printed circuit board when exposed to high temperatures. Literature pertaining to various measurement technique of glass transition temperature is outlined. Various statistical analyses that have been used in packaging industry to develop prediction model is also documented. The literature survey points at what analysis is relevant with which type of data. This section also outlines the current state of art for package warpage measurement and control. Technique used in this study such as digital image correlation (DIC) and the finite element method (FEM), are outlined.

Chapter 3 presents the study carried out on commercially available printed circuit boards to investigate the variation in their glass transition temperature as a function of reflow process parameter. The concentration of the study was to see the effect of peak temperature, time above

liquidus and multiple reflows on glass transition temperature. Two types of printed circuit board, classified as high Tg and mid Tg were used for the study. The chapter describes in detail the test carried out to measure the glass transition temperature. Also, the measured data were statistically analyzed to determine the statistical significance of the measured changes.

The following chapter 4 presents a study investigating the warpage of package on package (PoP) components. Digital image correlation (DIC) is used to measure the warpage of package in-situ during reflow. The study shows the effects of various process conditions and material selections on warpage. The primary focus of study was to measure warpge at reflow temperatures. Finite element models were developed to determine the effects of material variation and package architecture on warpage. Sensitivity analysis is also presented to show the influence of each parameter on package warpage. Lastly, all the data collected from experiment and augmented by FE results were used to perform regression analysis and develop statistical model for prediction of warpage. The chapter also shows to use the inverse relation for material selection guideline. Chapter 5 is the summary of the studies performed in this thesis and the scope of possible future work.

CHAPTER 2

Literature Review

Computer, telecommunications, automotive and consumer electronic products are undergoing dramatic changes. The new generation electronic products are characterized by very low cost, large volumes, portability, high performance and diverse functionalities characterize electronic products. As the significance of electronics has increased, the importance of their reliability is a major concern. This has caused the researchers in packaging industry to primarily focus on reliability issues associated with electronics. This chapter discusses the background of research done on electronic packaging reliability with special focus on the behavior of printed circuit board properties during exposure to high temperature; Warpage dependence of package on material and process parameters and statistical tools used to analyze the measured data for meaningful inference and to develop statistical prediction model.

2.1 Glass Transition Temperature of Printed Circuit Board (PCB)

Printed circuit boards are often exposed to high temperature both during assembly and in fielded products and the effect of temperature exposure has a known influence on glass transition temperature (Tg) of printed circuit board laminates. FR-4, which is a composite of epoxy resin with woven fiberglass reinforcement, is most commonly used material for manufacturing printed circuit boards. Glass transition temperature of PCB is an important design variable often quantified for defining of operating temperature window, accelerated test range and assembly process temperature. It is the temperature at which the resin system changes from a rigid or hard

material to a soft rubber like material [ISO 1999]. Several properties change as the glass transition temperature is exceeded, including the rate at which a material expands with temperature. Temperature above Tg results in higher moisture permeability, higher CTE and reduction in modulus. Therefore verification of the influence of thermal treatment on the glass transition temperature of epoxy laminates is an important requirement, which must be considered during design of electrical assembly. [Polansky, 2009] describes the influence of accelerated thermal treatment of thermosetting epoxy laminate on its glass transition temperature. The fact that glass transition temperature varies rapidly in reaction thermal stress was proven.

The transition to lead-free components from previously used leaded components has resulted in an increase of the peak reflow temperature by 30^0C-40^0C to 260^0C during reflow. SnAgCu commonly called as SAC alloys are the mostly widely used substitute for SnPb and has higher melting point. Though peak temperatures are not maintained for extended periods of time, multiple reflow cycles are not uncommon. So printed circuit board must be able to withstand these repeated exposures. The knowledge of PCB laminate material properties and their dependence on the material constituents, combined with their possible variations due to lead free soldering temperature exposure, is an essential input in the laminate selection process. A range of commercially available FR-4 PCB laminates material classified on the basis of glass transition temperature (high, mid and low) were studied and was shown that glass transition temperature of a laminate system is primarily a function of type of epoxy and its percentage composition [Sanpala, 2009] and the exposure tend to lower the glass transition temperature.

Thermal stability, glass transition temperature and dimensional stability of epoxy resins can be improved by adding inorganic fillers to epoxy to form organic-inorganic composite. [Jin, 2012] showed that the glass transition temperature of the composite was 10^0C higher than that of neat

epoxy resin. There is variety of thermal techniques to measure glass transition temperature and they vary as the optimized conditions differ between different techniques. The most predominant techniques used are differential scanning calorimetry (DSC), which measures the change in specific heat capacity, thermomechanical analysis (TMA), which measures the change in coefficient of thermal expansion, and dynamic mechanical analysis (DMA), which measures the change in viscoelastic properties. [Chew, 1996] showed that a difference of 40^0C was observed between the measured values of Tg using DSC and DMA. TMA measurements were about 15^0C higher than DSC measurements. This study also showed that the change in properties at glass transition temperature is most significant as detected by DMA and least significant as detected by DSC.

2.2 Package Warpage

For hand-held portable electronics domain, miniaturization, lightening, multi-functions and higher reliability with increased performance is the need in present time. The ever increasing demand for small form factors, better functionality and low cost assembly for wireless and embedded electronics system has pushed more and more component manufactures to adopt package on package (PoP) as a solution of highly integrated 3D packaging system to reduce package size and solve real state problem. In this system laminate substrate packages are stacked in vertical direction and interconnecting them with solder balls. In a PoP architecture the bottom package is generally a logic device while the top package is memory sub-system. Stacking the devices allows for vertical expansion while minimizing overall footprint.

The benefits of PoP are evident and they include:

- Less board space
- Better performance (Shorter communication paths between the micro and memory)
- Lower junction temperatures as compared to stacked die
- Greater control over the supply chain (opportunity to upgrade memory)
- Easier to debug and perform F/A

One of the greatest challenges in assembling PoP is managing out-of-plane Warpage. Warpage of the electronic package is a critical issue during reflow process in Surface Mount Technology (SMT) line while forming interconnection between top and bottom package through solder balls joints. Warpage is induced during thermal loading due to coefficient of thermal expansion (CTE) mismatch and stiffness mismatch between epoxy molding compound (EMC), substrate and silicon chip. Large warpage can cause loss of co-planarity between the top and bottom packages resulting in misshaped or open solder joints and substrate delamination leading to the electrical connection failure of the assembly. Thus it is important to have Warpage control between top and bottom package for high SMT yields of package stacking for PoP.

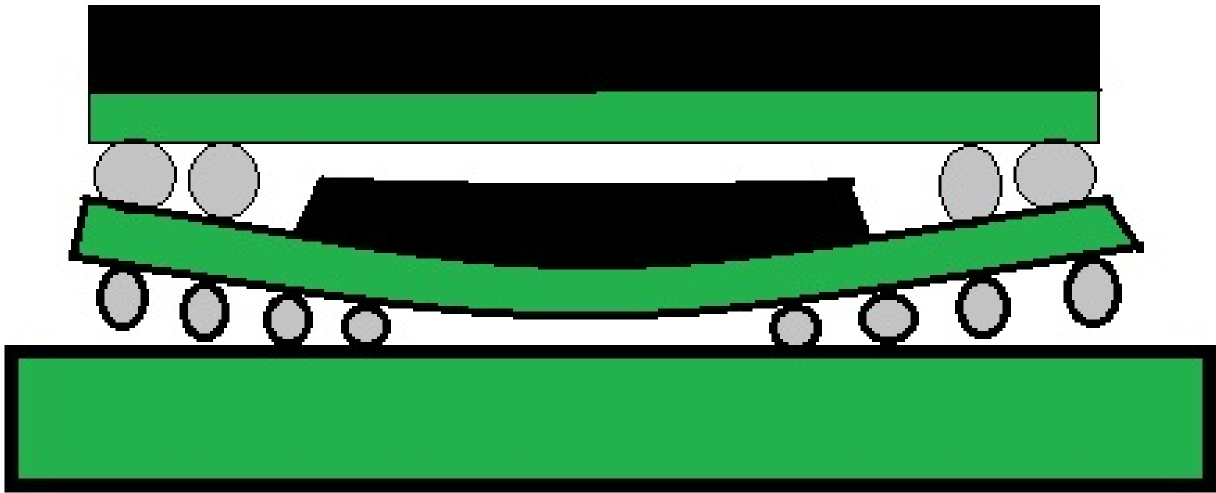

Figure 2.1: Open circuit Induced by Warpage in SMT Process I

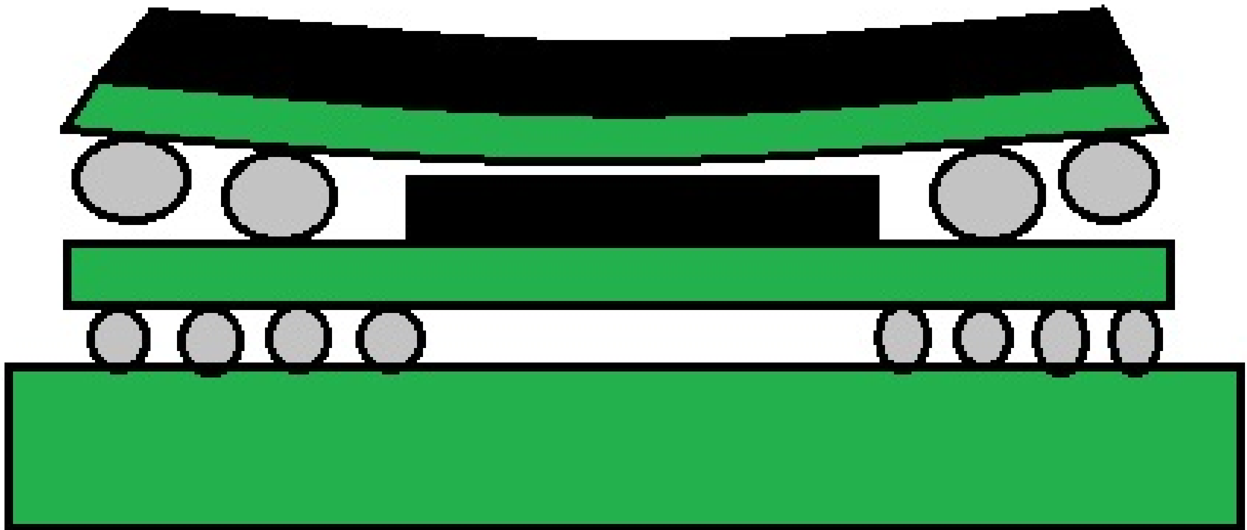

Figure 2.2: Open circuit Induced by Warpage in SMT Process II

The JEDEC standard JESD22-B112A defines Warpage according to the convex or concave shape of the warped package. Based on the shape of warpage, the standard assigns positive or negative sign convention to them. Warpage is measured from corner to corner along the diagonal

of the electronic package and convex shape warpage has positive value while concave shape Warpage has negative value. Figure 2-2 below shows the schematic representation of sign convention specified in the test standards. There are several methods to measure the Warpage which include digital image correlation (DIC), shadow moiré, laser reflection and projection moiré [JEDEC 2011].

[Blackshear 2010] showed an effective and accurate way of using digital image correlation (DIC) to measure warpage in electronic package. [Tzeng 2007, Sun 2008] used finite element method to predict warpage response for variation in different material properties such as die attaches, substrates and molding compound. PoP Warpage is a main reliability issue in surface mount assembly; [Zhang 2012] compared the different warpage effects induced by different SMT process. Since 3D packaging requires stacking in vertical direction, to maintain the mechanical compliance between the packages during stacking, the industry is continuously working to reduce the package height. One way of achieving this is by reducing mold cap thickness and distance between the top silicon die to the mold cap. But the major challenge in achieving this to control the Warpage while reducing the thickness. [Yim 2010, 2011] investigated the effects of compression mold process and material properties on thin PoP package Warpage during reflow. Previously researchers have shown that material properties are important selection criteria for warpage control. [Amagai 2010] studied the effects of the injection mold cure time (IMC) and post mold cure time (PMC) on warpage using visco-elastic finite element models. The multiple layers of the electronic package including the mold, substrate, die and die attach all play a vital role in the effect of Warpage. [Carson 2007] examined the effects of the epoxy molding compound, die attach, die thickness, and mold cap thickness on warpage.

2.3 Statistical Prediction Method

Researchers to analyze the experimental test data have long used statistical methods. Regression analysis is one of the most commonly used statistical method and has been widely used to correlate the reliability of a package with its geometric attributes, material properties and operating condition. Multiple Linear regression (MLR) based polynomial model was developed to correlate fatigue life of ceramic package with its design parameters [Perkins 2004]. There were five predictor variables, all design parameters, namely substrate size, substrate thickness, board thickness, solder ball pitch and CTE mismatch between substrate and board. Running finite element simulation for each data point to extract fatigue life populated the data matrix. Based on these data a regression model was developed.

[Muncy 2004] conducted thermal reliability test including air-to-air thermal cycling (AATC) and liquid-to-liquid thermal shock (LLTS) on various configurations of flip-chip on board packages. Multiple linear regression and analysis of variance was used to analyze the data for determining the parameters having influence on the reliability of the components in accelerated life testing. The parameters studied included, substrate metallization and mask opening area versus the UBM area of the flip chip bump, die size, perimeter or area array pattern, underfill material, location of die on the test board, frequency of cycling, number of I/O and percent area voiding. Multiple regression modeling and regression with life data modeling methodologies were used for obtaining the parameters of regression.

[Iyer 2005] used regression and back propagation neural networks based models to correlate the reliability of flip-chip package to properties of underfill and flux. Ninety-five different underfill flux combinations were tried and data from accelerated life testing of flip chip package was used

to develop model. A test data set was used to validate both regression and neural network model and was found that regression model was outperformed by neural networks model.

Data from published literature and accelerated test reliability based on the harsh environment testing of BGA packages by the researchers at NSF Center for Advanced Vehicle and Extreme Environment Electronics (CAVE[3]) was used to develop multivariate regression based models for life prediction of BGA packages [Singh 2006]. The predictor variable matrix consisted of die, die to body ratio, ball count, ball diameter, solder mask definition, printed circuit board surface finish and thickness, encapsulant mold compound filler content and deltaT. Regression analysis and analysis of variance was used to build linear, modified linear and non-linear models. The developed models were validated against experimental data.

[Stoyanov 2002] used a design of experiments and response surface modeling methodology for building a quadratic equation that related underfill modulus, underfill CTE, standoff height and substrate thickness with number of cycles to failure for flip chip package. Residual analysis, analysis of variance and statistical efficiency measure were used for validating the model.

Often for an electronic package the variables of interest are dependent on each other despite the fact that they contribute significantly to the final outcome being monitored. These inter dependency of input variables in a regression analysis gives rise to problem of multi-colinearity. This results in large variance and co-variance, high standard errors, fluctuation in magnitude of the regression coefficients for small changes in predictor variables and wider confidence intervals for regression coefficients. In some cases, the regression coefficients can have wrong sign or many predictors are not statistically significant even when the overall F-test is highly significant. Therefore it becomes very important to determine the possibility of linear dependency of predictor variable before building a regression model.

The most common way of solving a regression problem is using least square method. The disadvantage of this method lies in the requirement that βcap be an unbiased estimate of β. Least squares give unbiased estimates with minimum variance of all linear unbiased estimates but there is no upper limit bound on the variance of the estimates and presence of collinear variables may produce large variance. Thus the advantage of un-biasedness achieved using ordinary least square is lost due to large variance due to multi-colinearity.

One solution to multi-colinearity issues and obtain stable and meaningful estimates of regression coefficients is to use Principal component model [Fritts 1971]. In principal component analysis the set of X predictor variables are linearly transformed into new set of orthogonal Z predictor variables. These newly transformed variables are uncorrelated with each other and together account for much of variation in predictor variables. The principal component transformation is thus a rotation from the original x coordinate to the system defined by the principal axes of this ellipsoid [Massay 1965].

2.4 Digital Image Correlation

In last five years digital image correlation (DIC) has emerged as the leading method for strain measurement in complex electronic assemblies where it is not feasible to place deformation measuring devices such as strain gages on them. Additionally the immense advances in computer vision and processing power have made deformation measurements down to nanometer level easily possible. Conventional deformation measuring techniques require optimal placement of sensors such as strain gage on the structure, which is critical to collect true data. Also these techniques can only evaluate localized values. In present time where a single test assembly is

populated with multiple components, it is highly rewarding to have an estimate of full field deformation, which can be further used for evaluation of individual component response.

The digital image correlation method resolves the displacement field on the surface of a planar specimen by correlating sub images on a pair of images, one before deformation and the other after deformation. That is it tracks the movement of geometric point on specimen before and after loading capturing full field displacement and strain measurements during a transient dynamic event. This full field non-contact measurement technique provides the means that data can be captured in critical areas without distortion of desired test conditions. As it is a non-contact type technique the specimen preparation is very quick and easy. Test specimen is speckle coated which provide the means to distinguish the geometric points on the surface of interest. Earlier researcher has shown the dependence of accuracy of the method on the size, consistency and density of the speckle pattern [Zhou 2001, Amodio 2003, Srinivasan 2005].

The DIC technique has been previously used in industry to measure deformation and strain in sheet metal forming analysis, automotive crash testing, rail vehicle safety [Kirpatrick 2001], air-plane safety [Marzougui 1999], modal analysis of blades and disks dynamic fracture phenomenon and package hermiticity (MIL-STD-883) tests. High speed cameras in high speed photography measure impact speed, force, deformation due to shock and thermal loading. In plane deformation of geo-materials can also be quantitatively evaluated [Watanabe 2005].

[Lall 2007c, 2008b-d, 2009, Miller 2007, Park 2007a,b, 2008] shows the usage of DIC in electronic packaging field to measure full field deformation and deformation gradients in electronics. Previously, the DIC based measurement technique has been demonstrated for evaluation of stresses in solder interconnects of BGA packages under thermal loading conditions [Zhou 2001, Yogel 2001, Zhang 2004, Zhang 2005, Sun 2006], to calculate stresses and strain in

flip-chip dies under thermal loading [kehoe 2006], for material characterization [Park 2007] and to study deformations in printed circuit assemblies for mobile devices [Lall 2007, Miller 2007, Park 2007]. DIC has been used for evaluating elastic modulus of underfill material at elevated temperatures during four-point bending tests [Park 2007a, Shi 2007] DIC method has also been applied to SEM images to study the stresses released at the component surface before and after milling [Vogel 2007]. [Lall 2007, 2008] demonstrates that DIC technique is useful for transient strain measurements in electronic assemblies, in the presence of rigid body motion.

2.5 Finite Element Modeling

The Finite Element modeling is a very versatile, accurate tool used to simulate problem of complex nature. It has been widely used in packaging field for reliability prediction of solder interconnects in different environment such as drop and shock, vibration, thermal cycling. In second level interconnects, owing to their very small dimension, measurement of strain or stress is very complex. In such situations finite element analysis provides insight into the stress state and possible failure mechanism. The results obtained can be correlated with experimental results to check the accuracy of model.

Earlier researchers have used several modeling methods to simulate transient dynamic events. [Lall 2004,2005] used smeared property model, [Lall 2006, 2007, 2008] employed Timoshenko beam models with conventional and continuum shell, global-local sub-models [Tee 2003, Wong 2003, Zhu 2003, 2004] and studying warpage of package [Lin 2008; Verugd 2008; Che 2011].

Flexing and bending of the PCB is one of the major driver in failure of second level interconnects. Researchers have used finite element method to measure the warpage response of package when exposed to thermal loading [Feng 2008, Yim 2010]. Chip scale packages (CSP) have also been evaluated using finite element analysis to show that the critical location during testing is the corner copper wire [Wang 2004]. Since material properties have known effect on the warpage, simulations have been run to investigate their effect.

CHAPTER 3

Effect of Reflow Process on Glass Transition Temperature of Printed Circuit Board Laminates

3.1 Introduction

Glass transition temperature of PCB laminates is a key design variable often quantified for definition of operating temperature window, accelerated test range and assembly process temperatures. Glass transition temperature of typical PCB materials used in the electronics industry varies from 115°C to about 260°C. The glass transition temperature (Tg) of a resin system is typically defined as the temperature at which an amorphous material transforms from a hard, brittle, glassy-state to a molten, rubbery state [ISO 1999]. PCB laminates are often exposed to high temperatures above their glass transition temperature during reflow process. The transition to lead-free components from the previously used leaded components has resulted in an increase of the peak reflow temperature by 30°C-40°C to 260°C during reflow. Many alternate solder alloys have been developed as a substitute for SnPb but SnAgCu commonly known as SAC alloys are the most widely used. SAC alloys have higher melting point as compared to SnPb alloys. The melting point of SAC alloy is around 217°C as compared to 183°C of SnPb alloy. For proper wetting and solder joint formation the lead-free assemblies are reflowed at temperatures in excess of 240°C-260°C. Though peak temperatures are not maintained for extended periods of time, multiple reflow cycles are not uncommon. So printed circuit boards must be able to withstand these repeated exposures.

Exposure to high temperature above the Tg changes the material properties of the laminate and product reliability including, the coefficient of thermal expansion, and the elastic modulus changing the product reliability. Thus it is important to have the knowledge of material properties of circuit board and their dependence and variations due to lead free reflow process exposures to make appropriate selection of printed circuit board laminates and process variable for particular application. Previous researchers have observed the effect of thermal exposure associated with lead-free soldering on reduction of Tg of low-laminate Tg laminates [Sood 2009], and effect of thermal treatment on the increase in glass transition temperature of PCB laminates [Polansky 2009]. Quantification of the effect of various process variables including time above liquidous, peak temperature, and number of reflows is new. Effect of multiple reflow passes on Tg after reflow has been also been studied.

3.2 Test Vehicle

Commercially available FR-4 PCB laminates were used in this study. The PCB used for the study are broadly categorized on the basis of the glass transition temperatures as high Tg (Tg >145°C), mid Tg (125°C < Tg < 145°C) laminates. For the measurement purpose samples of size 6 mm x 6 mm was cut from each laminate. All laminates used were 1.5 mm thick. Identical area of the printed circuit board laminate was used for all measurements. Glass transition temperature of the laminates was measured before and after 2x-6x exposures to lead-free reflow cycle. Various reflow profiles were created by 3-level parameter variations for each parameter including peak temperature, time above liquidus, and number of reflows. Peak temperatures studied include 225°C, 255°C and 290°C. Time above liquidus values studied include, 30 sec, 90 sec and 150 sec. In each case the results were compared to a reference profile with a peak temperature of 255°C and a time above liquidus of 90 sec. The number of reflows was limited to 2x for the reference profile corresponding to double sided assemblies which are exposed to 2x reflow. Figure 3.1 below shows one set of the reflow profile used. Profile-3 (highlighted in red) is the reference profile. Profile-1 and profile -2 are with variation in time above liquidus, 30 second and 150 seconds respectively.

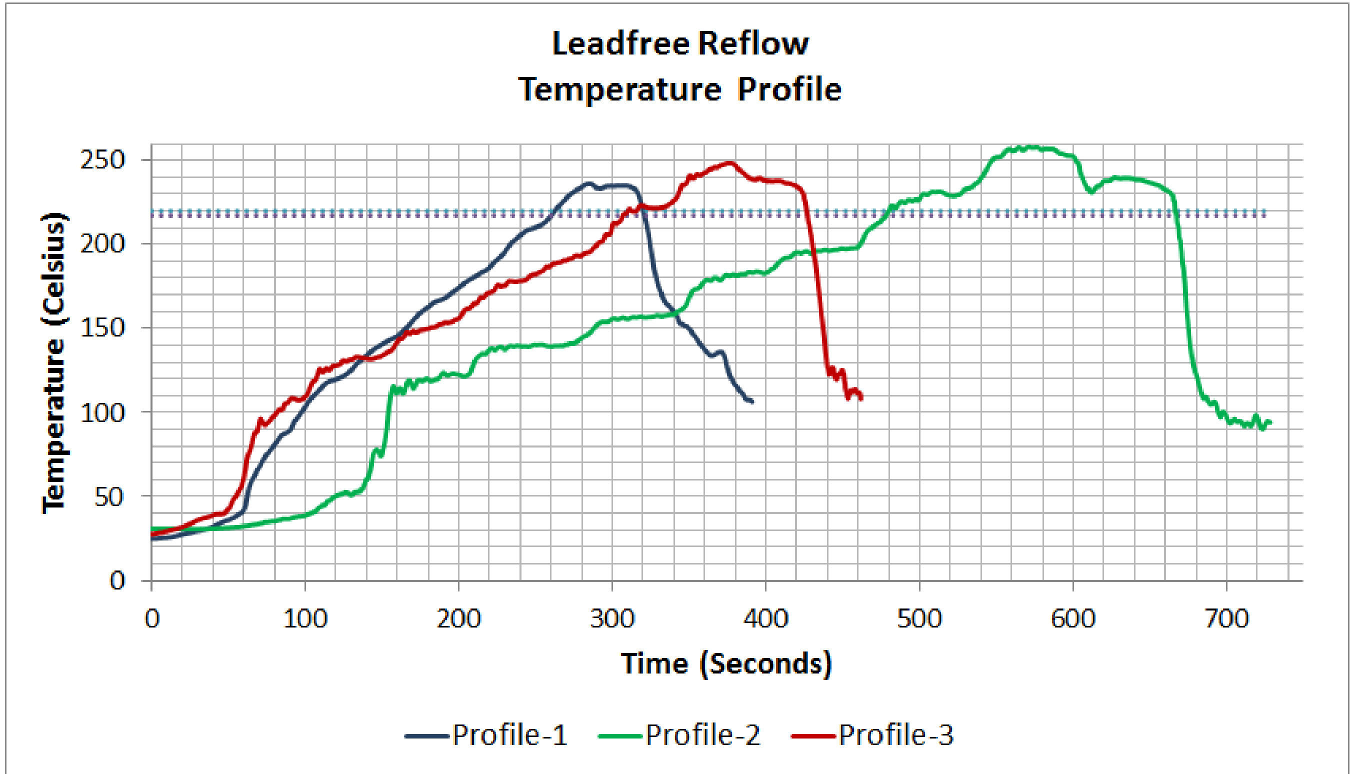

Figure 3.1: Reflow Profile

3.3 Measurement of Tg

The glass transition temperature of PCB laminates can be measured by a number of techniques including differential scanning calorimeter, thermo-mechanical analyzer, or dynamic mechanical analyzer. In this study, thermo- mechanical analyzer (TMA) was used to measure the glass transition temperature of the test-samples. The measurement setup is shown in Figure 3.2. The cut samples were placed in the sample holder made up of glass tube and was then covered with heater as shown in Figure 3.3. The heater heats up the sample causing it to expand. The expansion in Z-direction is then measured by the equipment and is plotted as a function of temperature.

Figure 3.2.a: TMA(Thermomechanical Analyzer)

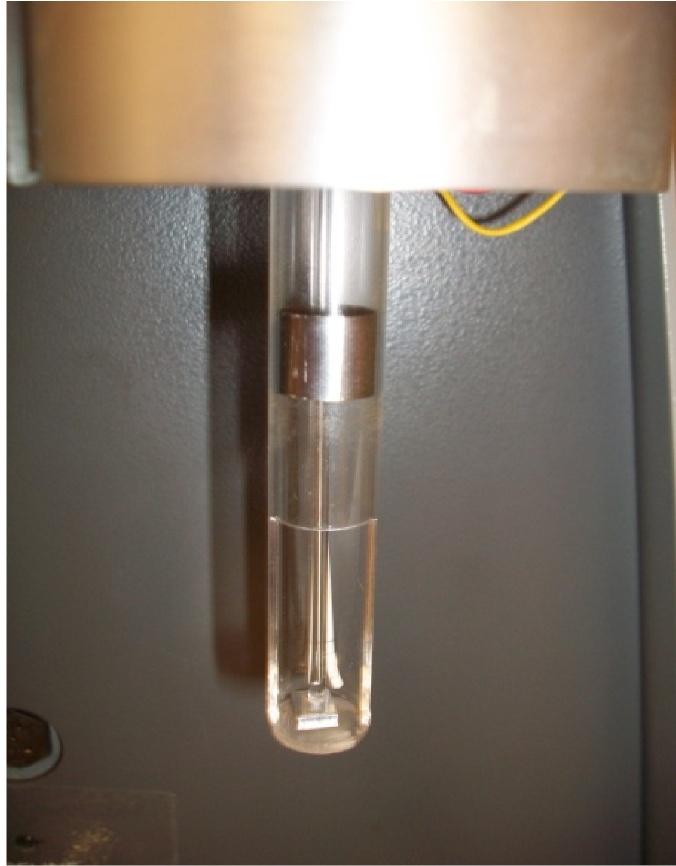

Figure 3.2.b: Sample Holder

Figure 3.2.c: Sample Holder with Heater

The rate of expansion of PCB laminates is 3x-5x higher above the T_g compared to expansion at temperatures below the T_g. Thermo-mechanical analysis (TMA) is a method to measure dimension changes versus temperature. Extrapolating the linear portion of curve (as shown below) to the point where they intersect provides the value of glass transition temperature (T_g). The slope of the linear portion of the curve above and below the T_g gives coefficient of thermal expansion (CTE). These values are important since they influence the reliability of finished circuit. So less thermal expansion will lead to better circuit reliability. Even though T_g is described by a precise temperature it is important to understand that the physical properties of material can begin to change as the T_g is approached (Figure 3.4).

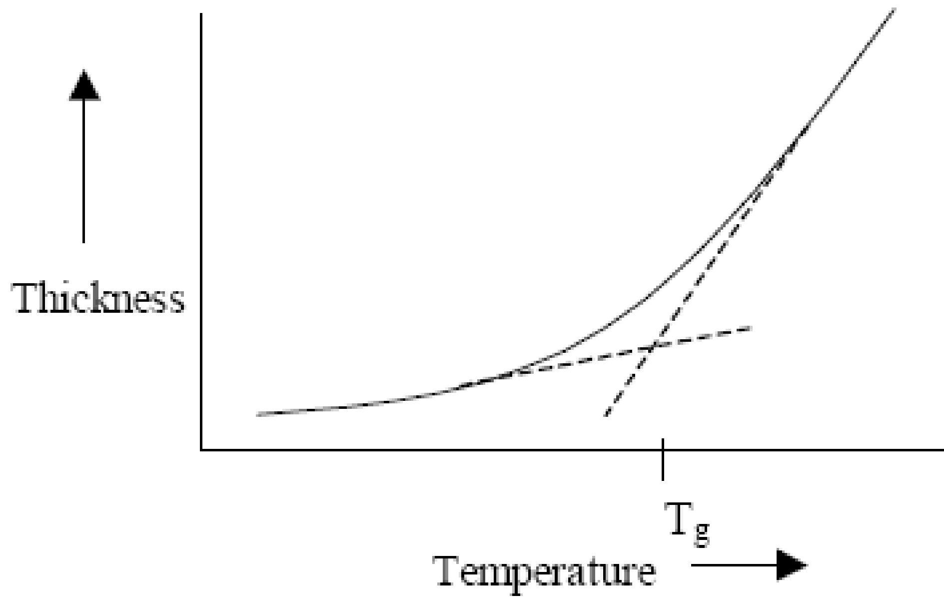

Figure 3.3: Representative CTE measurements from thermo- mechanical Analyzer.

3.4 Result and Analysis

The pre-exposure and post-exposure Tg measurement results have been grouped by Tg of the PCB laminate and reflow process variables (e.g., time above liquidus, peak reflow temperature, and number of reflows). In each case, multiple samples have been tested and group mean and variance used to ascertain the statistical significance of the differences observed.

3.4.1 *Mid Tg Laminates*

Table 3.1 shows the effect of time above liquidus on the Tg measurement for mid-Tg laminates. Results indicate a decrease in the glass transition temperature with the increase in time above liquidus. The Tg decreases to a mean value of 111.35°C for a TAL exposure of 150 sec from a mean value of 118.07°C for a TAL exposure of 30 sec. Table 3.2 shows the effect of peak temperature on the glass transition temperature for mid-Tg laminates. The mean Tg for peak reflow- temperature of 290°C drops to 111.96C from the mean Tg of 117.86C after peak exposure of 225°C. The pristine 0x reflow glass transition temperature mean-value of the mid-Tg laminate is 130.46C.

TAL(sec)	Peak Temperature (^{0}C)	Number of Reflows	Mean Tg (^{0}C)
30	255	2x	118.07
90	255	2x	114.37
150	255	2x	111.55

Table 3.1: Effect of Time above Liquidus on Tg

Peak Temperature (^{0}C)	TAL(sec)	Number of Reflows	Mean Tg (^{0}C)
225	90	2x	117.86
255	90	2x	114.37
290	90	2x	111.96

Table 3.2: Effect of Peak Temperature on Tg

Number of Reflows	Peak Temperature	TAL(sec)	Mean Tg
0x	255	90	130.45
2x	255	90	114.37
6x	255	90	117.97

Table 3.3: Effect of Number of Reflows on Tg

3.4.2 *Statistical Analysis of TAL Effect on T_g*

Figure 3.5 shows the statistical significance of difference in measured glass transition temperature in response to change in time above liquidus. The non-overlapping circles for the student's t-test and the tukey-kramer's test indicate that the differences are statistically significant at 95% confidence. It can be clearly seen from the plot that glass transition temperature drops corresponding to increase in time above liquidus. The mean squared error (MSE) is a way to quantify the difference between the estimated value and the true values of a quantity. The difference may occur because of unexplained sources of variation not captured in the measurement. The total sum of squares (SST) is a total of the squares of deviation of all measured values about their overall mean. Sum of Squares can be broken down to two components, (1) first, that measure the source of variation and is termed as the sum of squares for treatment (SST) and (2) second the sum of square of error (SSE).

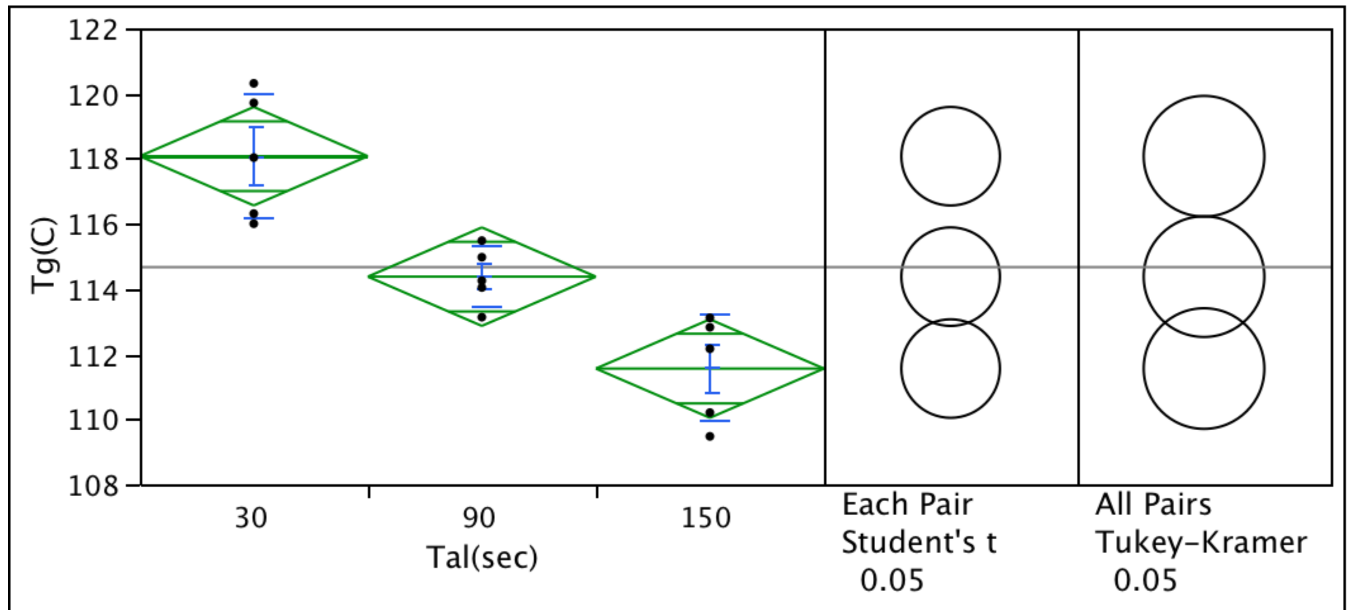

Figure 3.4: Analysis of statistical significance of TAL Effect on Tg of Mid-Tg Laminate

Source	Sum of Squares	Mean Square	F Ratio	Prob > F
Tal(sec)	106.91	53.45	22.18	<.0001
Error	28.91	2.40		
C.Total	135.82			

Table 3.4: ANOVA for Effect of TAL on Tg of Mid-Tg Laminate

When the null hypothesis of equal mean cannot be rejected, the two mean squares estimate the same quantity (error variance), and should be of approximately equal magnitude. In other words, their ratio should be close to 1. If the null hypothesis is rejected, then the mean square of treatment (MST) should be greater than mean square error (MSE). From the above shown ANOVA table it is evident that the difference in mean of glass transition temperature is significant as the value of MST is larger than MSE. The test statistic is the F value of 22.1880 (Table 3.4). The p-value for 22.1880 is 0.0001 which implies that there is a statistically significant difference among the population means.

Level	Mean	Std Error	Lower 95%	Upper 95%
30	**118.07**	**0.69**	**116.56**	**119.58**
90	**114.37**	**0.69**	**112.86**	**115.89**
150	**111.55**	**0.69**	**110.04**	**113.06**

Table 3.5: Means and Confidence Intervals for Effect of TAL on Tg of Mid-Tg Laminate

Table 3.5 shows means of measured glass transition temperature at three different values of TAL with corresponding standard error and a 95% confidence interval. Comparisons for each pair of TAL treatment on the T_g of mid-T_g laminate using Student's t are shown in Table 3.6. The results are tabulated by comparing the means of every treatment to the means of every other treatment that is it applies simultaneously to the set of all pairwise comparison. Positive values show pairs of means that are significantly different.

Abs (Dif)	30	90	150
30	-2.13	1.55	4.38
90	1.55	-2.13	0.68
150	4.38	0.68	-2.13

Table 3.6: Comparison of Tg from each TAL treatment using student's t-test

Table 3.7 shows the pairwise p-values for various TAL treatments on Tg for mid-Tg laminates. Results show that the differences in the measured T_g after various TAL treatments are statistically significant at greater than 95% confidence level in all the cases.

Level	-level	Difference	Lower CL	Upper CL	P- Value
225	255	3.49	1.78	5.19	0.0008
225	290	5.90	4.19	7.60	< .0001
255	290	2.41	0.70	4.11	0.0096

Table 3.7: Pairwise p-values for various TAL treatments on T_g for mid-T_g laminates

3.4.3 Statistical Analysis of Effect of Peak Temperature on Tg

Figure 3.6 shows the statistical significance of difference in measured glass transition temperature in response to change in peak temperature. The non-overlapping circles for the student's t-test and the tukey-kramer's test indicate that the differences are statistically significant at 95% confidence. It can be clearly seen from the plot that glass transition temperature drops corresponding to increase in the peak temperature.

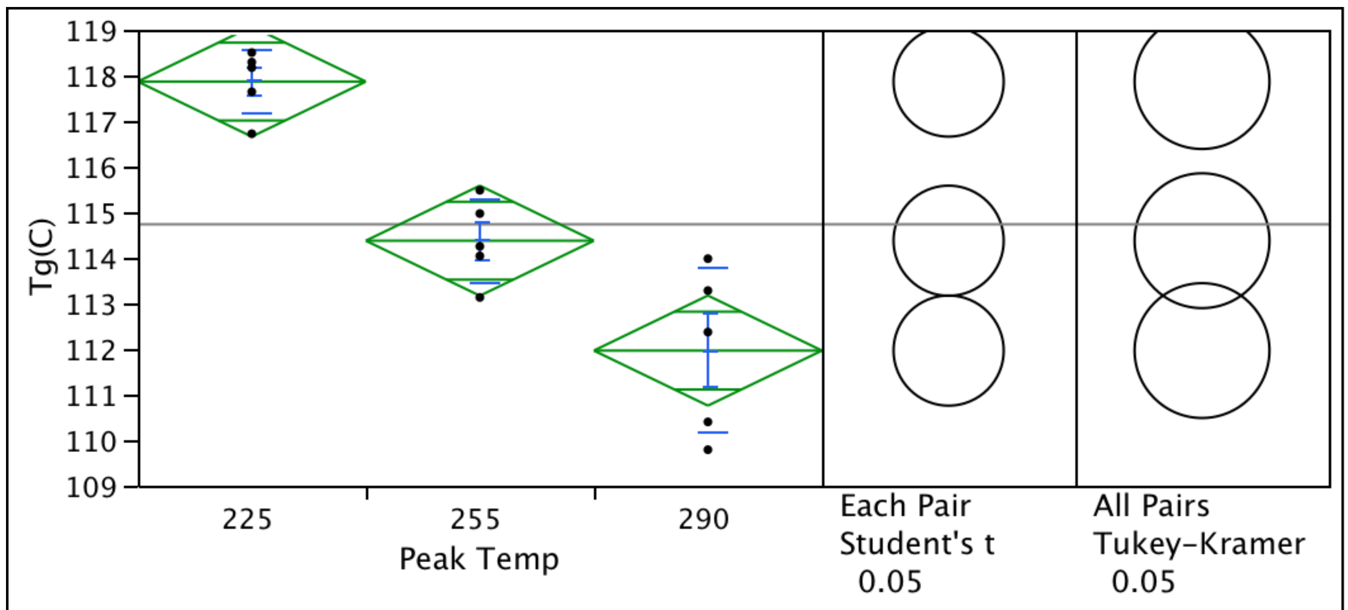

Figure 3.5: Analysis of Statistical Significance of Peak Temperature effect on Tg of Mid-Tg Laminate

To reject the null hypothesis or in other words to state that there is a statistically significant difference among the means of measured data, Mean square treatment (MST) should be larger than Mean square error (MSE). Also the F-value should be large and the corresponding p-value should be very small. Inferring from the Table 3.8, value of MST (43.9985) is very large compared to value of MSE (1.5354) and for the F-value (28.6561) the p-value is .0001(<.05).

These results imply that there is a statistically significant difference between the means of measured glass transition temperature at different peak temperature. Table 3.9 shows means of measured glass transition temperature at three different values of peak temperature with corresponding standard error and a 95% confidence interval.

Source	Sum of Squares	Mean Square	F Ratio	Prob > F
Peak Temp	**87.99**	**43.99**	**28.65**	**<.0001**
Error	**18.42**	**1.53**		
C.Total	**106.42**			

Table 3.8: ANOVA for effect of peak temperature on T_g of mid- T_g laminate

Level	Mean	Std Error	Lower 95%	Upper 95%
225	**117.86**	**0.55**	**116.66**	**119.07**
255	**114.37**	**0.55**	**113.17**	**115.58**
290	**111.96**	**0.55**	**110.76**	**113.17**

Table 3.9: Means and confidence intervals for effect of peak temperature on T_g for mid-T_g laminate.

Comparisons for each pair of peak temperature treatment on the T_g of mid-T_g laminate using Student's t are shown in Table 3.10. The results are tabulated by comparing the means of every treatment to the means of every other treatment that is it applies simultaneously to the set of all pairwise comparison. Positive values show pairs of means that are significantly different.

Abs (Dif)	**225**	**255**	**290**
225	**-1.70**	**1.78**	**4.19**
255	**1.78**	**-1.70**	**0.70**
290	**4.19**	**0.70**	**-1.70**

Table 3.10: Comparison of T_g from each peak temperature treatment using student's t-test

Table 11 shows the pairwise p-values for various peak temperature treatments on Tg for mid-Tg laminates. Results show that the differences in the measured T_g after various peak temperature treatments are statistically significant at greater than 95% confidence level in all the cases.

Level	-level	Difference	Lower CL	Upper CL	P- Value
225	255	3.49	1.78	5.19	0.0008
225	290	5.90	4.19	7.60	< .0001
255	290	2.41	0.70	4.11	0.0096

Table 3.11: Pairwise p-values for various peak temperature treatments on T_g for mid-T_g laminates

3.4.4 Statistical Significance of Effect of Number of Reflows on Tg

Figure 3.7 shows the statistical significance of difference in measured glass transition temperature in response to change in the number of reflows. The non-overlapping circles for the student's t-test and the tukey-kramer's test indicate that the differences are statistically significant at 95% confidence. It is seen here that there is a reversal in the trend. There is no continuous drop or increase in glass transition temperature. It first decreases and then again increases as number of reflow is increased.

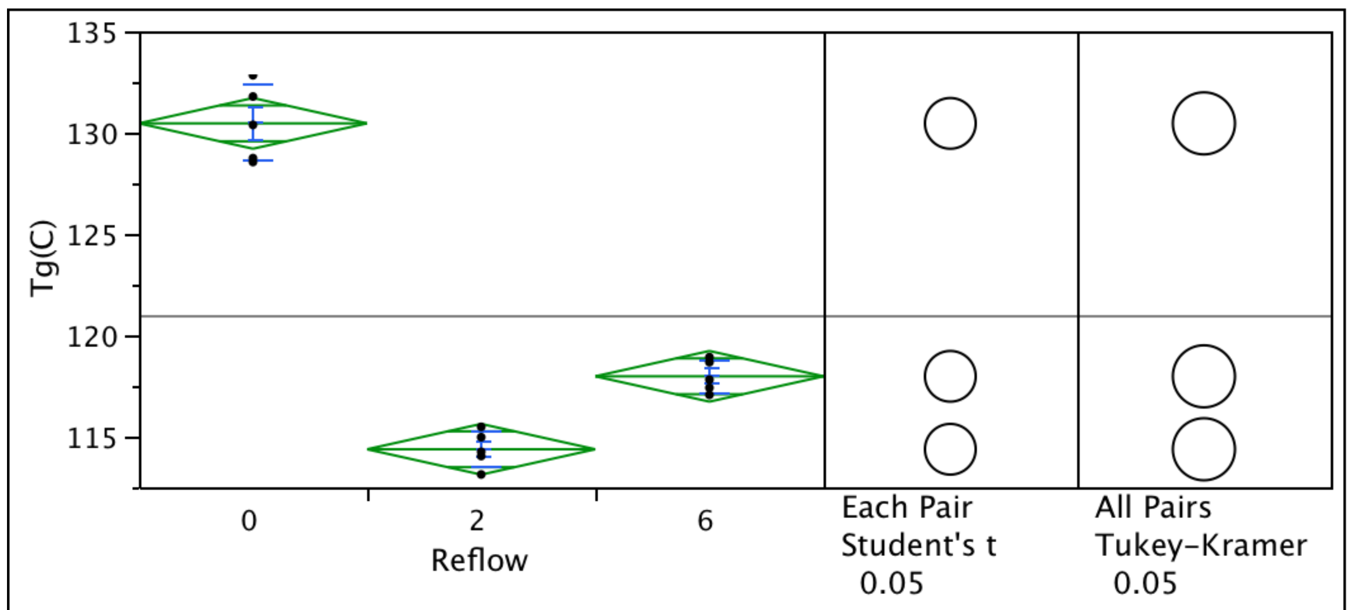

Figure 3.6: Analysis of statistical significance of number of reflows effect on T_g of mid-T_g laminate

To reject the null hypothesis or in other words to state that there is a statistically significant difference among the means of measured data, Mean square treatment (MST) should be larger than Mean square error (MSE). Also the F-value should be large and the corresponding p-value should be very small. Inferring from Table 3.12, it is seen that the difference in the values of

MST (356.159) and MSE (1.649) is large also the F- value (216.0203) is very large with very small corresponding p-value of .0001. These results fulfill the criteria to reject the null hypothesis of equal mean and it can be evidently stated that the means of glass transition temperature, measured for different number of reflows, show statistically significant difference. Table 3.13 shows means of measured glass transition temperature at three different numbers of reflow with corresponding standard error and a 95% confidence interval.

Source	Sum of Squares	Mean Square	F Ratio	Prob > F
Reflow	712.31	356.15	216.02	< .0001
Error	19.78	1.64		
C.Total	732.10			

Table 3.12: ANOVA for effect of number of reflows on T_g of mid-T_g laminate

Level	Mean	Std Error	Lower 95%	Upper 95%
0	130.45	0.57	129.20	131.71
2	114.37	0.57	113.12	115.63
6	117.97	0.57	116.72	119.23

Table 3.13: Means and confidence intervals for effect of number of reflows on T_g for mid T_g laminate

Comparisons for each pair of number of reflows treatment on the T_g of mid-T_g laminate using Student's t are shown in Table 3.14. The results are tabulated by comparing the means of every treatment to the means of every other treatment that is it applies simultaneously to the set of all pairwise comparison. Positive values show pairs of means that are significantly different.

Abs (Dif)	**0**	**6**	**2**
0	**-1.76**	**10.71**	**14.31**
6	**10.71**	**-1.76**	**1.83**
2	**14.31**	**1.83**	**-1.76**

Table 3.14: Comparison of T_g from each number of reflows treatment using student's t-test

Table 3.15 shows the pairwise p-values for various peak temperature treatments on Tg for mid-Tg laminates. Results show that the differences in the measured T_g after various peak temperature treatments are statistically significant at greater than 95% confidence level in all the cases.

Level	-level	Difference	Lower CL	Upper CL	P- Value
0	2	16.08	14.31	17.85	<.0001
0	6	12.48	10.71	14.25	<.0001
2	6	3.60	1.83	5.36	0.0008

Table 3.15: Pairwise p-values for various number of reflow treatments on Tg for mid-Tg laminates

3.5 High Tg Laminates

Table 3.16 shows the effect of time above liquidus on the T_g measurement for high-Tg laminates. Results indicate a decrease in the glass transition temperature with the increase in time above liquidus. The T_g decreases to a mean value of 150.26°C for a TAL exposure of 150 sec from a mean value of 151.03°C for a TAL exposure of 30 sec.

TAL(sec)	Peak Temperature (^{0}C)	Number of Reflows	Mean Tg (^{0}C)
30	255	2x	151.03
90	255	2x	148.03
150	255	2x	150.26

Table 3.16: Effect of time above liquidus on T_g for high-T_g Laminates

Table 3.17 shows the effect of peak temperature on the glass transition temperature for mid-T_g laminates. The mean T_g for peak reflow-temperature of 290°C increases to 150.82°C from the mean T_g of 147.46°C after peak exposure of 225°C. The pristine 0x reflow glass transition temperature mean-value of the mid-T_g laminate is 160.29°C. There was considerable drop in glass transition temperature as number of reflow was increased as shown in Table 3.18.

Peak Temperature (^{0}C)	TAL(sec)	Number of Reflows	Mean Tg (^{0}C)
225	90	2x	147.46
255	90	2x	150.44
290	90	2x	150.82

Table 3.17: Effect of Peak Temperature on Tg for high Tg Laminates

Number of Reflows	Peak Temperature (^{0}C)	TAL(sec)	Mean Tg (^{0}C)
0x	255	90	160.29
2x	255	90	150.44
6x	255	90	144.64

Table 3.18: Effect of Number of Reflows on Tg for high Tg Laminates

3.5.1 Statistical Significance of TAL Effect on Tg

Figure 3.8 shows the statistical significance of difference in measured glass transition temperature in response to change in time above liquidus. The non-overlapping circles for the student's t-test and the tukey-kramer's test indicate that the differences are statistically significant at 95% confidence. Overlapping circles indicate that the differences are not statistically significant at 95% confidence. It can be clearly seen from the plot that glass transition temperature exhibits a non-monotonic trend, decreasing and then increasing corresponding to an increase in time above liquidus. It is seen here that there is a reversal in the trend. There is no continuous drop or increase in glass transition temperature.

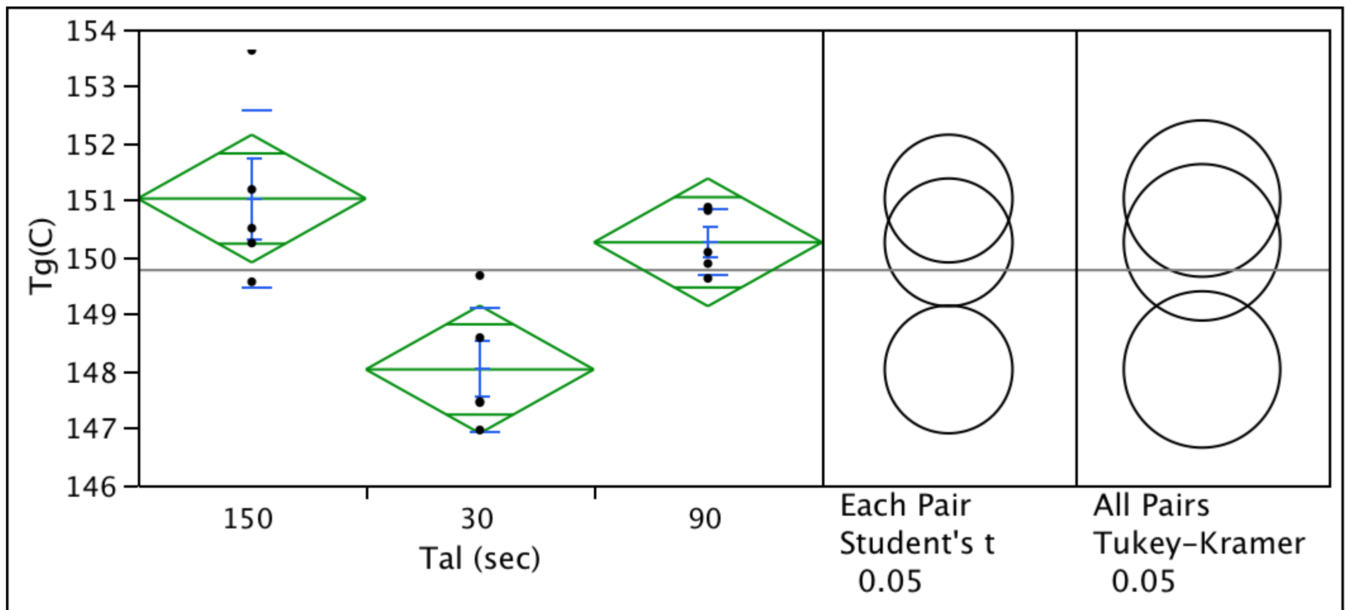

Figure 3.7: Analysis of statistical significance of TAL effect on T_g of high-T_g laminate

To reject the null hypothesis or in other words to state that there is a statistically significant difference among the means of measured data, Mean square treatment (MST) should be larger than Mean square error (MSE). Also, the F-value should be large and the corresponding p-value

should be very small. From Table 3.19, it is seen that the difference between the values of MST (12.1256) and MSE (1.322) is not very large as in some of above cases. This is due to the fact that the means of population are grouped very close together. But still the difference is significant enough as the F-value obtained is 9.1708 and the corresponding p-value is .0038 (<.05). From these results it can be said that though the difference in the population mean is small, there is still statistically significant difference among them. Table 3.20 shows means of measured glass transition temperature at three different values of time above liquidus with corresponding standard error and a 95% confidence interval.

Source	Sum of Squares	Mean Square	F Ratio	Prob > F
Tal(sec)	**24.25**	**12.12**	**9.17**	**.0038**
Error	**15.86**	**1.32**		
C.Total	**40.11**			

Table 3.19: ANOVA for effect of TAL on T_g of mid-T_g laminate

Comparisons for each pair of time above liquidus treatment on the T_g of mid-T_g laminate using Student's t are shown in Table 3.21. The results are tabulated by comparing the means of every treatment to the means of every other treatment that is it applies simultaneously to the set of all pairwise comparison. Positive values show pairs of means that are significantly different.

Level	Mean	Std Error	Lower 95%	Upper 95%
30	148.03	0.514	146.91	149.15
90	150.26	0.514	149.14	151.38
150	151.03	0.514	149.91	152.15

Table 3.20: Means and confidence intervals for effect of TAL on T_g for high-T_g laminate.

Abs (Dif)	30	90	150
30	-1.58	0.64	1.41
90	0.64	-1.58	-0.81
150	1.41	-0.81	-1.58

Table 3.21: Comparison of Tg from each TAL treatment using student's t-test

Table 22 shows the pairwise p-values for various peak temperature treatments on T_g for high-T_g laminates. Results show that the differences in the measured T_g after various peak temperature treatments are statistically significant at greater than 95% confidence level in all the cases.

Level	-level	Difference	Lower CL	Upper CL	P- Value
30	90	2.23	0.64	3.81	.00098
30	150	2.99	1.41	4.58	.0014
90	150	0.76	-0.81	2.35	0.3117

Table 3.22: Pairwise p-values for various time above liquidus treatments on Tg for high-Tg laminates

3.5.2 Statistical Analysis of Effect of Peak Temperature on Tg

Figure 3.9 shows the statistical significance of difference in measured glass transition temperature in response to change in peak temperature. The non-overlapping circles for the student's t-test and the tukey-kramer's test indicate that the differences are statistically significant at 95% confidence. Overlapping circles indicate that the differences are not statistically significant at 95% confidence. It can be clearly seen from the plot that glass transition temperature increases corresponding to increase in the peak temperature.

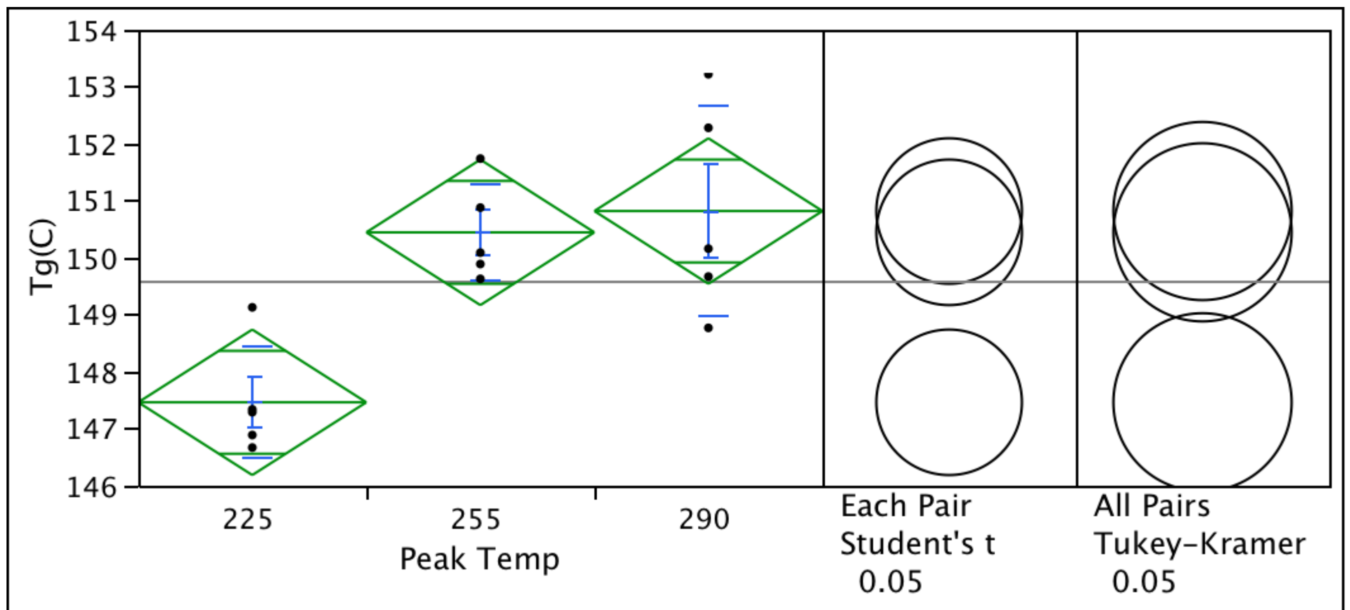

Figure 3.8: Analysis of statistical significance of Peak Temperature effect on T_g of high-T_g laminate

To reject the null hypothesis or in other words to state that there is statically significant difference among the means of measured data, Mean square treatment (MST) should be larger than Mean square error (MSE). Also the F-value should be large and the corresponding p-value should be very small. From Table 3.23 it is seen that the difference between the values of MST

(16.9124) and MSE (1.7165) is not very large as in some of above cases. This is due to the fact that the means of population are grouped very close together. But still the difference is significant enough as the F-value obtained is 9.8529 and the corresponding p-value is .0029 (<.05). From these results it can be said that though the difference in the population mean is small, there is still statistically significant difference among them. Table 3.24 shows means of measured glass transition temperature at three different values of peak temperature with corresponding standard error and a 95% confidence interval.

Source	Sum of Squares	Mean Square	F Ratio	Prob > F
Peak Temp	**33.82**	**16.91**	**9.8**	**.0029**
Error	**20.59**	**1.71**		
C.Total	**54.42**			

Table 3.23: ANOVA for effect of peak temperature on T_g of high-T_g laminate

Level	Mean	Std Error	Lower 95%	Upper 95%
225	147.46	0.58	146.19	148.74
255	150.44	0.58	149.17	151.72
290	150.82	0.58	149.54	152.10

Table 3.24: Means and confidence intervals for effect of peak temperature on T_g for high-T_g laminate.

Comparisons for each pair of peak temperature treatment on the T_g of high-T_g laminate using Student's t are shown in Table 3.25. The results are tabulated by comparing the means of every treatment to the means of every other treatment that is it applies simultaneously to the set of all pairwise comparison. Positive values show pairs of means that are significantly different.

Abs (Dif)	225	255	290
225	-1.80	1.17	1.55
255	1.17	-1.80	-1.43
290	1.55	-1.43	-1.80

Table 3.25: Comparison of Tg from each peak temperature treatment using student's t-test

Table 3.26 shows the pairwise p-values for various peak temperature treatments on T_g for high-T_g laminates. Results show that the differences in the measured T_g after various peak temperature treatments are statistically significant at greater than 95% confidence level in all the cases.

Level	-level	Difference	Lower CL	Upper CL	P- Value
225	**255**	**2.98**	**1.17**	**4.78**	**0.0037**
255	**290**	**0.37**	**1.55**	**5.16**	**0.6598**
290	**225**	**3.35**	**1.55**	**5.16**	**0.0016**

Table 3. 26: Pairwise p-values for various peak temperature treatments on T_g for high-T_g laminates

3.5.3 Statistical Analysis of Effect of Number of Reflows on Tg

Figure 3.9 shows the statistical significance of difference in measured glass transition temperature in response to change in number of reflows. The non-overlapping circles for the student's t-test and the tukey-kramer's test indicate that the differences are statistically significant at 95% confidence. Overlapping circles indicate that the differences are not statistically significant at 95% confidence. It can be clearly seen from the plot that glass transition temperature decreases corresponding to increase in the number of reflows.

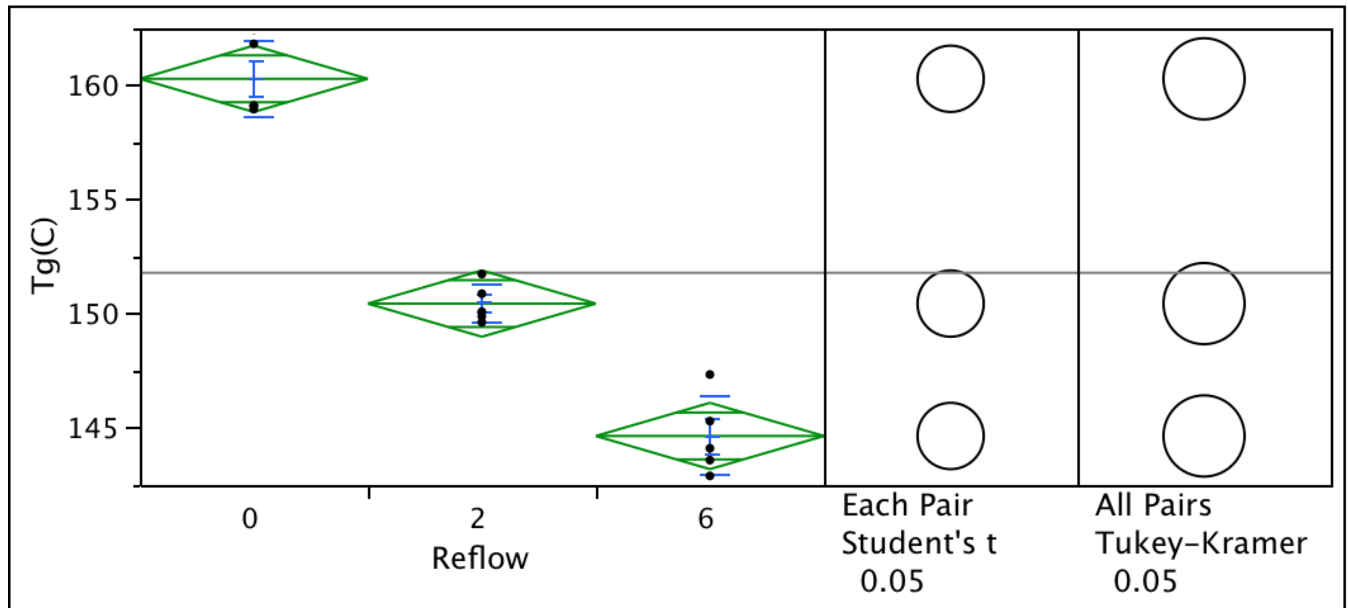

Figure 3.9: Analysis of statistical significance of Number of reflows effect on T_g of high-T_g laminate

To reject the null hypothesis or in other words to state that there is a statistically significant difference among the means of measured data, Mean square treatment (MST) should be larger than Mean square error (MSE). Also the F-value should be large and the corresponding p-value should be very small. Statistical significance of the measured data, can be inferred from Table 3.27. It is seen that the difference in the values of MST (312.661) and MSE (2.222) is large also the F-value (140.7263) is very large with very small corresponding p- value of .0001. These results fulfill the criteria to reject the null hypothesis of equal mean and it can be evidently stated that the means of glass transition temperature, measured for different number of reflows, show statistically significant difference. Table 3.28 shows means of measured glass transition temperature at three different values of number of reflows with corresponding standard error and a 95% confidence interval.

Source	Sum of Squares	Mean Square	F Ratio	Prob > F
Reflow	**625.32**	**312.66**	**140.72**	**< .0001**
Error	**26.66**	**2.22**		
C.Total	**651.98**			

Table 3. 27: ANOVA for effect of number of reflows on T_g of high-T_g laminate

Level	Mean	Std Error	Lower 95%	Upper 95%
0	160.29	0.66	158.84	161.74
2	150.44	0.66	148.99	151.90
6	144.64	0.66	143.20	146.10

Table 3.28: Means and confidence intervals for effect of number of reflow on T_g for high-T_g laminate.

Comparison for each pair of peak temperature treatment on the Tg of high Tg laminate using Student's t-test are shown in Table 3.29. The results are tabulated by comparing the means of every treatment to the means of every other treatment that is it applies simultaneously to the set of all pairwise comparison. Positive values show pairs of means that are significantly different.

Abs (Dif)	0	2	6
0	-2.05	7.79	13.58
2	7.79	-2.05	3.74
6	13.58	3.74	-2.05

Table 3.29: Comparison of T_g from each number of reflow treatment using student's t-test

Table 3.30 shows the pairwise p-values for various peak temperature treatments on T_g for high-T_g laminates. Results show that the differences in the measured T_g after various peak temperature treatments are statistically significant at greater than 95% confidence level in all the cases.

Level	-level	Difference	Lower CL	Upper CL	P- Value
0	**2**	**9.84**	**7.79**	**11.89**	**<.0001**
0	**6**	**15.64**	**13.58**	**17.69**	**<.0001**
2	**6**	**5.79**	**3.74**	**7.85**	**<.0001**

Table 3.30: Pairwise p-values for various number of reflow treatments on T_g for high-T_g laminates

CHAPTER 4

Model for Prediction of Package-on-Package (PoP) Warpage and the Effect of Process and Material Parameters

4.1 Introduction

The transition from conventional components and direct board level assembly to chip or package level system integration has improved package technology significantly over the past several years. In recent years miniaturization and high functionality have been demanded intensely by consumer electronics industry. Increasing the number of components within smaller housing to achieve high functionality leads to exhaustion of XY space. The demand for increases in I/Os and decrease in package size has led to the proliferation of 3D packaging technology. Three-dimensional packages exploit the availability of space in z-direction to pack more functionality in smaller form factor. Package-on-Package assemblies, commonly known as PoP assemblies have attracted a lot of interest, especially in portable electronics industry. In a PoP architecture, two or more packages are stacked on top of each other where the bottom package is generally a logic device while the top package is usually a memory sub-system. A schematic of a common PoP configuration is shown in Figure 4.1. For proper board-level assembly, great care must be taken to ensure co-planarity exists between the stacked packages. Package warpage is one of dominant issues for surface mount yields which is induced due to high temperature exposure during reflow process.

Figure 4.1: A common PoP configuration

In literature, a lot of researchers have discussed the key factors influencing PoP warpage such as package structures, package dimensions, material properties and processing conditions. Warpage is defined as the out-of-place displacement between the center of the package and the corner of the package. Previously, researchers [Yen 2008, Lin 2008, Sun 2008] have performed study to examine the warpage that occurs in packages during reflow processes. Warpage is characterized as positive or negative according to the shape it produces from a 2D perspective. The sign convention used for this study is shown in Figure 4.2. When looking from the ball side of package, convex surface is defined as a positive warpage while concave surface is defined as a negative warpage.

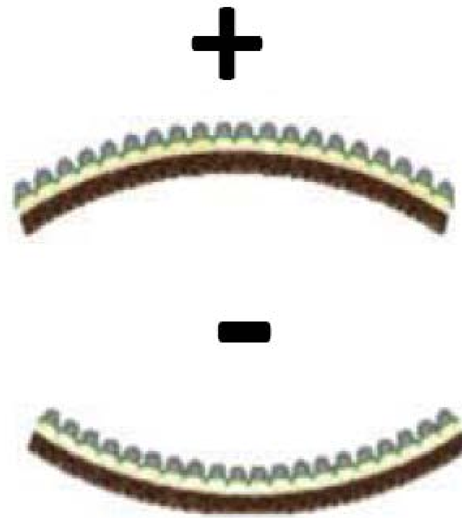

Figure 4.2: Warpage sign convention

Warpage is induced into electronic packages when they are exposed to high and low temperatures therefore solder reflow process is an important factor affecting the package warpage. Earlier shadow moiré interferometery is used to measure the warpage of a package during temperature changes. In this study, an image processing technique called DIC, digital image correlation, is also used. In the past, various researchers have used DIC successfully in electronic packaging field for measurement purpose in number of different studies. [Lall 2007b, 2008a,b, Miller 2007, Park 2007a,b, 2008] has shown the use of DIC to measure full field displacement and deformation in electronics subjected to drop events, [Bieler 2006, Rajendra 2002, Sun 2006, Xu 2006, Yogel 2001, Zhang 2005, Zhou 2001] used DIC to determine solder interconnect stresses under thermal loadings for BGA package types, warpage measurement on dual chip module [Ouimet 2008], [Peterson 2008] measured the damping ratio on the surface of a board, [Scheijgrond 2005] and [Kehoe 2006] measured velocity, rotation and bending on portable products subjected to impact testing and stresses and strains under thermal loading for

flip-chip dies respectively. Warpage values are greatly affected by process conditions, material properties and package architecture. [Amagai 2010, Sun 2008] used finite element analysis to study the effects of material properties on package warpage. Table 4.1 shows the ranges of package architecture and material properties that have been examined.

Parameter	Values
Package Dimensions	12-14 mm
EMC Thickness	0.2-0.3 mm
Substrate Thickness	80-120 um
EMC CTE1	10-16 ppm/C
EMC CTE2	34-74 ppm/C
EMC E1	18-26 GPa
EMC E2	0.6-3 GPa
Substrate CTE	3-7 ppm/C
Substrate Elastic Modulus	25-35 GPa
Chip Dimensions	7-10 mm
Chip Thickness	50-150 um
Chip CTE	2-3 ppm/C
Chip Elastic Modulus	140-170 GPa

Table 4.1: Range of values examined

4.2 Test Vehicle

This study used two different package types as test vehicles. Test Vehicle-1 is a PoP package which utilizes copper landing pads for 3D stacking. The package architecture is shown in Figure 4.3 and the package specifications are shown in Table 4.2.

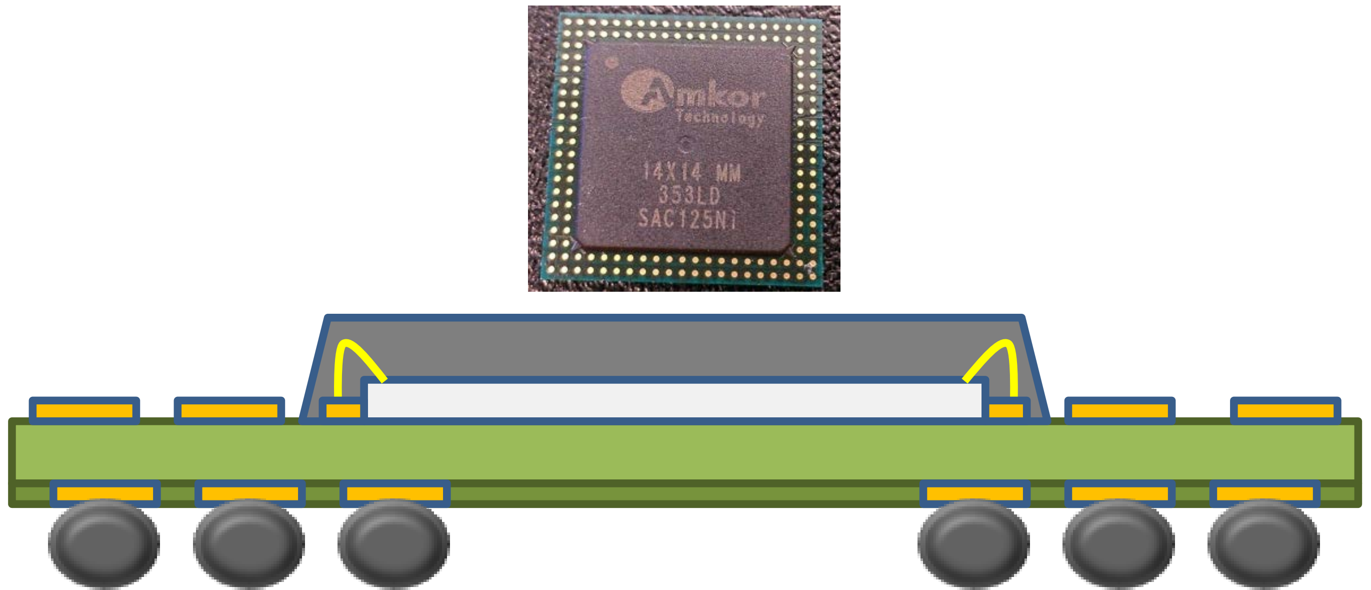

Figure 4.3: Test vehicle 1 package architecture

	Package-A	**Package-B**
Package Size	12mm x 12mm	14mm x 14mm
Package Thickness	0.6mm	0.6mm
Die Size	7mm x 7mm	8.9mm x 8.9mm
Die Thickness	100 µm	100 µm
Footprint Bottom Side	0.5mm Pitch, 305 I/O 23x23 Matrix 4 rows, 12NC, A1 Ball	0.5mm Pitch, 353 I/O 26x26 Matrix 4 rows, 12NC, A1 Ball

Table 4.2: Test vehicle 1 package specifications

Test Vehicle-2 is a PoP package that uses through mold via (TMV) technology for 3D stacking. The package architecture for Test Vehicle-2 is shown in Figure 4.4 and the package specifications are shown in Table 4.3.

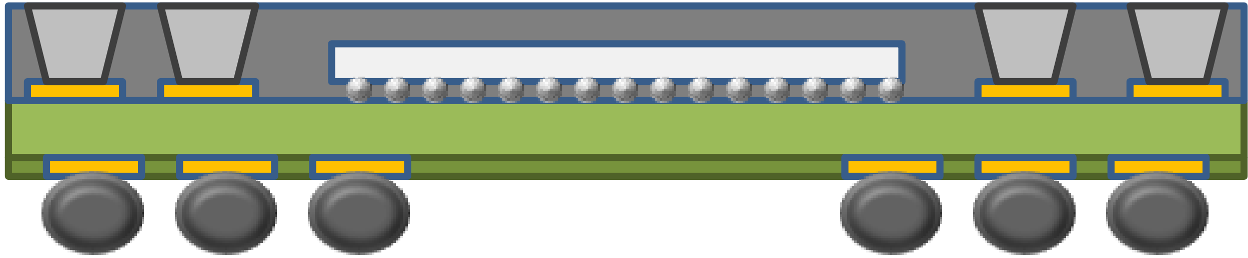

Figure 4.4: Test vehicle 2 package architecture

	Package-A	Package-B
Package Size	12mm x 12mm	14mm x 14mm
Package Thickness	0.6mm	0.50mm - 0.57mm
Die Size	8.47mm x 8.24mm	9mm x 9mm
Die Thickness	60 - 100 µm	100 µm
Footprint Bottom Side	0.4mm Pitch, 559 I/O 28x28 Matrix, De-Populated	0.5mm Pitch, 325 I/O

Table 4.3: Test vehicle 2 package specifications

4.3 Experimental Set Up

To determine the warpage of PoP packages in-situ during a reflow process, a single chamber conventional lead-free reflow oven is used. Test vehicles are speckle coated and then placed into the oven where they are exposed to the temperature changes present during an actual reflow process. The reflow profile has a peak temperature of 250 °C. The temperature profile used for this experiment is shown in Figure 4.5.

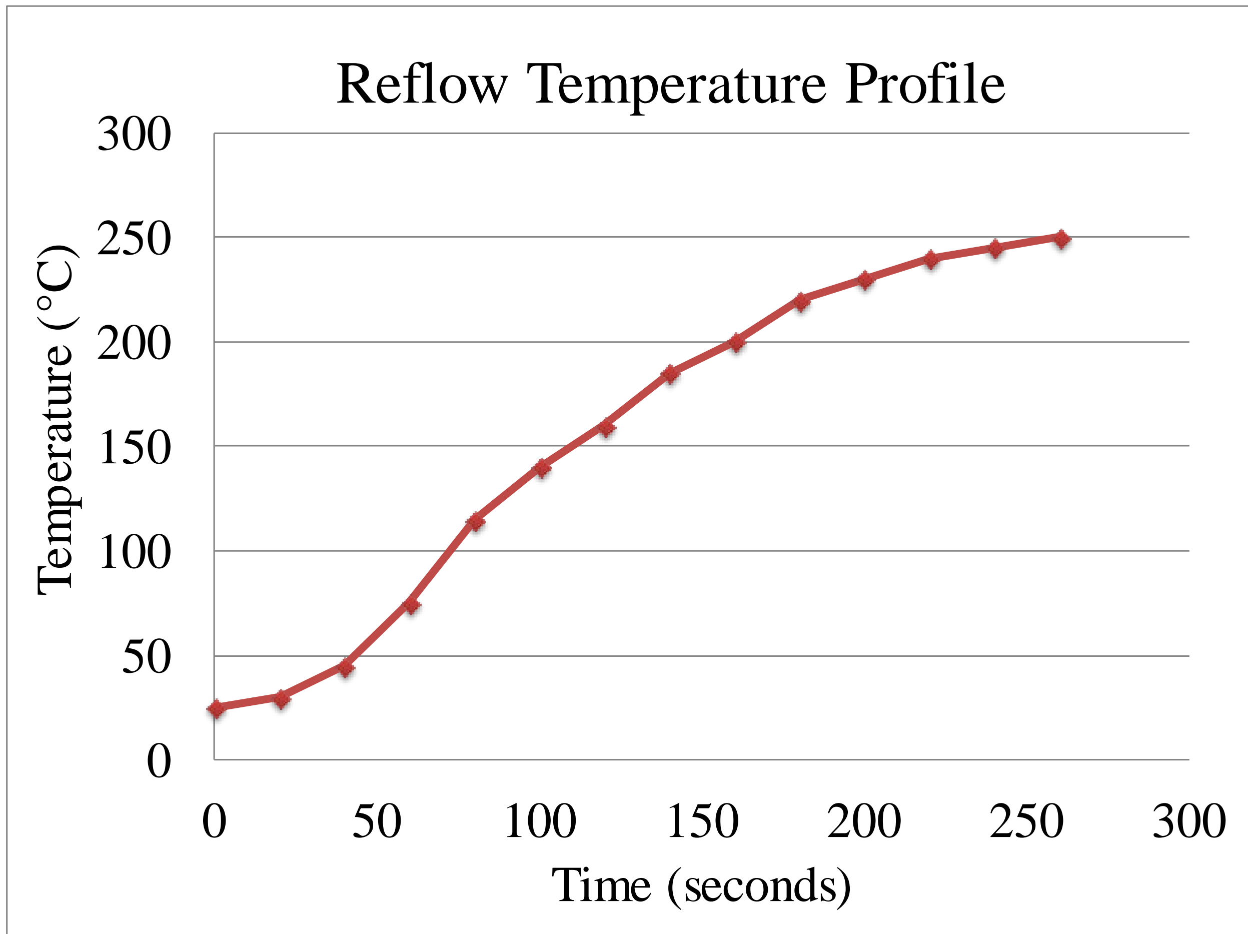

Figure 4.5: Temperature profile for reflow

The lead free reflow oven has a glass window installed on top which allows for visual inspection of components during reflow. Images of the test specimen, while being subjected to the reflow temperature profile is captured simultaneously by two high resolution low speed cameras. Figure 4.6 is a schematic showing the experimental set up used in this study.

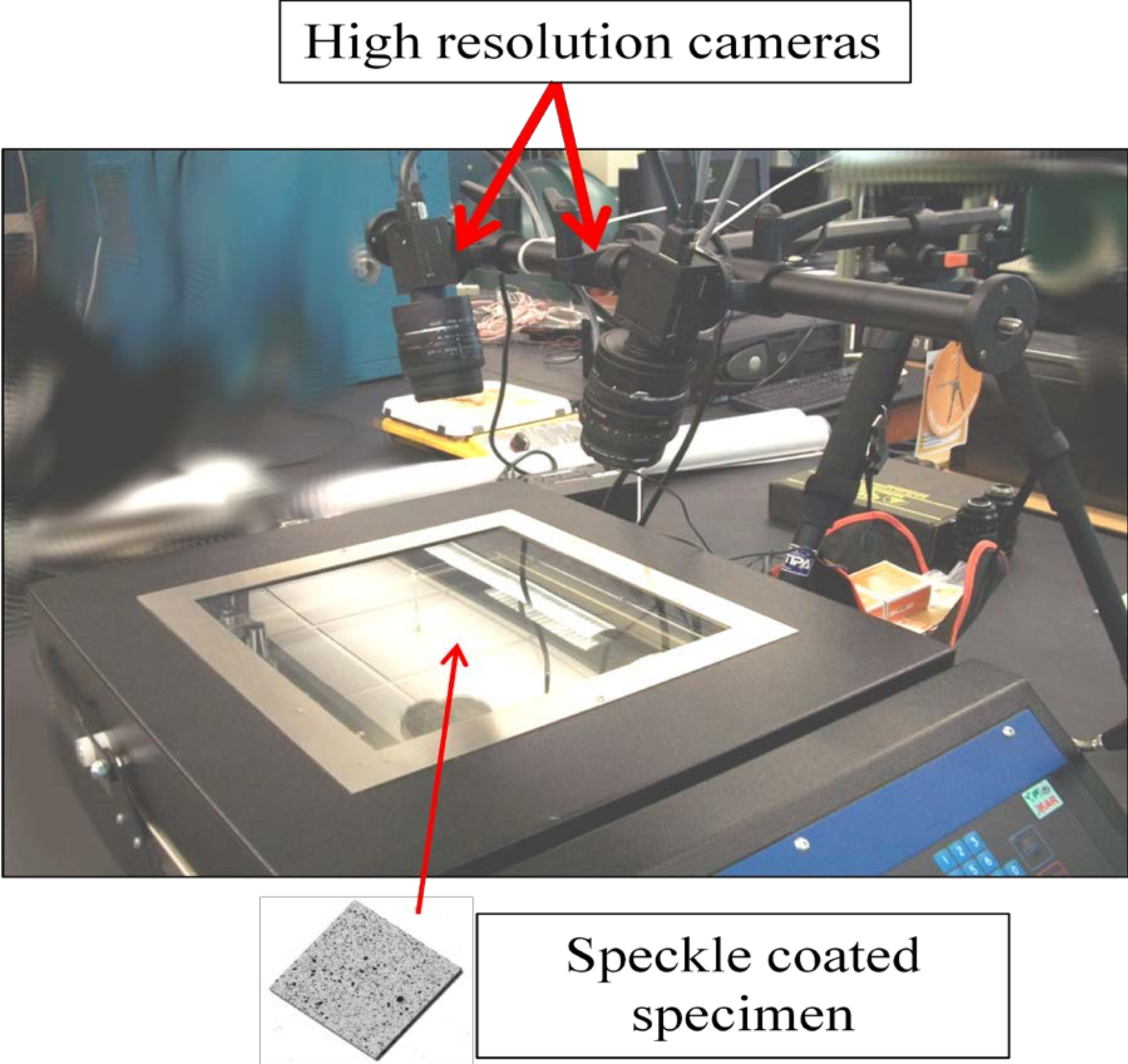

Figure 4.6: Experimental set up

In this study, the Digital Image Correlation (DIC) has been used to measure the warpage in packages during reflow. Digital image correlation (DIC) is an optical method, used to measure full field deformation and their derivatives on the surface of a loaded structure. This technique

involves coating the surface under investigation with speckle pattern and tracking a geometric point on the speckle patterned surface before and after the loading to determine out-of-plane deformation. Previously, [Lall 2007[a-e], 2008[a-d]] showed the use of DIC to measure full field displacement and deformation gradient. The specimens must be de-balled to provide a flat surface for speckle coating processes. Figure 4.7 is a schematic showing the principle of DIC for a three dimensional case.

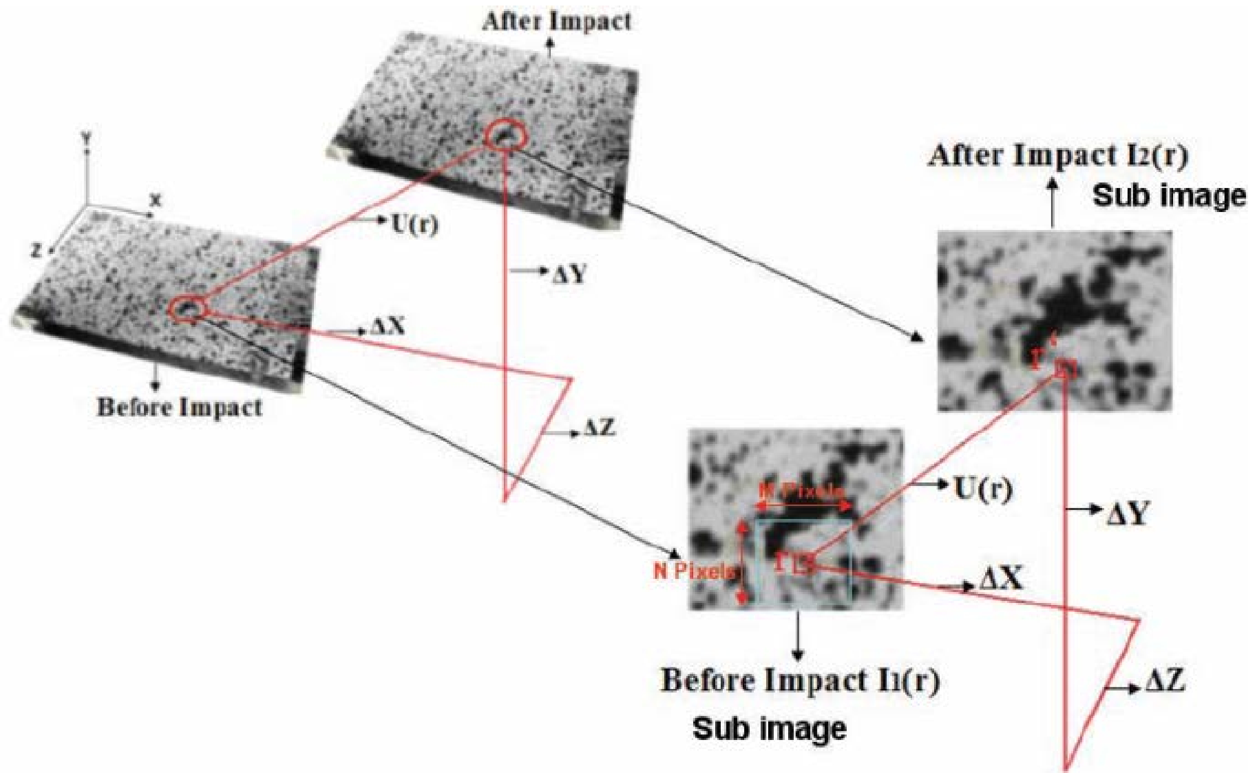

Figure 4.7: Digital image correlation for a 3D case [Lall 2010]

The sub image before loading is referred as I1(r) and the deformed image as I2(r) respectively. The two are related as follows:

$$I_2(r) = I_1[r - U(r)] \qquad (1)$$

$$I_1(r) = I_2[r + U(r)] \qquad (2)$$

Where U(r) is the displacement vector at pixel $r = (x, y, z)^T$. The difference in the positions

of the current pixel and the reference pixel gives the in-plane as well as out-of-plane displacement U(r) of this reference pixel. A sub image around a reference pixel 'r' in the undeformed image is then compared with the sub images corresponding to different pixels in the deformed image using a predefined correlation function. Statistical functions are used to correlate the change in a reference pixel in the original and in deformed image. Three such typical correlations include absolute difference, least square and cross correlation. There are three typical correlation functions which are used and are defined as follows: [Zhou 2001]

Absolute Difference:

$$C_A(r') = 1 - \frac{\iint_\Omega |I_2(r+r') - I_1(r)| dr}{\iint_\Omega I_1(r) dr} \quad (3)$$

Least square:

$$C_L(r') = 1 - \frac{\iint_\Omega [|I_2(r+r') - I_1(r)|]^2 dr}{\iint_\Omega I_1^2(r) dr} \quad (4)$$

and Cross-Correlation:

$$C_C(r') = 1 - \frac{\iint_\Omega I_1(r) I_2(r+r') dr}{[\iint_\Omega I_1^2(r) dr \iint_\Omega I_2^2(r+r') dr]^{1/2}} \quad (5)$$

Where Ω (M x N) is the area of the sub image around reference pixel r, r' is the current pixel, $C_A(r')$ is the current absolute correlation function, $C_L(r')$ is the current least square correlation function, and $C_C(r')$ is the current cross correlation function. The cross correlation provide the correspondence between matching subsets in images of undeformed and deformed states. A full field displacement contour is obtained from image processing.

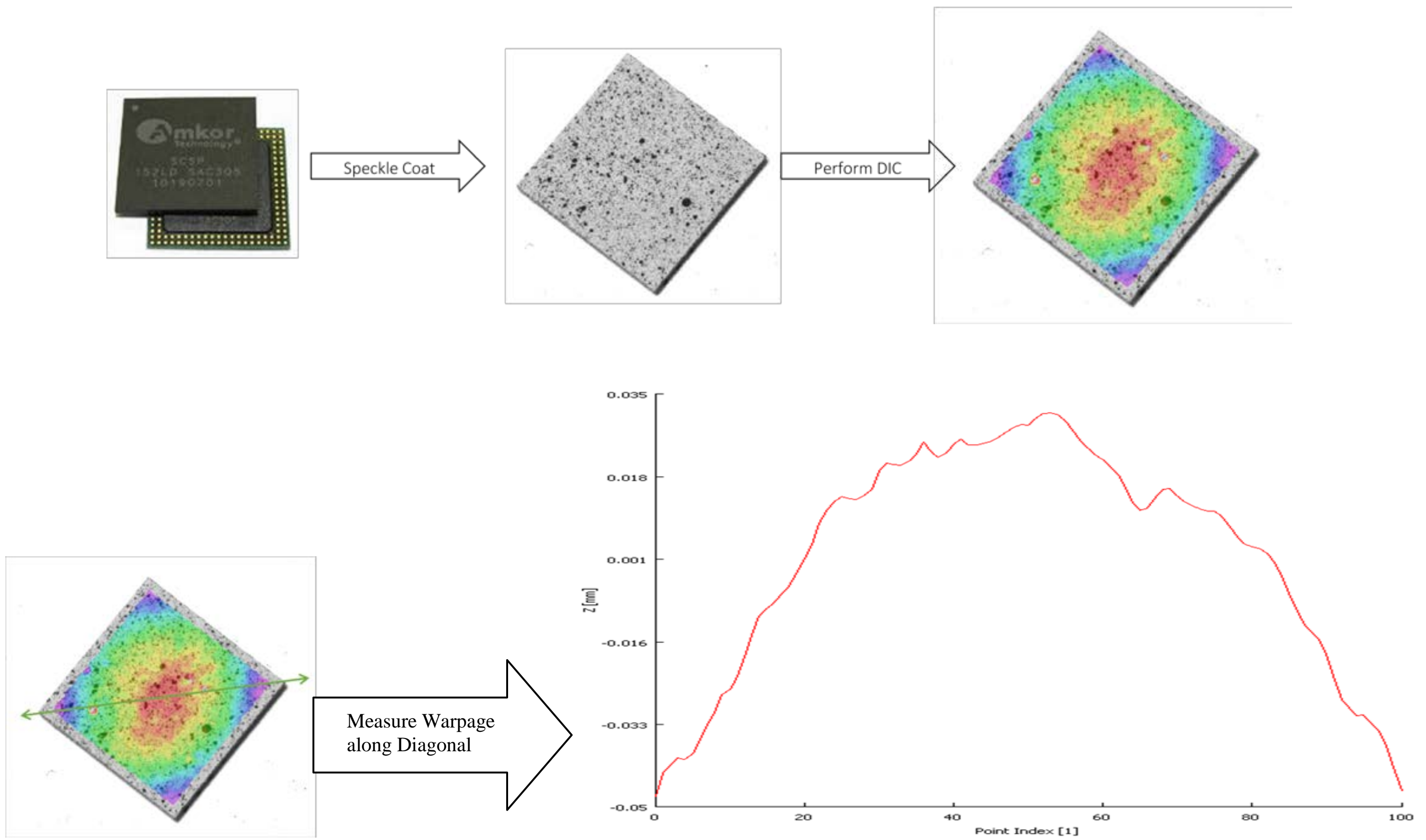

Figure 4.8: DIC Out-of-plane displacement contour

Warpage is typically measured from the corner of the package to the center. Figure 4.8 shows a representative warpage contour along with the diagonal along which warpage is measured.

4.4 Finite Element Analysis

Finite element analysis performed by Patel-[2013] to study the effect of material properties and package architecture on warpage has been used in this thesis to develop the statistical model for prediction of warpage. Patel-[2013] discusses about finite element model, analysis approach and results in detail. In this section a brief overview of package type modeled, constraints and analysis approach used in thesis by Patel-[2013] is given. A quarter symmetry model of TMV package with all the layers including epoxy molding compound (EMC), silicon die, copper layers, prepeg and laminate core were modeled [Patel 2013] in detail. To keep the finite element model as close to experimental test vehicle, the effect of through mold vias were considered and solder balls were not included to incorporate the effect of de-balling in experimentation. Linear properties model was used and solid elements were modeled using C3D8R elements. Quarter symmetry constraints were applied by constraining displacement in the X direction for nodes on the ZY plane and the Y direction for nodes on the XZ plane. Temperature boundary conditions were prescribed to reflect the reflow temperature profile used during experimentation. A static thermal analysis was performed using ABAQUS. Material properties required to define the baseline was determined using thermo-mechanical analyzer (TMA) and dynamic mechanical analyzer (DMA). [Patel 2013] has also considered the changes in material properties above and below the glass transition temperature (Tg). The mentioned thesis shows that there is a good correlation between the experimental and finite element results. Figure 4.9 shows a plot of correlation between the baseline experimental data and finite element analysis.

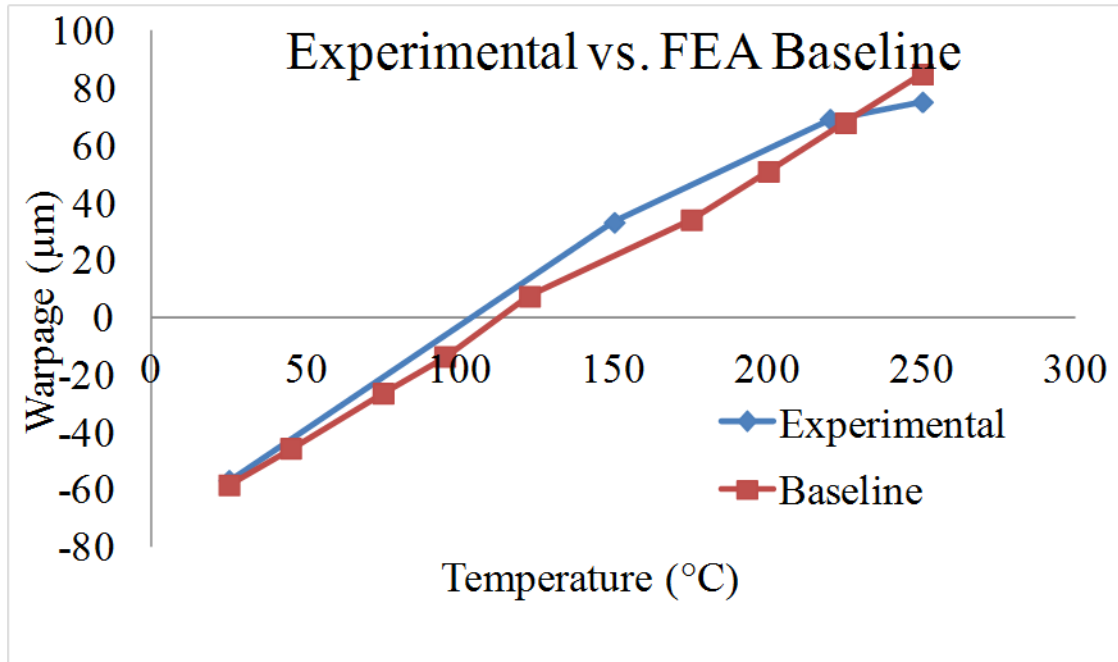

Figure 4.9: Experimental warpage Vs. FEA warpage [Patel 2013]

Once the correlation was established material properties such as CTE and elastic modulus were varied in finite element model to determine their effect on warpage. Similarly, package architecture such as package width, thickness, die width and thickness were varied to investigate their effect on warpage. The effect of these variations on warpage is documented in [Patel 2013].

4.5 Source of Data for Statistical Analysis

To develop the statistical model a complete data set is required which comprise of warpage response due to variation in material properties, package architecture and processing conditions. The experimental data were augmented with the finite element results for this purpose. Experiment showed the effect of process variable on glass transition temperature while the finite element results from thesis [Patel 2013], shed light on effects material selection has on warpage during reflow. The finite element results from aforementioned thesis were taken as is and both the experimental data and finite element results are used in conjunction to develop the statistical model. Combining both the results gave an input matrix consisting of all important variables which affect the warpage. Statistical analysis is done on this input variable matrix for model development.

4.6 Statistical Model Development Approach

To determine the relationship between a response variable and a set of predictor variables regression analysis has been performed. A particular regression analysis was selected to overcome the interdependency of predictor (input) variables. Multiple linear regression methods assume the predictor variables to be independent of each other. If predictor variables are related to each other, i.e. linearly dependent, it results in multi-collinearity, large variance and co-variance, high standard errors, fluctuation in magnitude of the regression coefficients for small changes in predictor variables and wider confidence intervals for regression coefficients. [Cook 1977]. One solution to multi-collinearity issues and obtain stable and meaningful estimates of regression coefficients is to use Principal components model [Fritts 1971]. In principal component analysis the set of X predictor variables are linearly transformed into new set of Z predictor variables known as principal components. The set of new orthogonal Z variables are uncorrelated with each other and together account for much of variation in predictor variables. The principal components correspond to the principal axes of the ellipsoid formed by scatter of simple points in the n dimensional space having X as a basis. The principal component transformation is thus a rotation from the original x coordinate system to the system defined by the principal axes of this ellipsoid [Massay 1965]. This transformation ranks the new orthogonal variables in order of their importance and the procedure then involves eliminating some of principal components to effect a reduction in variance. Scree plots, Eigen values and proportion of total variance explained by each principal component are then used to eliminate the least important principal components. After the elimination, multiple linear regressions have been performed with the original response variable and retained important set of principal components. The principal components estimators are then transformed back to original

predictor variables using the same linear transformation. Since the ordinary least square method has been used on principal components, which are pair wise independent, the new set of predictor coefficients are more reliable. Consider a data-set which consists of warpage as the response variable, y which depends on k-predictor variables including geometry, material properties and operating conditions. Assume that the data-set spans n-sets from the same package architecture and that the regression model is of the form,

$$y_i = \beta_0 + \beta_1 x_{1i} + \beta_2 x_{2i} + ... + \beta_k x_{ki} + \varepsilon_i \tag{6}$$

where x_1, x_2,…..x_k are the k-predictor variables, β_0, β_1, β_2,…… β_k are regression coefficients and ε_i is the model error for the ith data-set.

The model can be written in matrix notation as follows,

$$\{y\} = [X] + \{\beta\} + \{\varepsilon\} \tag{7}$$

Where,

$$\{y\} = \begin{Bmatrix} y_1 \\ y_2 \\ . \\ . \\ . \\ y_n \end{Bmatrix} \qquad \{\beta\} = \begin{Bmatrix} \beta_1 \\ \beta_2 \\ . \\ . \\ . \\ \beta_n \end{Bmatrix} \qquad \{\varepsilon\} = \begin{Bmatrix} \varepsilon_1 \\ \varepsilon_2 \\ . \\ . \\ . \\ \varepsilon_n \end{Bmatrix}$$

$$X = \overbrace{\begin{bmatrix} 1 & x_{11} & x_{21} & . & . & . & x_{k1} \\ 1 & x_{12} & x_{22} & . & . & . & x_{k2} \\ . & . & . & & & & \\ . & . & . & & & & \\ . & . & . & & & & \\ 1 & x_{1n} & x_{2n} & & & & x_{kn} \end{bmatrix}}^{\text{k predictor variables}} \tag{8}$$

The least squares estimator, {b}, of the regression coefficients, {β}, assuming that [X] is of full column rank,

$$\{b\} = [b_0 \quad b_1 \quad b_2 \quad . \quad . \quad . \quad b_k]^T = \left([X]^T [X]\right)^{-1} [X]^T \{y\} \tag{9}$$

The variance and co-variance matrix of the estimated regression coefficients in vector {b} is,

$$\text{var}\{b\} = \sigma^2 \left([X]^T [X]\right)^{-1} \tag{10}$$

Where each column of [X] indicates measurement of a particular predictor variable. One way of performing multiple linear regressions is to first either center and scale or standardize the independent variables. These transformations in the independent variables are useful as it allows results from different studies to be comparable. Once the Independent variables are centered and scaled, and then the variable, x_{ji}, is transformed as follows,

$$X^*_{ji} = \frac{x_{ji} - \bar{x}_j}{s_j} \tag{11}$$

Where,

$$S_j = \sqrt{\sum_{i=1}^{n} \left(x_{ji} - \bar{x}_{\ j}\right)^2} \tag{12}$$

The input variables matrix has been centered and scaled to develop an alternative formulation as follows,

$$y_i = \beta_0^* + \beta_1^* x_{1i}^* + \beta_2^* x_{2i}^* + \ldots. + \beta_k^* x_{ki}^* + \varepsilon_i \tag{13}$$

$$= \beta_0^* + \beta_1^* \frac{x_{ji} - \bar{x}_j}{s_j} + \ldots. + \beta_k^* \frac{x_{ki} - \bar{x}_k}{s_k} + \varepsilon_i$$

In matrix form the equation is written as follows,

$$\{y\} = \beta_0^* \{1\} + [X^*]\{\beta^*\} + \varepsilon_i \tag{14}$$

Where {1} is the unit vector, of size n x 1, and β^* is the vector of transformed coefficients. Centering and scaling makes $[X^*]^T[X^*]$ the k x k correlation matrix of the independent variables.

$$C = [X^*]^T [X^*] \tag{15}$$

where C is correlation matrix. Principal components regression is the method to deal with problem of multicollinearity and results in estimation and predictions better than ordinary least squares. With this method, the original k predictor-variables have been transformed into a new set of orthogonal or uncorrelated variables called principal components of the correlation matrix. The transformation has been used to rank the new orthogonal variables in the order of their importance. Some of the principal components have been eliminated for reduction in variance. Multiple regression analysis of response variables using ordinary least squares has been done against a reduced set of principal components. The regression coefficients of the reduced set of principal components have then been transformed into new set of coefficients that correspond to the original correlated variables. The new coefficients are called principal component estimators. Eigenvalues of the Correlation Matrix, [C], have been calculated using the following determinant equation,

$$([C] - \lambda[I])[V] \tag{16}$$

$$\Rightarrow \left|[C] - \lambda[I]\right| = 0 \quad \text{or} \quad \left|[X^*]^T [X^*] - \lambda[I]\right| = 0$$

Where $\lambda_1, \lambda_2, \ldots, \lambda_k$ are the eigenvalues of the correlation matrix, and $[V]$ is a k x k eigenvector matrix consisting of normalized eigenvectors associated with each eigenvalues. Since, the eigenvectors are orthogonal, $[V][V]^T = I$. The regression equation of centered and scaled variables can be written as follows,

$$\{y\} = \beta_0^* + [X^*]\{\beta^*\} + \{\varepsilon\} \tag{17}$$

$$\Rightarrow \{y\} = \beta_0^*\{1\} + [X^*][V][V]^T\{\beta^*\} + \{\varepsilon\}$$

$$\Rightarrow \{y\} = \beta^*\{1\} + [Z]\{\alpha\} + \{\varepsilon\}$$

Where $[Z]$ is an n x k matrix of principal components and $\{\alpha\}$ is a vector of new regression coefficients. The new model formulation is then written as follows,

$$y_i\big|_{1<i<n} = \beta_0^* + \alpha_1 z_1 + \alpha_2 z_2 + \ldots + \alpha_k z_k + \varepsilon_i \tag{18}$$

Where $z_1, z_2, \ldots, z_k$ are the new variables called principal components of the correlation matrix $[C]$. The principal components are orthogonal to each other. Each principal component is a linear combination of transformed predictor variables.

where,

$$z_j = \left[x_1^* \quad x_2^* \quad . \quad . \quad . \quad x_k^* .\right] \underbrace{\begin{Bmatrix} v_{1j} \\ v_{2j} \\ . \\ . \\ . \\ v_{kj} \end{Bmatrix}}_{\text{Eigenvector associated with } \lambda_1} \tag{19}$$

Based on the rationale that the principal component with smallest eigenvalue is the least informative, principal components have been eliminated by discarding the component associated with the smallest eigenvalue. Using this procedure, principal components are eliminated until the remaining components explain some pre-selected percentage of the total variance (for example, 85 percent or more). The coefficients for the centered and scaled variables are obtained as follows,

$$\{\alpha\}_{kx1} = [V]^T \{\beta^*\}$$

$$\Rightarrow [V]\{\alpha\}_{kx1} = [V][V]^T \{\beta^*\} \tag{20}$$

$$\Rightarrow \{\beta\}_{kx1} = [V]_{kx1} \{\alpha\}_{kx1}$$

Where $[V]$ is the eigenvector matrix and $\{\alpha\}$ is a vector of new regression coefficients. Assume that r-variables have been dropped. A principal component analysis has been performed on this original predictor variable matrix X and its eigenvalues and corresponding Eigen vectors have been extracted. The transformation to coefficients of the natural variables is done as follows,

$b_{j,pc} = (b^*_{j,\,pc} / s_j)$ where, j = 1, 2,…, k (21)

The first four eigen vectors explained more than 85% of the original matrix and had eigen values greater than 1. A kink in scree plot supports the selection of first four eigen vectors. A transformation matrix, V has been created with first four eigen vectors.

4.7 Failure Modes

Final equation is formulated based on the natural log transformed PCR. Natural log of all the predictor variables are taken and then based on this new transformed variables the regressions coefficients are calculated. When converted back to original scale the final equation is of power form and is shown below

$$Y = A * X_1^{\beta_1} * X_2^{\beta_2} * X_3^{\beta_3} * .... * X_n^{\beta_n} \quad (22)$$

Where,

Y = Response (Warpage)

A = Constant

X_1, X2, X3, X4…. = Predictor Variables

$\beta 1,\ \beta 2,\ \beta 3,\ \beta 4$….= Coefficients from PCR

Table 4 shows all predictor variables along with their calculated regression coefficients. The response variable is delta-warpage, which is defined as the absolute change in warpage from the initial warpage of the package-on-package. The initial warpage of the package-on-package is an input variable in equation 24. The delta warpage is defined by the following equation:

$$Warpage_{FINAL} = Warpage_{INITIAL} + \Delta Warpage \quad (23)$$

In order to compute the final warpage the user can (1) first compute the delta-warpage using equation (24), then (2) add the delta warpage to the initial warpage of the assembly to get the value of final warpage after reflow.

Variables	Beta
Bo	-6.175812824
Pkg_Width (mm)	-4.002694876
Die_Width (mm)	1.119915688
Die_Thicknes s(µm)	-0.300239659
Die_E (Gpa)	0.266884426
Die_CTE (ppm)	-0.301377463
Core_Thickness (µm)	-0.002835812
Core_E (Gpa)	-0.250345809
Core_CTE (ppm)	0.150896399
Mold_Thickness (µm)	-0.187471596
Mold_E1 (Gpa)	-0.175263209
Mold_E2 (Gpa)	-0.235199487
Mold_CTE1 (ppm)	-0.474303101
Mold_CTE2 (ppm)	-0.381094443
Peak Temp (C)	2.069406884
Temp (C)	1.238669196
absIW (µm)	1.135436023

Table 4.4: PCR Beta Coefficients

The final form of the equation is shown below.

$$\Delta Warpage = e^{-6.17} * PkgWdtMM^{-4.00} * ChipWdtMM^{1.12} * ChipThkMICM^{-0.30} * ChipEmodGPA^{0.27} * ChipCtePPMC^{-0.30} * CoreThkMICM^{-0.0028} * CoreEmodGPA^{-0.25} * CoreCtePPMC^{0.15} * MoldThkMICM^{-0.19} * MoldEmod1GPA^{-0.18} * MoldEmod2GPA^{-0.23} * MoldCte1PPMC^{-0.47} * MoldCte2PPMC^{-0.38} * PeakTempC^{2.07} * TempC^{1.24} * absInitWarpMICM^{1.14}$$

4.8 Convergence of Predicted Vs Measured Values

Convergence of warpage predictions from the statistical model and experimental values is investigated. The statistical model is used to predict the warpage for variation in any one predictor variable while keeping all other constant. Figure 4.10 through Figure 4.24 are plots showing the correlation between the statistical models and finite element with the experimental data. The effect of individual parameters on the delta warpage has been categorized into three categories including (1) effect of process variables (2) effect of material properties (3) effect of assembly dimensions.

4.8.1 *Effect of Process Variables*

Figure 4.10 to Figure 4.12 show the effect of process variables on the delta warpage of a package-on-package assembly. Experimental data in Figure 4.10 shows that the delta warpage increases with the increase in value of initial warpage. The PCR model captures the magnitude and rate of change of the delta warpage with the absolute value of initial warpage quite well. Figure 4.11 shows the effect of ambient temperature on the delta warpage of the package-on-package assembly

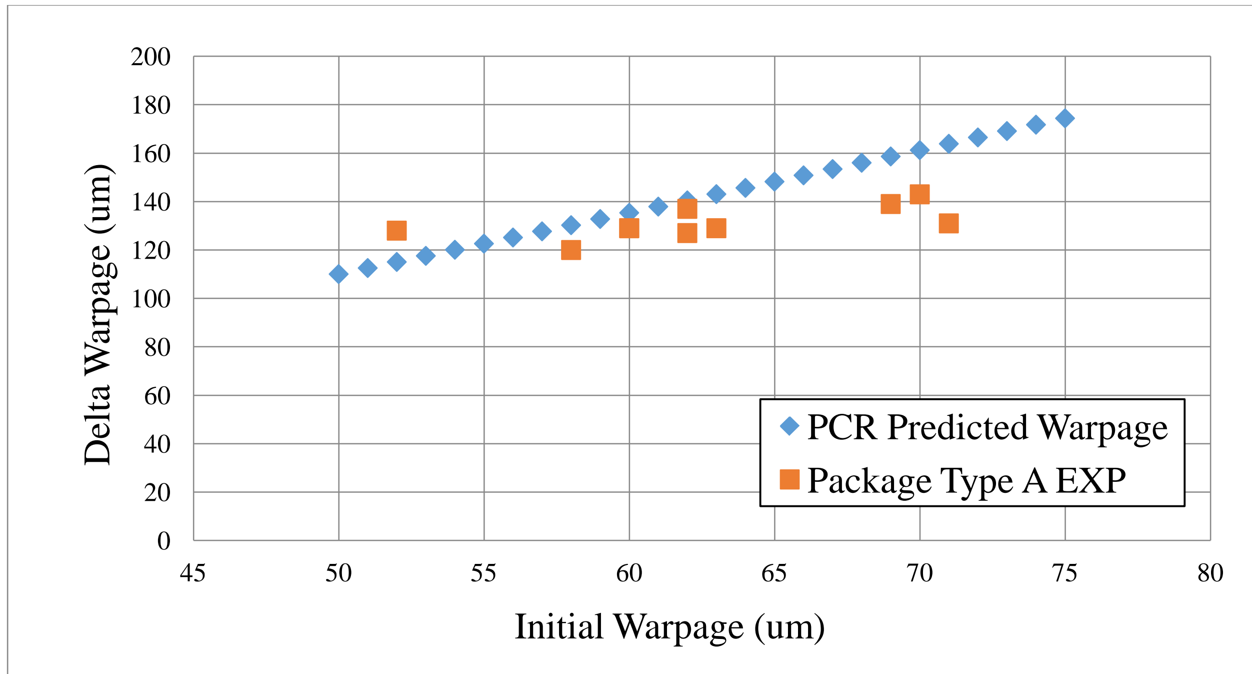

Figure 4.10: PCR Predicted vs Measured for change in Initial Warpage

Experimental data shows that the delta warpage increases with the increase in the ambient temperature of the package- on-package assembly. The PCR model captures the magnitude and rate of change of the delta warpage with the ambient temperature quite well. Figure 4.12 shows the effect of peak reflow temperature on the delta warpage after reflow. Experimental and simulation data shows that the delta warpage after reflow increases with the increase in the peak reflow temperature. The PCR model captures the magnitude and rate of change of the delta warpage with the peak reflow temperature quite well.

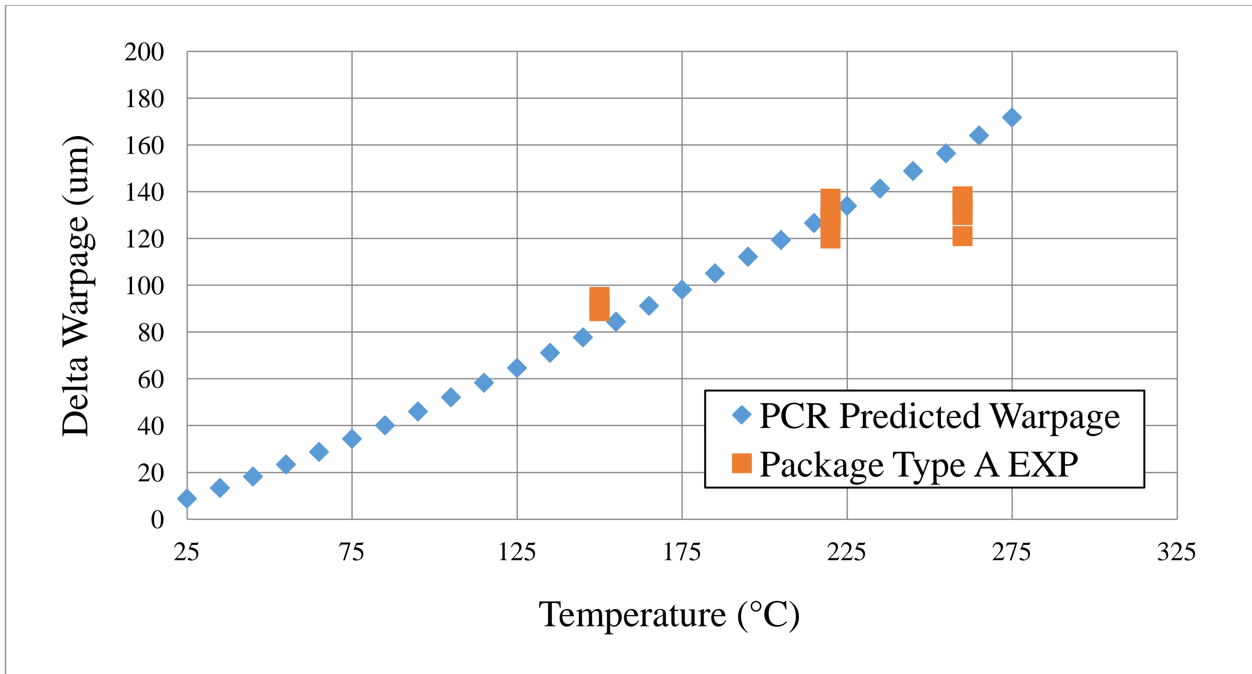

Figure 4.11: PCR Predicted vs Measured for change in Temperature

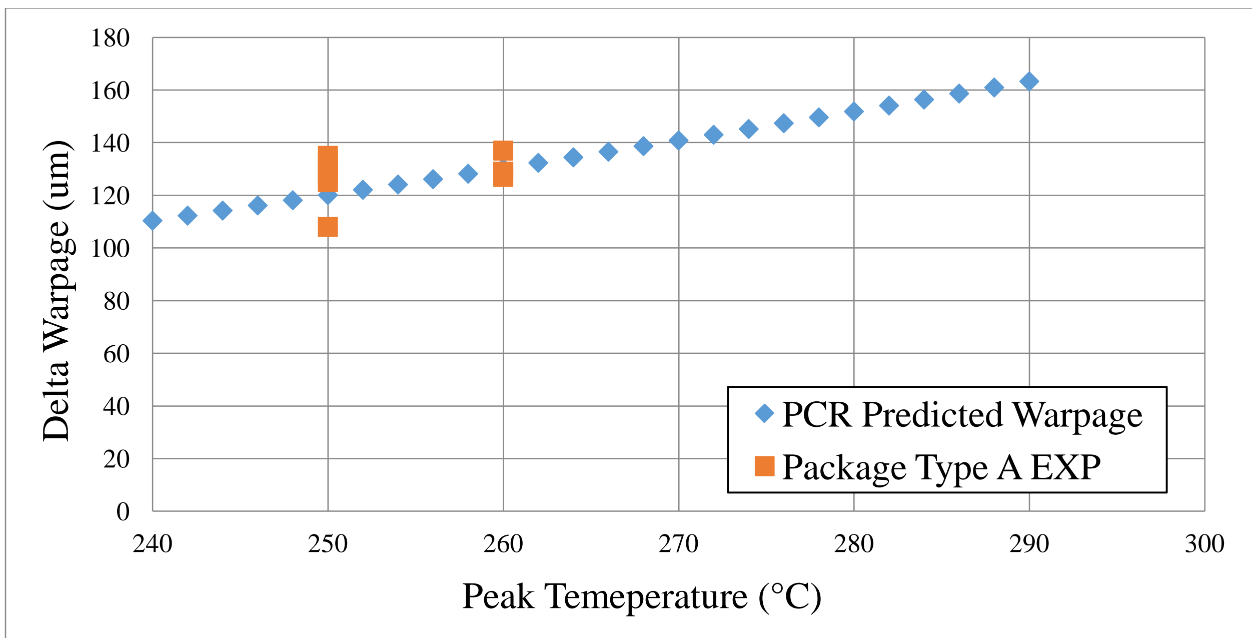

Figure 4.12: PCR Predicted vs Measured for change in Peak Temperature

4.8.2 *Effect of Material Properties*

Figure 4.13 to Figure 4.19 show the effect of the material properties on the delta warpage of the package-on-package assembly. The delta warpage of the package-on-package assembly increases with the increase in the elastic modulus of the chip or the stiffness of the chip.

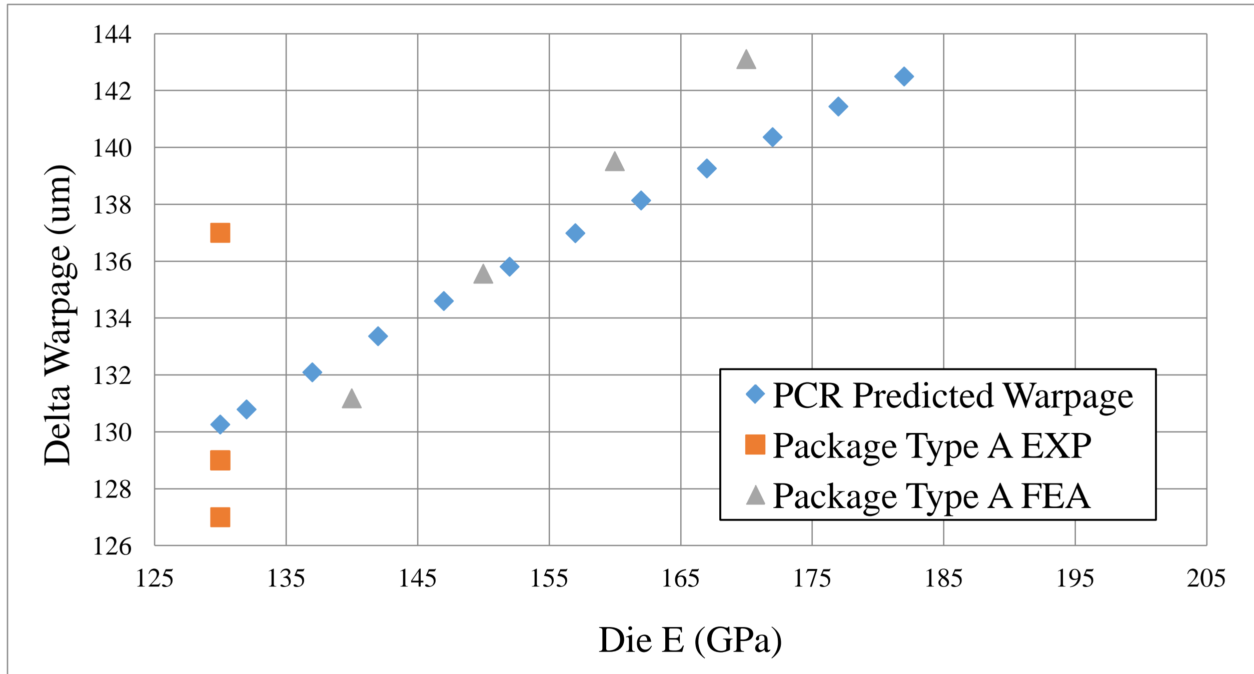

Figure 4.13: PCR Predicted vs Measured for change in Die E

The trend has been found to hold true for multiple package types. The PCR model predictions correlate well with the experimental data and finite element model predictions both in terms of magnitude and the rate of change of delta warpage with the change in elastic modulus of the chip.

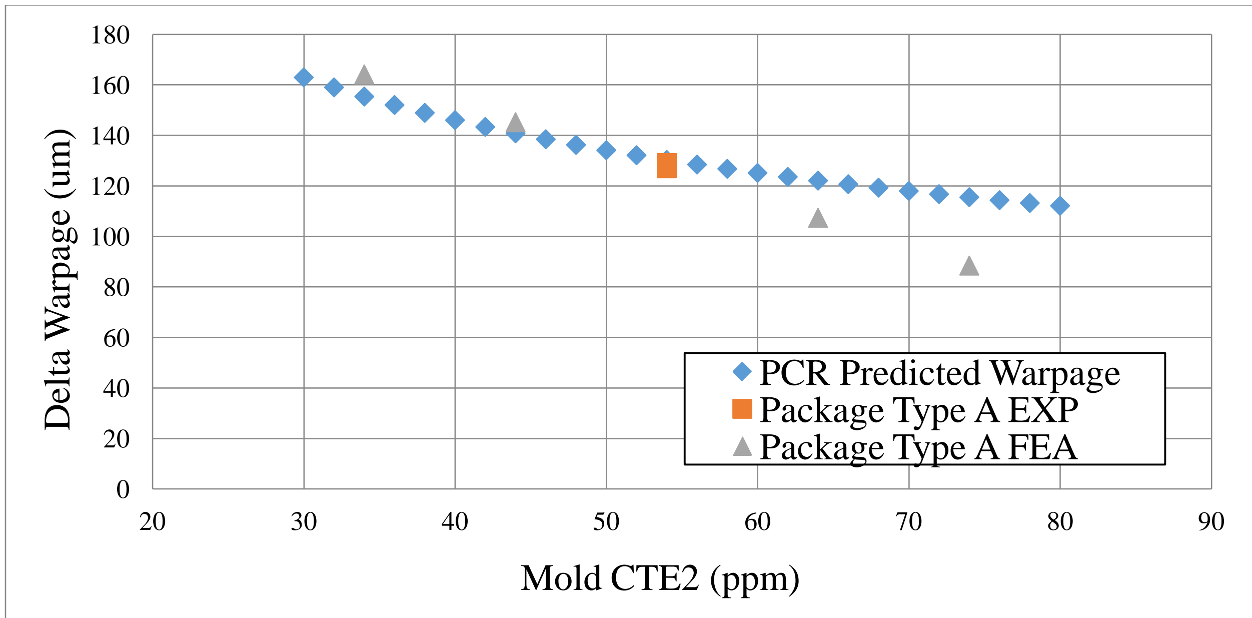

Figure 4.14: PCR Predicted vs Measured for change in Mold CTE2

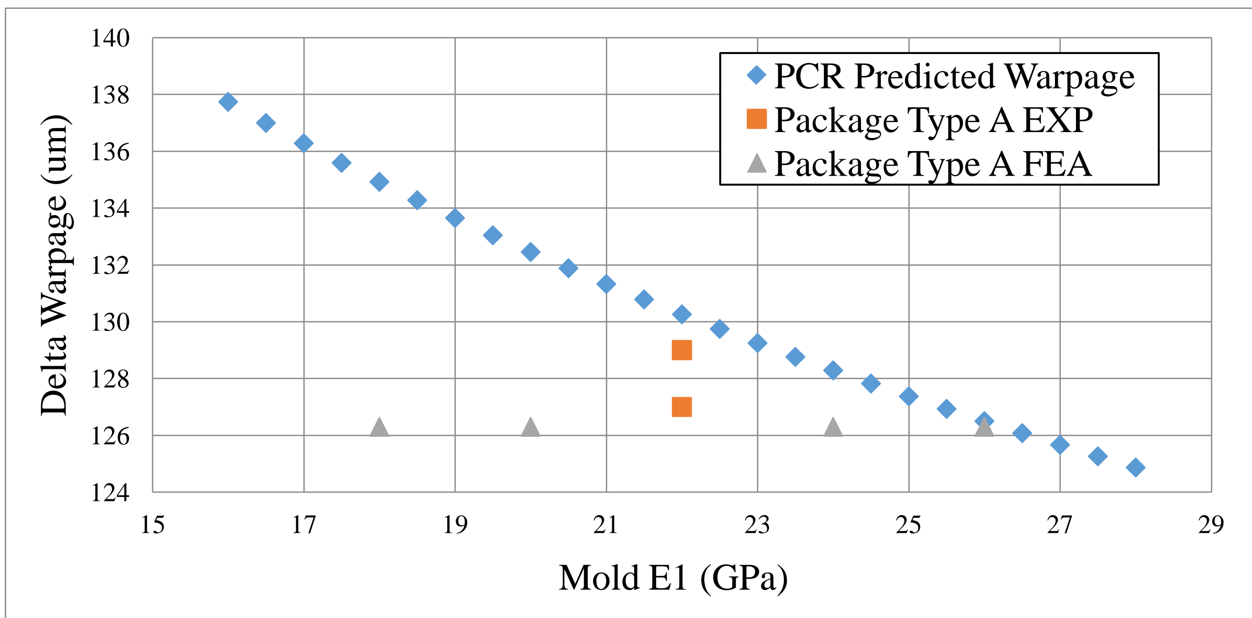

Figure 4.15: PCR Predicted vs Measured for change in Mold E1

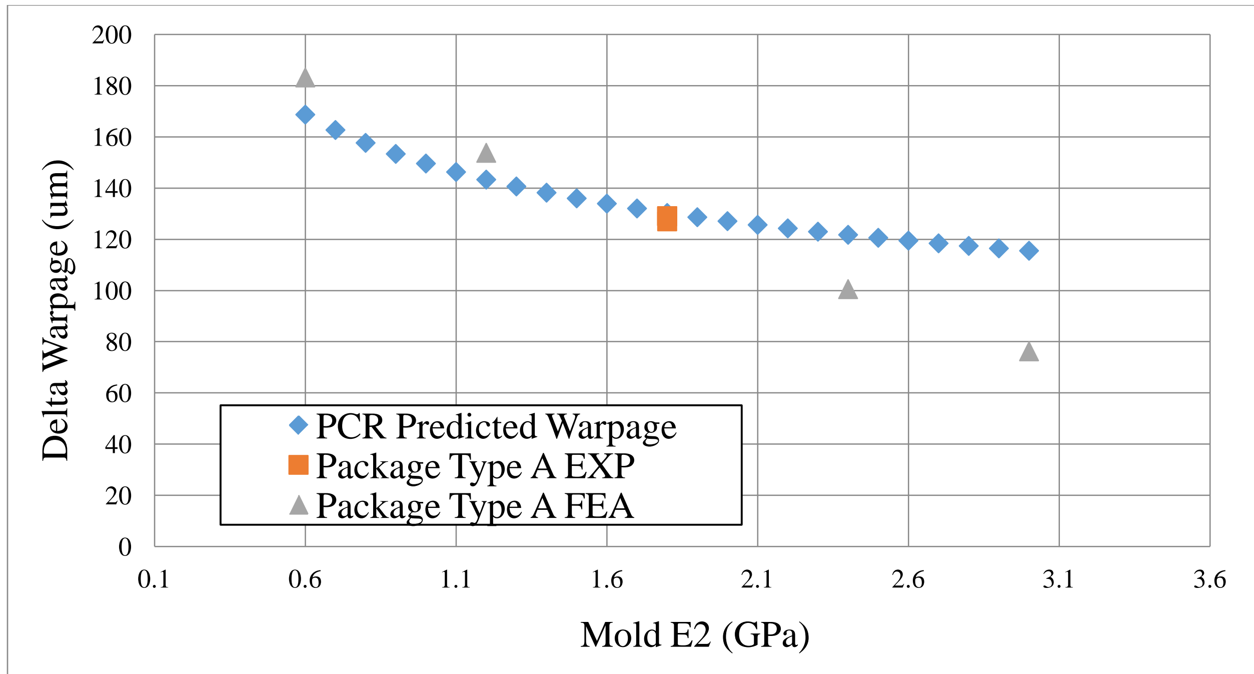

Figure 4.16: PCR Predicted vs Measured for change in Mold E2

Figure 4.14 shows the effect of electronic molding compound's coefficient of thermal expansion above the glass transition temperature (MoldCTE2 in ppm/°C) on the delta warpage of the package-on-package assembly after reflow. Experimental and simulation data across multiple package-on- package assemblies show a decrease on the delta warpage with increase in the molding compound's coefficient of thermal expansion above the glass transition temperature. The PCR model correlates well with the experimental and finite element model predictions of delta warpage in terms of both magnitude and rate of change of delta warpage versus molding compound's coefficient of thermal expansion above the glass transition temperature.

Figure 4.15 shows the effect of electronic molding compound's elastic modulus below the glass transition temperature (MoldE1 in GPa) on the delta warpage of the package-on-package assembly after reflow. Experimental and simulation data across multiple package-on-package

assemblies show a relatively minimal effect on the delta warpage with increase in the molding compound's elastic modulus below the glass transition temperature. The PCR model over predicts the experimental and finite element model predictions of delta warpage in terms of both magnitude and rate of change of delta warpage versus molding compound's elastic modulus below the glass transition temperature. Figure 4.16 shows the effect of electronic molding compound's elastic modulus above the glass transition temperature (MoldE2 in GPa) on the delta warpage of the package-on- package assembly after reflow. Experimental and simulation data across multiple package-on-package assemblies show a decrease in the delta warpage with increase in the molding compound's elastic modulus above the glass transition temperature. The PCR model correlates well with experiment data and the finite element model results in terms of both magnitude and rate of change of delta warpage versus molding compound's elastic modulus above the glass transition temperature.

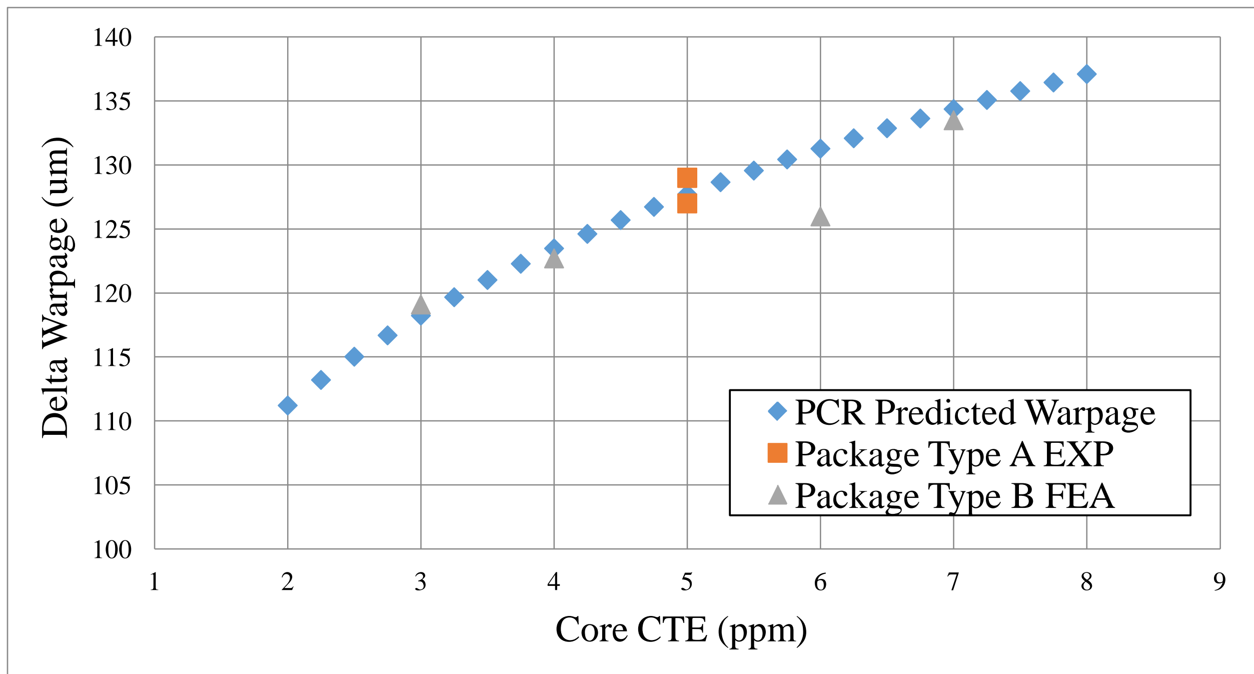

Figure 4.17: PCR Predicted vs Measured for change in Core CTE

Figure 4.17 shows the effect of package substrate core's coefficient of thermal expansion below the glass transition temperature (CoreCTE in ppm/°C) on the delta warpage of multiple types of package-on-package assemblies after reflow. Experimental and simulation data across multiple package-on-package assemblies show an increase in the delta warpage with increase in the substrate core's coefficient of thermal expansion below the glass transition temperature. The PCR model correlates well with the experimental and finite element predicted values of delta warpage in terms of both magnitude and rate of change of delta warpage versus substrate core's coefficient of thermal expansion below the glass transition temperature. Figure 4.18 shows the effect of substrate core's elastic modulus below the glass transition temperature (CoreE in GPa) on the delta warpage of the package-on-package assembly after reflow. Experimental and simulation data across multiple package-on-package assemblies show a decrease of the delta warpage with increase in the substrate core's elastic modulus below the glass transition temperature. The PCR model correlates well with the experimental and finite element model values of delta warpage in terms of both magnitude and rate of change of delta warpage versus substrate core's elastic modulus below the glass transition temperature.

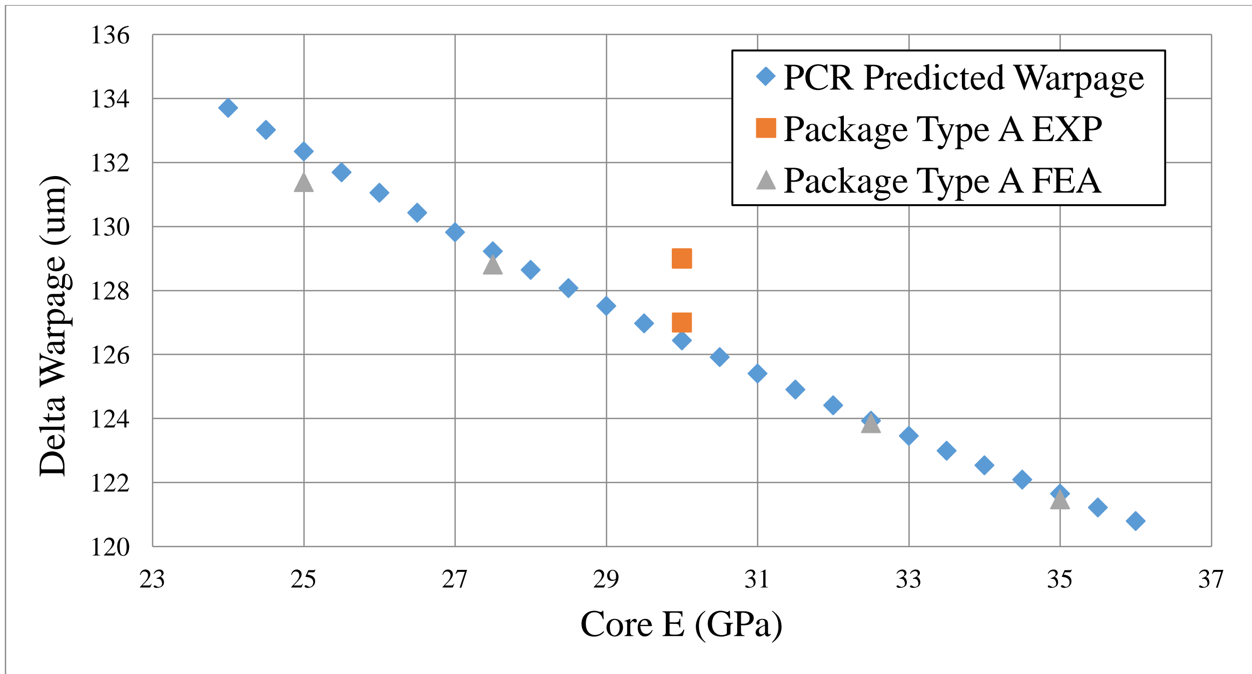

Figure 4.18: PCR Predicted vs Measured for change in Core E

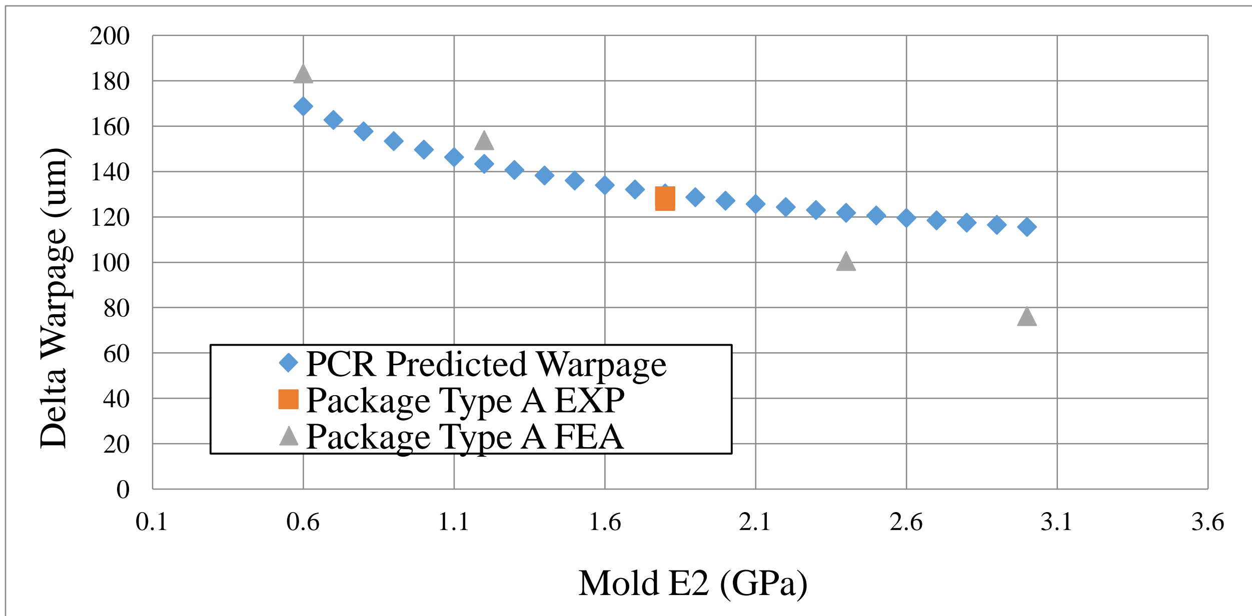

Figure 4.19: PCR Predicted vs Measured for change in Die CTE

Figure 4.19 shows the effect of package chip's coefficient of thermal expansion (ChipCTE in ppm/°C) on the delta warpage of multiple types of package-on-package assemblies after

reflow. Experimental and simulation data across multiple package-on-package assemblies show a decrease in the delta warpage with increase in the package chip's coefficient of thermal expansion. The PCR model correlates well with the experimental and finite element model's delta warpage in terms of both magnitude and rate of change of delta warpage versus package chip's coefficient of thermal expansion.

4.8.3 *Effect of Assembly Dimensions*

Figure 4.20 to Figure 4.24 shows the effect of the change in the package element dimensions on the package-on-package assembly warpage after reflow.

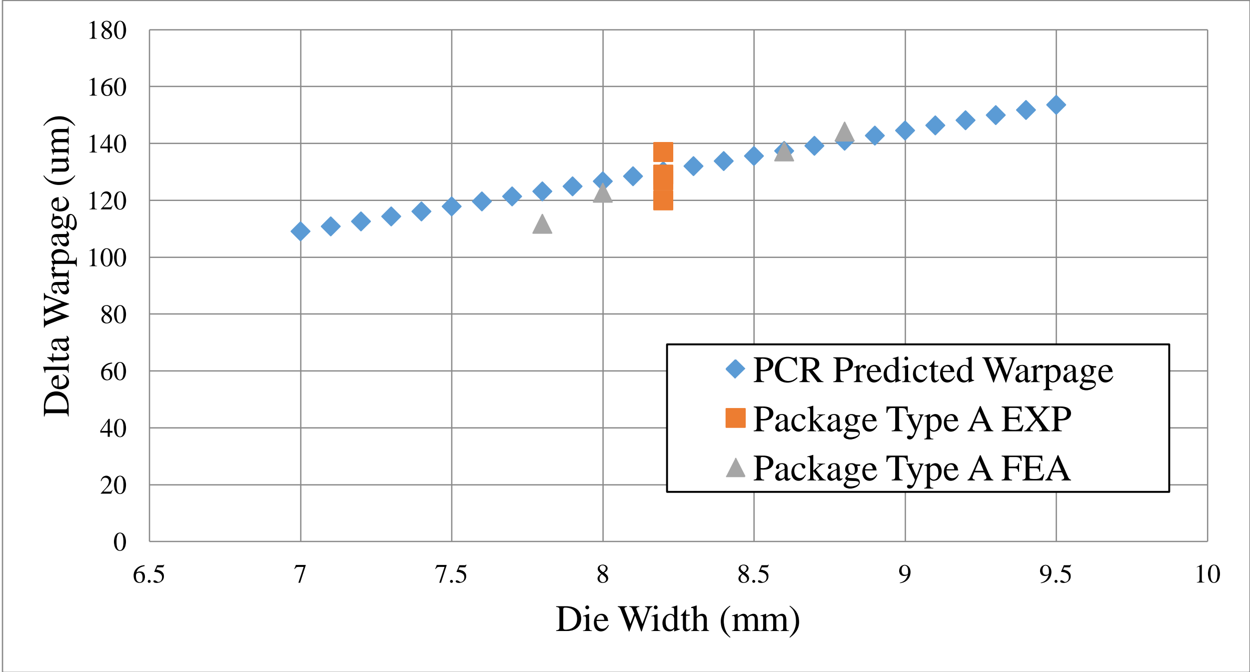

Figure 4.20: PCR Predicted vs Measured for change in Die Width

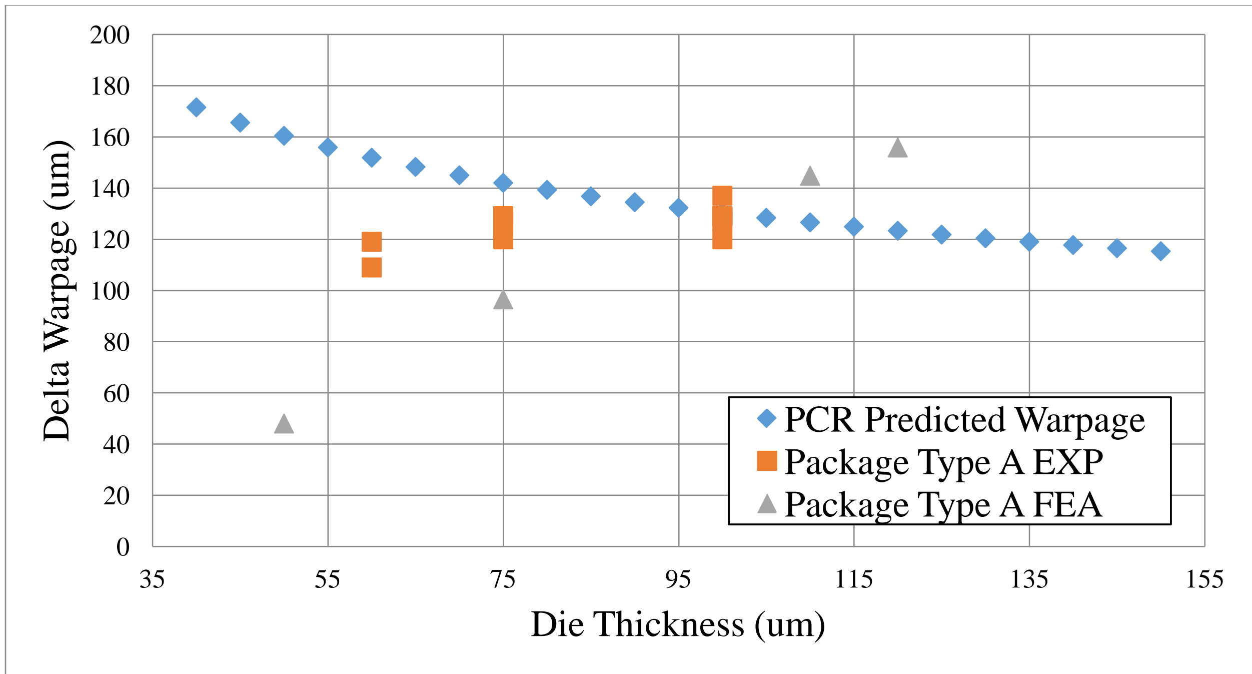

Figure 4.21: PCR Predicted vs Measured for change in Die Thickness

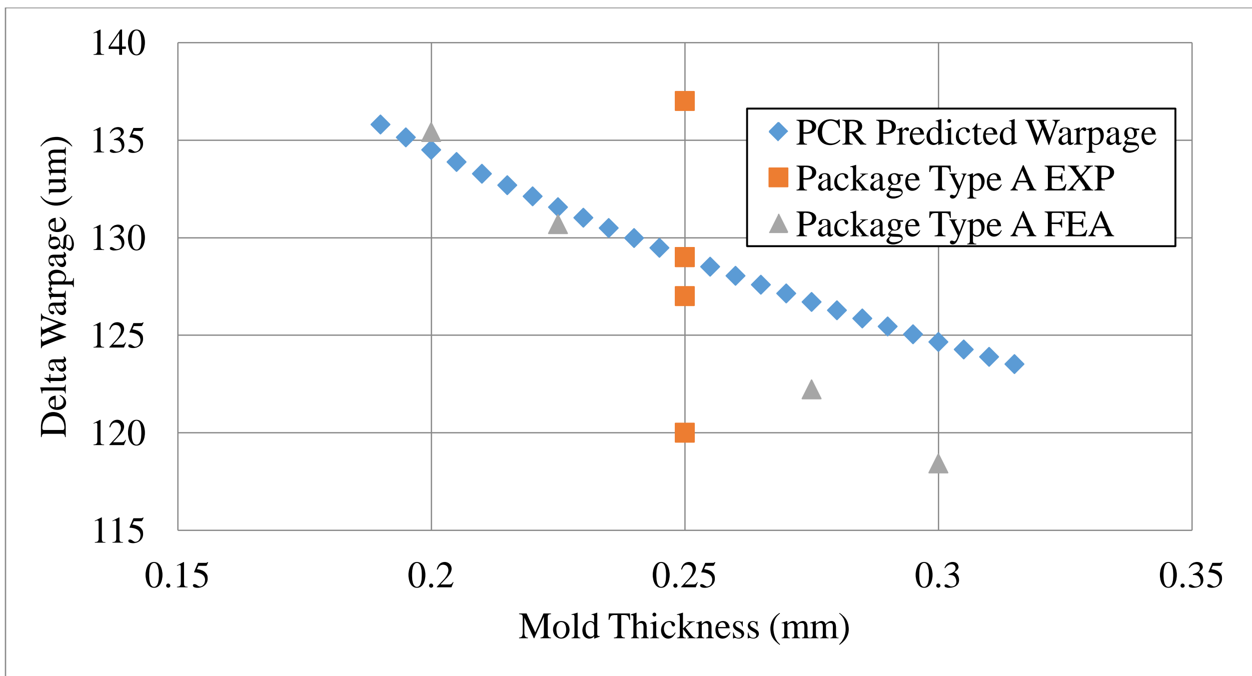

Figure 4.22: PCR Predicted vs Measured for change in Mold Thickness

Figure 4.20 shows the effect of chip width (mm) on the delta warpage of multiple types of package-on-package assemblies after reflow. Experimental and simulation data across multiple package-on-package assemblies show an increase in the delta warpage with increase in the package chip's width. The PCR model correlates well with the experimental and finite element model's delta warpage in terms of both magnitude and rate of change of delta warpage versus package chip's width. Figure 4.21 shows the effect of chip thickness (mm) on the delta warpage of multiple types of package-on-package assemblies after reflow. Experimental and simulation data across multiple package-on-package assemblies show an increase in the delta warpage with increase in the package chip's thickness. The PCR model does not capture the trend shown by the experimental and finite element model's delta warpage in terms of both magnitude and rate of change of delta warpage versus package chip's thickness. Figure 4.22 shows the effect of mold thickness (mm) on the delta warpage of multiple types of package-on-package assemblies after reflow. Experimental and simulation data across multiple package-on-package assemblies show a decrease in the delta warpage with increase in the mold's thickness. The PCR model captures the trend shown by the experimental and finite element model's delta warpage in terms of both magnitude and rate of change of delta warpage versus mold's thickness.

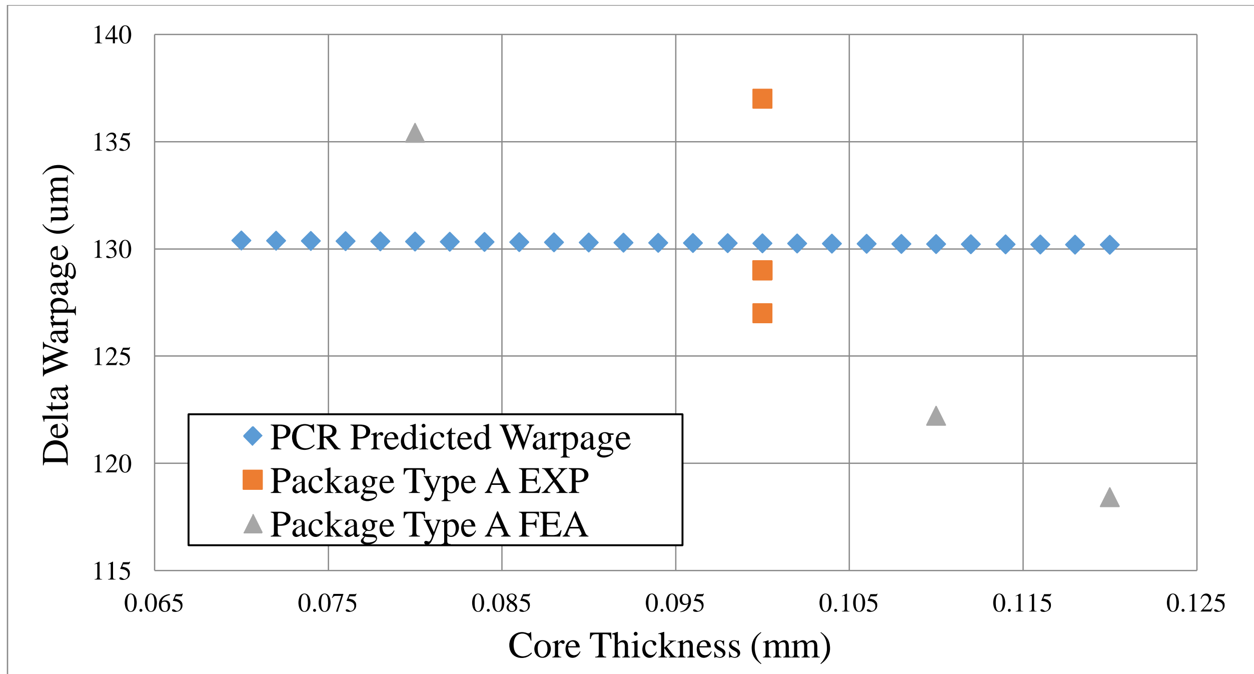

Figure 4.23: PCR Predicted vs Measured for change in Core Thickness

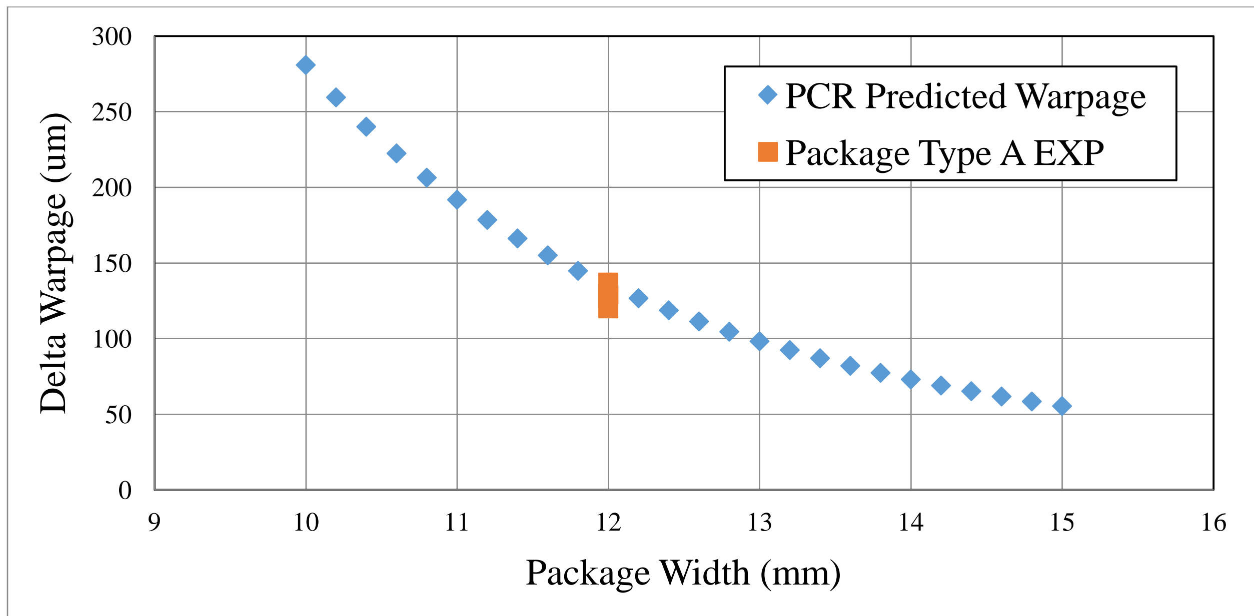

Figure 4.24: PCR Predicted vs Measured for change in Package Width

Figure 4.23 shows the effect of core thickness (mm) on the delta warpage of multiple types of package-on-package assemblies after reflow. Experimental and simulation data across multiple

package-on-package assemblies show a decrease in the delta warpage with increase in the core's thickness. The PCR model does not capture the trend shown by the experimental and finite element model's delta warpage in terms of both magnitude and rate of change of delta warpage versus core's thickness. Figure 4.24 shows the effect of package width (mm) on the delta warpage of multiple types of package-on-package assemblies after reflow. Experimental and simulation data across multiple package-on-package assemblies show a decrease in the delta warpage with increase in the package width. The PCR model captures the trend shown by the experimental and finite element model's delta warpage in terms of both magnitude and rate of change of delta warpage versus package width.

4.9 Inverse Determination of Desired Material Properties, Process Conditions and Package Element Dimensions

In order to determine the desired material properties, process conditions and package element dimensions to get the desired upper bound on the warpage after reflow, Equation (24) has been used to solve for the desired range of parameters. In general, it is not possible to vary all the parameters in a package-on-package assembly. For example, an end-user or an assembly house may only be able to vary the process conditions of assembly of the package-on-package assembly. On the other hand, the part manufacturer may recommend process conditions but may have no actual control over the actual process conditions used by the end-users of the package-on-package assembly. A part manufacturer may be able to control the package dimensions and the material selection much more effectively. A base configuration of the package-on-package assembly may be taken as a given value. This base configuration may consist of either a given set of process conditions or a given sent of material properties and package dimensions (Table 4.5). The use of the inverse model may then vary one or more parameters at a time and evaluate the effect of the variation on the warpage of the package-on-package assembly after reflow. The desired range of the values of input parameters may then be identified in this manner. Table 4.6 shows an example where a maximum warpage of -80μm is desired. The mold CTE1 is varied and the corresponding warpage is calculated. All other values are kept constant.

Parameter	Value
Pkg_Width (mm)	12
Die_Width (mm)	8
Die_Thickness (µm)	100
Die Elastic Modulus (Gpa)	130
Die CTE (ppm/°C)	2.9
Core Thickness (µm)	0.12
Core Elastic Modulus (Gpa)	25
Core CTE (ppm/C)	4
Mold Thickness (µm)	0.3
Mold E1 (Gpa)	20
Mold E2 (Gpa)	1
Mold CTE1 (ppm/°C)	Varies
Mold CTE2(ppm)	60
Peak Temp (°C)	260
Temp (°C)	250
Absolute IW(µm)	50

Table 4.5: Example Base Configuration for Package-on-Package Warpage

Mold CTE1	Warpage
13	-87.52
13.25	-86.28
13.5	-85.08
13.75	-83.91
14	-82.77
14.25	-81.66
14.5	-80.58
14.75	-79.52
15	-78.50
15.25	-77.49
15.5	-76.51
15.75	-75.56
16	-74.62

Table 4.6: Effect of Mold CTE1 on the Package-on-Package Warpage

It can be seen in Table 6 that for Mold CTE1 values less than 14.5 ppm/°C the warpage is greater than the desired value of -80µm. In order to keep the package-on-package assembly warpage within the desired limit Mold CTE1 should be greater than 14.5 ppm/°C. Similarly,

individual parameters in the base configuration have been varied to determine the allowable variation in the base value. Required range of input parameters for the desired upper bound of package-on-package assembly warpage has been computed using a similar process and shown in Table 4.7.

Desired Maximum Warpage @ 250°C (μm)	PCR Predicted ΔWarpage	PCR Predicted Warpage	Material Selection Guideline
-80	130.57	-80.57	MoldCTE1≥14.5 ppm
-80	129.32	-80.16	Mold CTE2≥58 ppm
-80	132.12	-80.12	Mold E1 ≥22 GPa
-80	134.61	-79.61	Mold E2 ≥1.3 GPa
-80	115.37	-79.78	Core E ≥27 GPa
-80	116.21	-80.79	Core CTE ≤4.5 ppm

Table 4.7: Usability of PCR Model

Chapter 5

Summary and Future Work

The aim of this study has been to use statistical tool to evaluate and analyze the measured experimental data. Statistical based modeling methodologies have been presented in this work. These methods have been used to investigate the significance of change in glass transition temperature of printed circuit board and also to develop mathematical model to predict warpage of PoP package. This study also shows the feasibility of FE modeling for performing investigative studies to augment experimental data. Models were developed to study the effect of material properties on warpage of package.

In chapter 3, the study showed the high-temperature exposure associated with lead free reflow process produced noticeable change in the glass transition temperature of the laminates. The Tg of a polymer is dependent on several parameters such as degree of cross-linking, molecular weight and entrapped plasticizers. For Mid Tg laminates time above liquidus and peak temperature had significant effect on the glass transition temperature. The variation in mean of Tg between control and other reflowed samples was more than 10^{0}C. The drop in glass transition temperature for TAL 30sec to 150sec and for peak temperature 225°C to 290°C was not very high but the change was significant. On the other hand for different number of passage through reflow chamber, mid Tg Laminates first showed decrease and then a slight increase. From control sample to 2x reflow there was a drop but for 6x reflow there was an increase in glass transition temperature. Statistical analysis showed that the variation was significant. For High Tg

laminates when time above liquidus was varied the drop was significant for all the three cases when compared to control sample. Analysis showed that there was no significant change in glass transition temperature between samples reflowed at 90sec and 150sec but they both varied significantly from samples reflowed at 30sec.Same hold true for peak temperature where the change in glass transition temperature at higher temperatures was not significant. These high Tg laminates showed significant drop in glass transition temperature as the number of reflow is increased. Study results show that the manufacturing process variables do affect the glass transition temperature in a statistically significant.

For this study, in future it would be interesting to investigate the effect of thermal cycling, aging with and without humidity on not only glass transition temperature of printed circuit board but also on other material properties. The study can also be expanded to various PCB available in market to see if the behavior is generic or certain factor dependent.

Chapter 4 talks about Physics based statistical model capable of predicting warpage values based on an input variable matrix has been presented. The statistical model was based on a data set with provided from both experimental analysis and finite element analysis. Experimental warpage results were determined using an optical examination technique called digital image correlation or DIC. Finite element analysis has been correlated with experimental values [Patel 2013]. Physics based statistical model capable of predicting warpage values based on an input variable matrix has been presented. The statistical model was based on a multivariate method called principal component regression or PCR. The developed model has been validated with experimental data and finite element analysis. The model has been used to solve for the desired range of parameters in order to determine the desired material properties, process conditions and package element dimension to get the wanted upper bound on the warpage after

reflow. It allows user to use the inverse model to evaluate the effect of the variation of one or more parameters on the warpage of PoP assembly after reflow and identify the desired range of the values of input parameters. The developed model is a time effective solution for assessing the range of various input parameters required to keep the warpage within the tolerable limits.

For warpage study only reflow temperatures were investigated but as electronics are subjected to a wide range of temperature, it would be interesting to see warpage response corresponding to very high and low temperature.

BIBLIOGRAPHY

Chew, S., E. Lim. Monitoring Glass Transition of Epoxy Encapsulant Using Thermal Analysis Techniques,Penang, Malaysia, ICSE'96 Proceedings, Nov. 1996

Ganesan, S., M. Pecht, *Lead-Free Electronics*. Piscataway, NJ, IEEE Press, Wiley-Interscience, 2006.

ISO 11357-2: Plastics - Differential scanning calorimetry (DSC) - Part 2: Determination of glass transition temperature (1999).

Peng, Y., X. Qi, and C. Chrisafides, The influence of curing systems on epoxide-based PCB laminate performance, *Circuit World*, vol. 31,no. 4, pp. 14–20,2005.

Polansky, R., V. Mentlık, P. Prosr, J. Susir. Influence of thermal treatment on the glass transition temperature of thermosetting epoxy laminate. Polymer Testing, Vol. 28, pp. 428–436, 2009.

Ritchey, L. W., A survey and tutorial of dielectric materials used in the manufacture of printed circuit boards. Speeding Edge, Circuitree Magazine, November 1999.

Sanapala,*R.,* B. Sood, D. Das, M. Pecht, Effect of Lead- Free Soldering on Key Material Properties of FR-4 Printed Circuit Board Laminates. IEEE Transactions on Electronics Packaging Manufacturing, Vol. 32, No. 4, October 2009.

Sood, B., R. Sanapala, D. Das, M. Pecht, C. Y. Huang, and M. Y. Tsai. Comparison of Printed Circuit Board Property Variations in Response to Simulated Lead-Free Soldering. IEEE Transactions on Electronics Packaging Manufacturing, Vol. 33, No. 2, 2010.

Amagai M.; Yutaka S., A study of package warpage for package on package (PoP), 60th Electronic Components and Technology Conference, pp.226-233, 1-4 June 2010.

Amkor Technology, http://www.amkor.com/

Bieler, T., Jiang, H., Influence of Sn Grain Size and Orientation on the Thermomechanical Response and Reliability of Pb-free Solder Joints, Proceedings of the 56th ECTC, pp. 1462- 1471, May 2006.

Cook, E.R.; Jacoby, G.C. Jr., Tree-ring-drought relationships in the Hudson Valley, New York. Science, Vol. 198, pp.399-401, 1977

.

Draper, N.R.; Smith, H., Applied regression analysis, 2nd edition, New York: John Wiley, and Sons. 709 p 1981.

Fritts, H.C.; Blasing, T.J.; Hayden, B.P.; Kutzbach, J.E., Multivariate techniques for specifying tree-growth and climate relationships and for reconstructing anomalies in paleoclimate, Journal of Applied Meteorology, Vol. 10, pp. 845-864, 1971.

Gunst, R.F.; Mason, R.L., Regression analysis and its application: a data-oriented approach, New York: Marcel Dekker, 402 p., 1980.

Kehoe, L., Lynch, P., Guénebaut, V., Measurement of Deformation and Strain in First Level C4 Interconnect and Stacked Die using Optical Digital Image Correlation, Proceedings of the 56th ECTC, pp. 1874-1881, May 2006.

Lall, P., Choudhary, P., Gupte, S., Suhling, J., Hofmeister, J., Statistical Pattern Recognition and Built-In Reliability Test for Feature Extraction and Health Monitoring of Electronics under Shock Loads, 57th Electronics Components and Technology Conference, Reno, Nevada, pp. 1161-1178, May 30-June 1, 2007a.

Lall, P., Gupte, S., Choudhary, P., Suhling, J., Solder-Joint Reliability in Electronics Under Shock and Vibration using Explicit Finite Element Sub-modeling, IEEE Transactions on Electronic Packaging Manufacturing, Volume 30, No. 1, pp. 74-83, January 2007b.

Lall, P., Panchagade, D., Iyengar, D., Shantaram, S., Suhling, J., Schrier, H., High Speed Digital Image Correlation for Transient-Shock Reliability of Electronics, Proceedings of the 57th ECTC, Reno, Nevada, pp. 924-939, May 29 – June 1, 2007c.

Lall, P. Panchagade, D., Liu, Y., Johnson, W., Suhling, J., Smeared Property Models for Shock-Impact Reliability of Area-Array Packages, ASME Journal of Electronic Packaging, Volume 129, pp. 373-381, December 2007d.

Lall, P., Hande, M., Bhat, C., Islam, N., Suhling, J., Lee, J., Feature Extraction and Damage-Precursors for Prognostication of Lead-Free Electronics, Microelectronics Reliability, Volume 47, pp. 1907–1920, December 2007e.

Lall, P., Choudhary, P., Gupte, S., Suhling, J., Health Monitoring for Damage Initiation and Progression during Mechanical Shock in Electronic Assemblies, IEEE Transactions on Components and Packaging Technologies, Vol. 31, No. 1, pp. 173-183, March 2008a.

Lall, P., Panchagade, D., Choudhary, P., Gupte, S., Suhling, J., Failure-Envelope Approach to Modeling Shock and Vibration Survivability of Electronic and MEMS Packaging, IEEE Transactions on Components and Packaging Technologies, Vol. 31, No. 1, pp. 104-113, March 2008b.

Lall, P., Iyengar, D., Shantaram, S., S., Gupta, P., Panchagade, D., Suhling, J., KEYNOTE PRESENTATION: Feature Extraction and Health Monitoring using Image Correlation for survivability of Leadfree Packaging under Shock and Vibration, Proceedings of the 9th International Conference on Thermal, Mechanical, and Multi Physics Simulation and Experiments in Micro-Electronics and Micro-Systems (EuroSIME), Freiburg, Germany, pp. 594-608, April 16-18, 2008c.

Lall, P., Iyengar, D., Shantaram, S., Pandher, R., Panchagade, D., Suhling, J., Design Envelopes and Optical Feature Extraction Techniques for Survivability of SnAg Leadfree Packaging Architectures under Shock and Vibration, Proceedings of the 58th Electronic Components and Technology Conference (ECTC), Orlando, Florida, pp. 1036-1047, May 27-30, 2008d.

Lall, P., Shirgaokar, A., Drake, J., Moore, T., Suhling, J., Principal Component Regression Models for Life Prediction of PBGAs on Copper Core and No-Core Assemblies, ITherm '08, Orlando, Florida, pp. 770-785, May 28-31, 2008.

Lall, P., Shirgaokar, A., Arunachalam, D, "Principal Component Analysis Based Development of Norris-Landzberg Acceleration Factors and Goldmann Constants for Leadfree Electronics," Electronic Components and Technology Conference (ECTC), 26-29 May 2009

Lall, P., Kulkarni, M., Angral, A, Digital-Image Correlation and XFEM Based Shock-Reliability Models for Leadfree and Advanced Interconnects, Proceedings of the 60th Electronic Components and Technology Conference (ECTC), Las Vegas, Nevada, June 1-4, 2010

Lall, P., Narayan, V., Suhling, J., Blanche, J., Effect of Reflow Process on Glass Transition Temperature pf Printed Circuit Board Laminates, ITherm, May 30 – June 1, 2012

Lall, P., Patel, K., Narayan, V., Model for Prediction of Package-on-Package Warpage and the Effect of Process and Material Parameters, Proceedings of the 63rd Electronic Components and Technology Conference (ECTC), Las Vegas, Nevada, May 28–3, 2013

Mansfield, E.R.; Webster, J.T.; Gunst, R.F., An analytic variable selection technique for principal components regression, Applied Statistics. Vol. 6, pp. 34-40, 1977.

Massey, W., Principal component regression in exploratory statistical research, Journal of the American Statistical Association, 60, pp.234-246, 1965.

Miller, T., Schreier, H., Reu, P, High-speed DIC Data Analysis from a Shaking Camera System, Proceedings of the SEM Conference, Springfield, Massachusetts, June 4-6, 2007.

Park, S., Shah, C., Kwak, J., Jang, C., Pitarresi, J., Transient Dynamic Simulation and Full-Field Test Validation for A Slim-PCB of Mobile Phone under Drop Impact, Proceedings of the 57th ECTC, Reno, Nevada, pp. 914-923, May 29 – June 1, 2007a.

Park, S., Reichman, A., Kwak, J., Chung, S., Whole Field Analysis of Polymer Film, Proceedings of the SEM Conference, Springfield, Massachusetts, June 4-6, 2007b. 554 2009 Electronic Components and Technology Conference

Peterson, D., Cheng, C., Karulkar, P.C., Characterization of Drop Impact Survivability of a 3D-CSP Stack Module, Proceedings of the 58th Electronic Component and Technology Conference, Orlando, Florida, pp. 1648-1653, May 27-30, 2008.

Patel, K.; Modeling and Reliability Characterization of Area-Array Electronics Subjected to High-G Mechanical Shock Up To 50,000G and Finite Element Analysis of Package on Package (PoP) Components for Warpage During Reflow, Master’s Thesis, Auburn University, pp. 95-122, 2013

Rajendra, Pendse, D., Zhou, P., Methodology For Predicting Solder Joint Reliability In Semiconductor Packages, Microelectronics Reliability, Vol. 42, pp. 301-305, 2002.

Scheijgrond,P.L.W., Shi, D.X.Q., Driel, W.D.V., Zhang,G.Q., Nijmeijer, H., Digital Image Correlation for Analyzing Poratable Electronic Products during Drop Impact Tests, 6th International Conference on Electronic Packaging Technology, pp. 121 – 126, Aug 30.-Sept 2. 2005.

Sun, Y., Pang, J., Shi, X., Tew, J., Thermal Deformation Measurement by Digital Image Correlation Method, Proceedings of ITherm Conference, pp. 921-927, May 2006.

Sun P.; Leung V.C.; Xie B.; Ma V.W.; Shi, D.X., Warpage reduction of package-on-package (PoP) module by material selection & process optimization, Electronic Packaging Technology & High Density Packaging, pp.1-6, 28-31 July 2008

Yen, F.; Chen, E.; Lai J.Y.; Wang Y.P.,The Introduction of Warpage Improvement Guidelines for BGA's Performance within SMT Temperature Profile, Microsystems, Packaging, Assembly & Circuits Technology Conference, 2008. IMPACT 2008. 3rd International , pp.278-282, 22-24 October 2008

Yogel, D., Grosser, V., Schubert, A., Michel, B., MicroDAC Strain Measurement for Electronics Packaging Structures, Optics and Lasers in Engineering, Vol. 36, pp. 195-211, 2001.

Zhang, F., Li, M., Xiong, C., Fang, F., Yi, S., Thermal Deformation Analysis of BGA Package by Digital Image Correlation Technique, Microelectronics International, Vol. 22, No. 1, pp. 34-42, 2005.

Zhou, P., Goodson, K. E., Sub-pixel Displacement and Deformation Gradient Measurement Using Digital Image- Speckle Correlation (DISC), Optical Engineering, Vol. 40, No. 8, pp 1613-1620, August 2001.